Contents of issue 5 vol. XLV

Polish Academy of Sciences

Institute of Fundamental Technological Research

Archives of Mechanics

Archiwum Mechaniki Stosowanej

volume 45 issue 5

Polish Scientific Publishers PWN

Warszawa 1993

ARCHIVES OF MECHANICS IS DEVOTED TO
Theory of elasticity and plasticity • Theory of nonclassical continua • Physics of continuous media • Mechanics of discrete media • Nonlinear mechanics • Rheology • Fluid gas-mechanics • Rarefied gases • Thermodynamics

---

Printed in Poland, Editorial Office: Świętokrzyska 21,
00-049 Warszawa (Poland)

Arkuszy wydawniczych 8,25. Arkuszy drukarskich 8,25
Papier offset. kl. III 70 g. B1. Oddano do składania w grudniu 1993 r.
Druk ukończono w kwietniu 1994 r.
Skład i łamanie: CENTRUM Warszawa, ul. Husarii 12
Druk i oprawa: Drukarnia Braci Grodzickich, Żabieniec ul. Przelotowa 7

Arch. Mech., 45, 5, pp. 507-525, Warszawa 1993

Growth of circular cylindrical voids in shear bands

K. L. PAN (SHANGHAI)

THE CIRCULAR cylindrical void growth in a finite representative volume element (RVE) is analyzed for a nonlinear power law viscous material undergoing simple shearing combined with triaxial tension (or pressure). To establish the macroscopic constitutive relation, a constitutive potential theory is developed for the porous viscous material. A microscopic velocity field is constructed by assuming incompressibility of the matrix and the uniform velocity boundary conditions of RVE. Basing on the velocity field, the macroscopic constitutive potential function and the corresponding constitutive relation are found. From the constitutive relation obtained, the relative void growth rate is computed numerically, which is a function of the stress triaxiality, the void volume fraction and the strain rate sensitivity exponent of the matrix. When the matrix material becomes infinite, the present result is reduced to that of MCCLINTOCK *et al.* [1] or FLECK and HUTCHINSON [2].

1. Introduction. General theory of constitutive potential

IN FRACTURE EXPERIMENTS, a phenomenon of the nucleation, growth and coalescence of the microvoids has been observed in ductile materials. However, the fracture often occurs in shear bands as well. The void growth in such bands was investigated early by MCCLINTOCK *et al.* [1] for an infinite viscous material containing an elliptical cylindrical void. The same problem was discussed by FLECK and HUTCHINSON [2] according to their proposed constitutive potential. But these discussions have not considered the void interaction effects. The void is isolated in an infinite block of the material. In order to consider such effects, a widely applied physical model is a "unit cell" (or RVE) containing a single void. A strict treatment of the interaction of neighbouring voids requires the non-uniformity of the strain rate or stress on the boundary of the unit cell. A comprehensive discussion was given by GILORMINI *et al.* [3]. However, for possible computation, the uniform boundary conditions are still employed in many papers including the present one. The early work dealing with this problem was made by TRACEY [4] and NEEDLEMAN [5] who investigated the growth of a void in a finite body. Later, a more detailed discussion on the growth of both cylindrical and spherical voids in ductile materials was made by GURSON [6] who used the concept of unit cell and an upper bound approach of the constitutive potential in his analysis. Gurson's result has been employed and extended by several authors, for instance, by NEEDLEMAN and RICE [7], TVERGAARD [8], KOPLIK and NEEDLEMAN [9] and MEAR [10]. The other studies on the void growth in a finite body were given by DUVA [11], LICHT and SUQUET [12] and WORSWICK and PICK [13]. Recently, a new method to investigate the dynamic void growth in viscoplastic materials has been developed by PAN and HUANG [14].

This paper concerns the cylindrical void growth in shear bands and is based on a macroscopic constitutive potential theory and a unit cell model. The following assumptions are also adopted: a. The void growth rate is negligibly small during the initial elastic phase and the transitional elastic-plastic phase. Thus only the fully plastic phase needs to be considered. b. The voids preserve the same shape during their deformation (for small deformations). c. The evolution of the void volume fraction is governed by the formula

$$df = (1 - f)\, dE_{kk} \qquad (f = V_v/V),$$

which leads to

$$\dot{E}_{kk} = \dot{f}/(1 - f), \qquad \text{and} \qquad \dot{V}_v = \dot{V}. \tag{1.1}$$

Equation (1.1) indicates that the macroscopic volume dilatation is contributed only by the volume change of voids in the material.

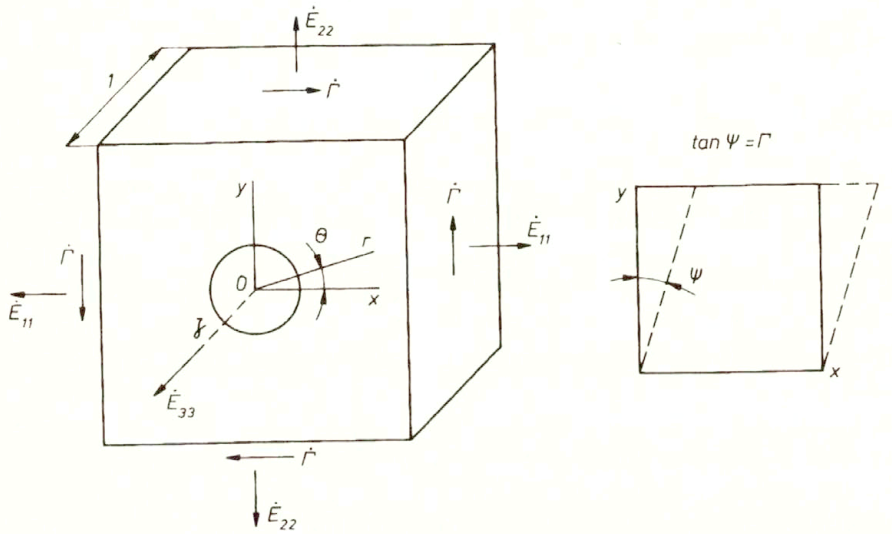

FIG. 1. Unit cell and its deformation with outer strain rate.

The geometry and the notation of the unit cell are displayed in Fig. 1. The volume of the unit cell is $V = V_m + V_v$, where V_m and V_v are, respectively, the volumes of the matrix and the void. The macroscopic stress and strain rate (i.e., the overall stress and strain rate) acting on the cell are denoted by upper-case letters Σ_{ij} and $\dot{E}_{ij}$, while the corresponding microscopic stress and strain rate (the ones appearing in the matrix) are denoted by lower-case letters σ_{ij} and $\dot{\varepsilon}_{ij}$. Thus the following boundary conditions can be given:

(i) Traction-free condition on the inner surface of the cell.

(ii) On the outer boundary of the unit cell, the velocity boundary conditions for the simple shear with triaxial tension or pressure states (see Fig. 1.) are satisfied,

(1.2) $$v_1 = \dot{E}_{11} x_1 + \dot{\Gamma} x_2, \qquad v_2 = \dot{E}_{22} x_2, \qquad v_3 = \dot{E}_{33} x_3,$$

where $\dot{\Gamma}$ is the macroscopic shear strain rate. The corresponding tensorial components of the strain rate are

(1.3) $$\dot{E}_{12} = \dot{E}_{21} = \dot{\Gamma}/2.$$

The matrix is assumed to be governed by a nonlinear power law viscous and incompressible material:

(1.4) $$s_{ij} = (2\mu/3)(\dot{\varepsilon}_e)^{n-1} \dot{\varepsilon}_{ij}, \qquad \dot{\varepsilon}_{ii} = 0,$$

where μ is a viscous constant defined by

$$\mu = \sigma_0/\dot{\varepsilon}_0^n;$$

here σ_0 and $\dot{\varepsilon}_0$ are constants for no strain-hardening materials, and n $(0 \geqslant n \geqslant 1)$ is a strain-rate sensitivity exponent, $\dot{\varepsilon}_e = (2\dot{\varepsilon}_{ij}\dot{\varepsilon}_{ij}/3)^{1/2}$ is the equivalent strain rate, s_{ij} is the deviatoric stress. It has been assumed that in Eq. (1.4) the elastic part of the strain rate can be neglected. The overall response of the damaged material is measured in terms of the macroscopic stress and strain rate which can, respectively, be expressed as

$$\Sigma_{ij} = \frac{1}{V}\int_v \sigma_{ij}\, dV = \frac{1}{V}\int_{\partial v} \sigma_{ik} n_k x_j\, dS,$$

$$\dot{E}_{ij} = \frac{1}{2V}\int_{\partial v} (v_i n_j + v_j n_i)\, dS,$$

where $\mathbf{v}$ is the velocity field corresponding to $\dot{\boldsymbol{\varepsilon}}$ and $\mathbf{n}$ is the outwardly directed unit normal to the boundary. The measures Σ and $\dot{\mathbf{E}}$ are work conjugate, and what is sought is the constitutive relation which relates these macroscopic quantities. It can be shown that the constitutive equation (1.4) can also be expressed in the form:

$$S_{ij} = \partial\varphi(\dot{\varepsilon}_{kl})/\partial\dot{\varepsilon}_{ij} \qquad \text{or} \qquad \dot{\varepsilon}_{ij} = \partial\psi(\sigma_{kl})/\partial\sigma_{ij},$$

where

$$\varphi = \mu\left[\frac{1}{(n+1)}(\dot{\varepsilon}_e)^{(n+1)}\right],$$

(1.5) $$\psi = \mu^{-1/n}\left(\frac{1}{n}+1\right)^{-1}(\sigma_e)^{(1/n+1)}.$$

Note that, in Eq. (1.5), φ and ψ are convex functions of their variables and they satisfy the condition $\partial\psi/\partial\sigma_{ii} = 0$. Hence for two arbitrarily specified stress-strain rate states $\left(\sigma_{ij}^{(1)}, \dot{\varepsilon}_{ij}^{(1)}\right)$ and $\left(\sigma_{ij}^{(2)}, \dot{\varepsilon}_{ij}^{(2)}\right)$, the following relation can be obtained

(1.6) $$\psi(\sigma_{ij}^{(2)}) \geqslant \sigma_{ij}^{(2)}\dot{\varepsilon}_{ij}^{(1)} - \varphi(\dot{\varepsilon}_{ij}^{(1)}).$$

Let us choose $\sigma_{ij}^{(2)}$ as the true stress field corresponding to macroscopic stress Σ_{ij}, and $\dot{\varepsilon}_{ij}^{(1)}$ as any kinematically admissible strain rate field corresponding to the macroscopic strain rate $\dot{E}_{ij}^{(1)}$. Integrating inequality (1.6) we obtain

$$\Psi \geqslant \frac{1}{V}\int_{Vm} \sigma_{ij}^{(2)} \dot{\varepsilon}_{ij}^{(1)} dV - \Phi_1, \tag{1.7}$$

where

$$\Psi = \frac{1}{V}\int_{Vm} \psi(\sigma_{ij}^{(2)})\, dV, \tag{1.8}$$

$$\Phi_1 = \frac{1}{V}\int_{Vm} \varphi(\dot{\varepsilon}_{ij}^{(1)})\, dV. \tag{1.9}$$

Using the classical relation given by HILL [15]

$$\frac{1}{V}\int_{Vm} \sigma_{ij}^{(2)} \dot{\varepsilon}_{ij}^{(1)} dV = \Sigma_{ij} \dot{E}_{ij}^{(1)}$$

the inequality (1.7) can be expressed as

$$\Psi \geqslant \Sigma_{ij} \dot{E}_{ij}^{(1)} - \Phi_1. \tag{1.10}$$

It is obvious that for a given Σ_{ij}, the corresponding $\dot{E}_{ij}$ should be chosen to maximize the right-hand side of the inequality (1.10). This can be accomplished through the following procedure: a) for a given $\dot{E}_{ij}^{(1)}$, seek the corresponding kinematically admissible strain rate field $\dot{\varepsilon}_{ij}^{(1)}$ which minimizes the value of Φ_1; b) from the condition $\delta\Psi = 0$, the relation between the macroscopic stress and strain rate can be obtained by

$$\Sigma_{ij} = \left.\frac{\partial \Phi_1\left(\dot{E}_{ij}^{(1)}\right)}{\partial \dot{E}_{ij}^{(1)}}\right|_{\dot{E}_{ij}^{(1)}}. \tag{1.11}$$

Equation (1.11) indicates that the macroscopic constitutive relation can be found from a known potential function Φ_1 which is related to the microscopic potential function φ by Eq. (1.9) through $\dot{\varepsilon}^{(1)}$ and $\mathbf{v}^{(1)}$. If $\mathbf{v}^{(1)}$ were an actual velocity field, Eq. (1.11) would give an actual macroscopic stress field. When an approximate velocity field $\mathbf{v}$ is given, Eq. (1.11) gives an approximate macroscopic stress field. The $\mathbf{v}$ field considered here has the following function form:

$$\mathbf{v} = \mathbf{v}(\dot{\mathbf{E}}, n, \mathbf{x}, f, c_1, c_2, \ldots),$$

where c_i is chosen so as to minimize the potential Φ_1 and to make $\mathbf{v}$ reach the actual velocity field.

2. Macroscopic potential function and corresponding constitutive relation

It is convenient to decompose the velocity field $\mathbf{v}$ into three parts

$$\mathbf{v} = \mathbf{v}' + \mathbf{v}^v + \mathbf{v}^*,$$

where $\mathbf{v}'$ and $\mathbf{v}^v$ correspond, respectively, to the deviatoric part and the dilatational part of the field $\dot{\varepsilon}$, each satisfying the incompressibility and the boundary conditions. $\mathbf{v}^*$ is so constructed that it satisfies the zero boundary condition and incompressibility condition.

For a circular cylindrical void, the cylindrical coordinates (r, θ, z) with $x_3 = z$ can be chosen to compute the $\dot{\varepsilon}$ and $\mathbf{v}$ fields. Using the coordinates (r, θ, z), the boundary conditions can be expressed as

$$v_r' = b\left(\frac{1}{3}\dot{E} - \frac{1}{2}\dot{E}_3 - \dot{E}'\cos 2\theta + \frac{1}{2}\dot{\Gamma}\sin 2\theta\right), \qquad v_r^v = b\,\dot{E}_m,$$

$$v_\theta' = b\,(\dot{E}'\sin 2\theta - \dot{\Gamma}\sin^2\theta), \qquad v_\theta^v = 0, \tag{2.1}$$

$$v_z' = (\dot{E}_3 - \dot{E}_m)\,z_0, \qquad v_z^v = \dot{E}_m\,z_0,$$

where

$$\dot{E}' = (\dot{E}_{22} - \dot{E}_{11})/2, \qquad \dot{E} = \dot{E}_{kk}/2, \qquad \dot{E}_m = \dot{E}_{kk}/3, \qquad \dot{E}_3 = \dot{E}_{33},$$

and z_0 is a given unit length in z direction. The components of the microscopic strain rate written in (r, θ, z) can be expressed in terms of the velocity field $\mathbf{v}$ as follows:

$$\begin{aligned}
\dot{\varepsilon}_{rr} &= \partial v_r/\partial r,\\
\dot{\varepsilon}_{\theta\theta} &= r^{-1}\,\partial v_\theta/\partial\theta + v_r/r,\\
\dot{\varepsilon}_{r\theta} &= (1/2)(r^{-1}\,\partial v_r/\partial\theta + \partial v_\theta/\partial r - \partial v_\theta/r),\\
\dot{\varepsilon}_{zz} &= \partial v_z/\partial z.
\end{aligned} \tag{2.2}$$

From the boundary condition (2.1) and the incompressibility condition $\dot{\varepsilon}_{zz} + \dot{\varepsilon}_{\theta\theta} + \dot{\varepsilon}_{rr} = 0$, a microscopic velocity field $\mathbf{v}^0 = \mathbf{v}' + \mathbf{v}^v$ can be obtained:

$$v_r^0 = r\left(-\frac{1}{2}\dot{E}_3 - \dot{E}'\cos 2\theta + \frac{1}{2}\dot{\Gamma}\sin 2\theta\right) + A/r,$$

$$v_\theta^0 = r\,(\dot{E}'\sin 2\theta - \dot{\Gamma}\sin^2\theta),$$

$$v_z^0 = \dot{E}_3\,z.$$

The corresponding strain rate field is

$$\dot{\varepsilon}^0_{rr} = -\frac{1}{2}\dot{E}_3 - \dot{E}'\cos 2\theta + \frac{1}{2}\dot{\Gamma}\sin 2\theta - A/r^2,$$

$$\dot{\varepsilon}^0_{\theta\theta} = -\frac{1}{2}\dot{E}_3 + \dot{E}'\cos 2\theta - \frac{1}{2}\dot{\Gamma}\sin 2\theta + A/r^2,$$

(2.3)

$$\dot{\varepsilon}^0_{r\theta} = \dot{E}'\sin 2\theta + \frac{1}{2}\dot{\Gamma}\cos 2\theta,$$

$$\dot{\varepsilon}^0_{zz} = \dot{E}_3,$$

where

$$A = \dot{E}\,b^2.$$

Another part $\mathbf{v}^*$ of the velocity field can be given by

(2.4) $$v^*_r = -\eta_{,\theta}(r,\theta)/r, \qquad v^*_\theta = -\eta_{,r}(r,\theta) \qquad v^*_z = 0,$$

where

$$\eta(r,\theta) = \dot{E}'(b-r)^2 \sum_{k=0,\,2,\,4,\,\ldots} (f_{1k}(r)\cos k\theta + f_{2k}(r)\sin k\theta),$$

$$f_{1k}(r) = \sum_{s=-1,\,0,\,1,\,\ldots} A_{ks}\,r^s, \qquad f_{2k}(r) = \sum_{s=-1,\,0,\,1,\,\ldots} B_{ks}\,r^s,$$

whereas $\eta_{,\theta}$ and $\eta_{,r}$ are derivatives of $\eta(r,\theta)$ with respect to coordinates θ and r. For axisymmetric loading, i. e. $\dot{E}_{11} = \dot{E}_{22}$, we have $\eta(r,\theta) = 0$ and $\mathbf{v} = \mathbf{v}^s + \mathbf{v}^v$. The strain rate field $\dot{\boldsymbol{\varepsilon}}^*$ can be computed by substituting Eq. (2.4) into Eq. (2.2), which gives

$$\dot{\varepsilon}^*_{rr} = \dot{E}'(b/r-1)\sum_k \sum_s g_1(r,k,s)\,(-A_{ks}\sin k\theta + B_{ks}\cos k\theta),$$

$$\dot{\varepsilon}^*_{r\theta} = (1/2)\,\dot{E}'\sum_k \sum_s g_2(r,k,s)\,(A_{ks}\cos k\theta + B_{ks}\sin k\theta),$$

(2.5)

$$\dot{\varepsilon}^*_{\theta\theta} = -\dot{\varepsilon}^*_{rr}$$

$$\dot{\varepsilon}^*_{zz} = 0,$$

where

$$g_1 = (r,k,s) = kr^s[1+s+(1-s)\,b/r],$$

$$g_2(r,k,s) = r^s\{k^2(b/r-1)^2 - (b/r-1)[s(2+s)+s(2-s)\,b/r-2]+2\}.$$

Then the strain rate field $\dot{\varepsilon}$ can be expressed as $\dot{\boldsymbol{\varepsilon}} = \dot{\boldsymbol{\varepsilon}}^0 + \dot{\boldsymbol{\varepsilon}}^*$, from which the equivalent strain rate can be expressed by

$$(2.6)\qquad \dot{\varepsilon}_e = (2\dot{\varepsilon}_{ij}\dot{\varepsilon}_{ij}/3)^{1/2}$$
$$= \frac{2}{\sqrt{3}}\left[\frac{3}{4}\dot{E}_3' + \dot{E}'^2 + \frac{1}{4}\dot{\Gamma}^2 - \dot{E}^2 x^2 - 2\dot{E}\dot{\varepsilon}x + \dot{\varepsilon}_{rr}^{*2} + \dot{\varepsilon}_{r\theta}^{*2} + 2\dot{\varepsilon}\,\dot{\varepsilon}_{rr}^{*} + 2\dot{\varepsilon}_{r\theta}^{0}\dot{\varepsilon}_{r\theta}^{*}\right]^{1/2},$$

where

$$x = b^2/r^2, \qquad \dot{\varepsilon} = -\dot{E}'\cos 2\theta + \frac{1}{2}\dot{\Gamma}\sin 2\theta - \dot{E}x.$$

The potential function Φ_1 can be computed from Eqs. (1.9) and (1.5) as

$$(2.7)\qquad \Phi_1 = \frac{1}{V}\int_{Vm}\int s_{ij}(\dot{\varepsilon}_{ij})\,d\dot{\varepsilon}_{ij}\,dV = \frac{\mu}{\pi}\int_0^{2\pi}\int_1^{1/f}\left[\frac{1}{(n+1)}(\dot{\varepsilon}_e)^{(n+1)}\right]x^{-2}\,dx\,d\theta,$$

where f is void volume fraction which is a micromechanical quantity and is defined by $f = V_v/V = a^2/b^2$. It can be used to describe the isotropic damage of the material. In this way, some account is taken of the interaction of the neighboring voids. When the matrix becomes infinite, f is zero, which corresponds to an isolated void in an infinite matrix. The parameters A_{ks} and B_{ks} in Eq. (2.7) are chosen to minimize Φ_1. A numerical scheme is shown in Appendix A. An upper bound solution of Eq. (2.7) can be obtained by omitting $\dot{\varepsilon}_{ij}^{*}$ and it will be denoted by Φ_1^0. A comparison of Φ_1 with Φ_1^0 is given in Table 1 for several ratios: $\dot{E}_3/\dot{\Gamma}$, $\dot{E}'/\dot{\Gamma}$ and $\dot{E}/\dot{\Gamma}$. The results show that the difference between Φ_1^0 and Φ_1 is in general small. Namely, $\dot{\varepsilon}_{ij}^{*}$ obtained in this manner gives a small contribution to the value of Φ_1. Therefore the upper bound solution Φ_1^0 is accurate enough in practical application. Thus in the following analyses the upper bound potential function Φ_1^0 will be considered.

Table 1. Potential values with $n = 0.2$, $\dot{\Gamma} = \dot{\varepsilon}_0 = 1$.

	void volume fraction	$\Phi_1^0/\sigma_0\dot{\varepsilon}_0$	$\Phi_1/\sigma_0\dot{\varepsilon}_0$	$\Delta\Phi_1$
$\dot{E}_3/\dot{\Gamma} = 0.5$,	$f = 0.05$	1.8510	1.7493	0.0581
$\dot{E}'/\dot{\Gamma} = 0.1$,	$f = 0.1$	1.5032	1.4138	0.0632
$\dot{E}/\dot{\Gamma} = 0.2$,	$f = 0.2$	1.1762	1.0980	0.0712
$\dot{E}_3/\dot{\Gamma} = 1.0$,	$f = 0.05$	19.0692	18.1574	0.0502
$\dot{E}'/\dot{\Gamma} = 0.5$,	$f = 0.1$	13.7011	13.0128	0.0529
$\dot{E}/\dot{\Gamma} = 2.0$,	$f = 0.2$	9.0161	8.5233	0.0578

In the above table $\Delta\Phi_1 = (\Phi_1^0 - \Phi_1)/\Phi_1$.

The upper bound of the constitutive relation corresponding to Φ_1^0 can be found from Eqs. (1.11) and (2.7) by taking $\dot{\varepsilon}_{ij}^* = 0$. This leads to

$$\Sigma_{ij} = \partial \Phi_1^0 / \partial \dot{E}_{ij} = \frac{\mu}{\pi} \int_0^{2\pi} \int_1^{1/f} \left[(2^n / \sqrt{3^{n+1}}) H^{(n-1)/2} \right] H_{,ij} x^{-2} \, dx \, d\theta, \tag{2.8}$$

where

$$\dot{\varepsilon}_e = 2\sqrt{H}/\sqrt{3},$$

$$H = \frac{3}{4}\dot{E}_3^2 + \dot{E}'^2 + \frac{1}{4}\dot{\Gamma}^2 + \dot{E}^2 x^2 + 2\dot{E}' \dot{E} x \cos 2\theta - \dot{\Gamma} \dot{E} x \sin 2\theta,$$

$$H_{,11} = -\dot{E}' + \dot{E} x^2 + (\dot{E}' - \dot{E}) x \cos 2\theta - \frac{1}{2}\dot{\Gamma} x \sin 2\theta,$$

$$H_{,22} = \dot{E}' + \dot{E} x^2 + (\dot{E}' + \dot{E}) x \cos 2\theta - \frac{1}{2}\dot{\Gamma} x \sin 2\theta, \tag{2.9}$$

$$H_{,33} = \frac{3}{2}\dot{E}_3 + \dot{E} x^2 + \dot{E}' x \cos 2\theta - \frac{1}{2}\dot{\Gamma} x \sin 2\theta,$$

$$H_{,12} = \frac{1}{2}\dot{\Gamma} - \dot{E} x \sin 2\theta.$$

Note

$$\Sigma_{12} = \frac{1}{2}\partial \Phi_1^0 / \partial \dot{E}_{12} = \partial \Phi_1^0 / \partial \dot{\Gamma}.$$

Up to now, the macroscopic constitutive relation has been completed by Eqs. (2.8) and (2.9). Thus for any given macroscopic strain rates $\dot{E}_{ij}$ $(i = j)$ and $\dot{\Gamma}$, the macroscopic stress Σ_{ij} can be determined from Eqs. (2.8) and (2.9) by the numerical integration.

3. The void growth in a shear band

Consider a unit cell in a shear band which is inclined by 45° to the axis of the tension Σ. The unit cell is in a plane strain state with hydrostatic tension (or pressure), as adopted by MCCLINTOCK *et al.*[1] and FLECK *et al.* [2], i.e., in the present case: $\dot{E}_{33} = 0$, $\dot{E}_{11} = \dot{E}_{22}$. Then, Eq. (2.9) gives

$$H = \frac{1}{4}\dot{\Gamma}^2(1 + \omega^2 x^2 - 2\omega x \sin 2\theta),$$

$$H_{,11} = \frac{1}{2}\dot{\Gamma}(\omega x^2 - \omega x \cos 2\theta - x \sin 2\theta),$$

$$H_{,22} = \frac{1}{2}\dot{\Gamma}(\omega x^2 + \omega x \cos 2\theta - x \sin 2\theta), \tag{3.1}$$

$$H_{,33} = \frac{1}{2}\dot{\Gamma}(\omega x^2 - x \sin 2\theta),$$

$$H_{,12} = \frac{1}{2}\dot{\Gamma}(1 - \omega x \sin 2\theta),$$

where (note Eq. (1.1))

$$\omega \equiv 2\dot{E}/\dot{\Gamma} = \dot{E}_{kk}/\dot{\Gamma} = (\dot{V}_v/\dot{\Gamma}V_v)f = \lambda f, \tag{3.2}$$

whereas $\lambda \equiv \dot{V}_v/\dot{\Gamma}V_v$ is called the relative void growth rate.

Consider the substitution $t = \omega x$ and expressions (2.8) and (3.1); the stress triaxiality can be defined by

$$\chi \equiv \Sigma_m/\Sigma_{12} = \Sigma_{kk}/3\,\Sigma_{12} = \int_0^{2\pi\,\omega/f}\int_{\omega} [H(t,\theta)^{(n-1)/2}](1 - \sin 2\theta/t)\,dt\,d\theta \Big/ \int_0^{2\pi\,\omega/f}\int_{\omega} [H(t,\theta)^{(n-1)/2}](1 - t\sin 2\theta)\,t^{-2}\omega\,dt\,d\theta, \tag{3.3}$$

where

$$H(t,\theta) \equiv 1 + t^2 - 2t\sin 2\theta.$$

Note that $|\sin 2\theta| \leqslant 1$ and, therefore, $|2t\sin 2\theta|/(1+t^2) \leqslant 1$. $H(t,\theta)^{(n-1)/2}$ can be expanded into the series

$$H(t,\theta)^{(n-1)/2} = P^{(n-1)/2}\left[1 + \sum_{k=1}^{\infty} \frac{(2k-1-n)!!}{(2k)!!}\left(\frac{2t}{P}h\right)^k\right], \tag{3.4}$$

where

$$P \equiv P(t) = 1 + t^2, \qquad h \equiv h(\theta) = \sin 2\theta.$$

The first order approximation of Eq. (3.4) gives

$$H(t,\theta)^{(n-1)/2} = P^{(n-1)/2}\left[1 + (1-n)\left(\frac{t}{P}h\right)\right]. \tag{3.5}$$

The following integral (see Eq. (B.2) in Appendix B) is necessary for the computation of the triaxiality (3.3),

$$\int_0^{2\pi} \sin^k 2\theta = \begin{cases} 0, & \text{for} \quad k = 2m-1, \\ \dfrac{2(2m-1)!!}{(2m)!!}\pi, & \text{for} \quad k = 2m, \end{cases} \tag{3.6}$$

where $m = 1, 2, 3, \ldots$. In terms of Eqs. (3.4) and (3.6), formula (3.3) can be expressed as

$$\chi = \int_{\lambda f}^{\lambda} \left[2P^{(n-1)/2} + F_m\right] dt \Big/ \int_{\lambda f}^{\lambda} \left[2P^{(n-1)/2} + G_m\right] t^{-2}\, \lambda f\, dt, \tag{3.7}$$

where the substitution $\omega = \lambda f$ from Eq. (3.2) has been made. The first order approximation can be found by Eq. (3.5) and (3.6)

$$\chi = \int_{\lambda f}^{\lambda} \left[P^{(n-1)/2}\right] dt \Big/ \int_{\lambda f}^{\lambda} \left[P^{(n-1)/2}\right] t^{-2}\, \lambda f\, dt. \tag{3.8}$$

The expressions of F_m and G_m are given by Eq. (B.4) in Appendix B. Their integrals are, in general, functions of λ. However, in the case of a large void growth rate and an isolated void, these expressions are independent of λ as proved in Appendix B. The numerical analysis made with different m in F_m and G_m shows that their change is determined with the accuracy better than 1%, when $m \geqslant 5$, as long as the λ is larger

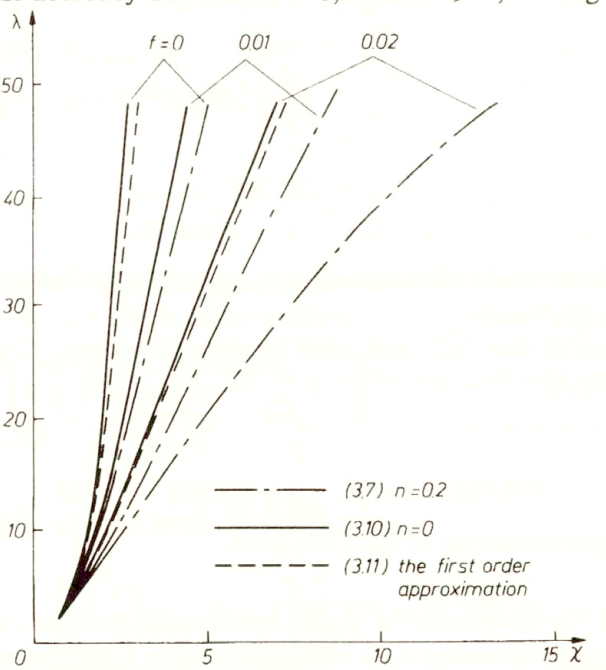

FIG. 2. Relation of void growth rate λ and triaxiality χ with different void volume fraction f.

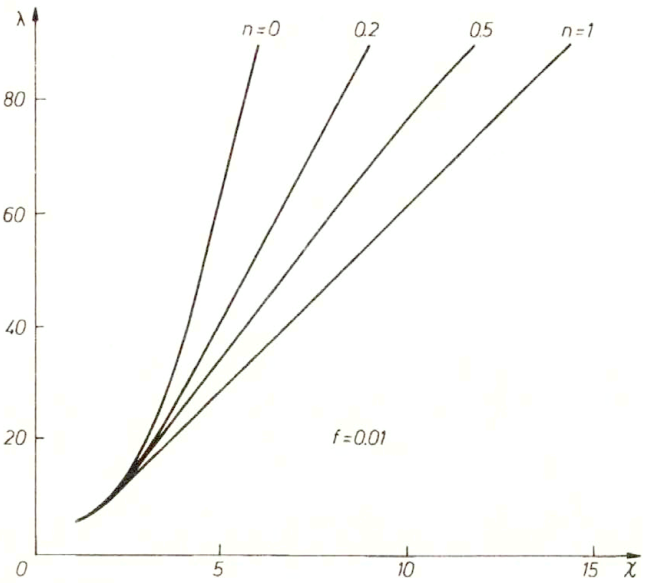

FIG. 3. Relation of void growth rate λ and triaxiality χ with different strain rate sensitivity exponen n.

than 10. Therefore, in the computation, $m = 5$ is always considered. The cylindrical void growth in a shear band can be analyzed numerically from Eq. (3.7), which is shown in Figs. 2 and 3 for different void volume fractions f and strain rate sensitivity exponents n. Figure 2 shows the effect of the void volume fraction. The results show that the void growth rate is a decreasing function of the void volume fraction, which means that theinteractions of the voids make the void growth difficult. Figure 3 demonstrates the effect of the strain rate sensitivity exponent, which indicates that the largest void growth rate occurs for the perfectly plastic material ($n = 0$), and the smallest one — for the Newtonian material ($n = 1$). The most general form of the triaxiality can be expressed as

$$\chi = \chi(\lambda, f, n). \tag{3.9}$$

It is obvious that the relative void growth rate λ is an implicit function of the triaxiality, void volume fraction and strain rate sensitivity exponent. Some special cases can be obtained from Eq. (3.9),

a. $\chi = \chi(\lambda, f)$, for the perfectly plastic material (when $n = 0$), or for Newtonian material (when $n = 1$).

b. $\chi = \chi(\lambda, n)$, for the infinite matrix material.

They can be discussed in detail as follows:

a. $n = 0$, *the perfectly plastic material*

In this case, the triaxiality in Eq. (3.7) can be expressed as

$$\chi = \int_{\lambda f}^{\lambda} [2P^{(-1/2)} + F_{0m}]\, dt \Big/ \int_{\lambda f}^{\lambda} [2P^{(-1/2)} + G_{0m}]\, t^{-2}\, \lambda f\, dt. \tag{3.10}$$

If the second term of the integrand in Eq. (3.10) is omitted, the first order approximation of the triaxiality (see Eq. (3.8)) can be obtained, which gives an analytical expression

$$\chi = \ln\{[\lambda + \sqrt{(\lambda^2+1)}]/[\lambda f + \sqrt{\lambda^2 f^2 + 1)}]\} / [f\sqrt{(\lambda^2+1)} + \sqrt{(\lambda^2 f^2+1)}]. \tag{3.11}$$

When the matrix material is infinite, Eq. (3.11) becomes $\lambda = \sinh\chi$, which has the same form as that given by McClintock for $n = 0$. The comparison of Eq. (3.11) with Eq. (3.10) is made in Fig. 2, in which the dashed line curves come from Eq. (3.11).

b. $n = 1$, *the Newtonian material*

In this case Eq. (B.4) in Appendix B gives $F_m = G_m = 0$. Then Eq. (3.7) becomes

$$\chi = \lambda \tag{3.12}$$

which is an exact expression.

c. $f = 0$, *the infinite matrix material*

Note the following limitation, when the matrix material becomes infinite

$$\int_{\lambda f}^{\lambda} [2P^{(n-1)/2} + G_m]\, t^{-2}\, \lambda f\, dt \to 2; \tag{3.13}$$

then, the triaxiality (3.7) can be expressed by

$$\chi = \int_0^{\lambda} [P^{(n-1)/2} + \frac{1}{2} F_m]\, dt. \tag{3.14}$$

The first order approximation is

$$\chi = \int_0^{\lambda} P^{(n-1)/2}\, dt. \tag{3.15}$$

For comparison, the formula given by MCCLINTOCK [1] and FLECK [2] are also given as follows:

$$\chi = \ln\{(1-n)\lambda + \sqrt{[(1-n)^2\lambda^2 + 1]}\}/(1-n), \tag{3.16}$$

$$\chi = [\lambda^n - (1-n)(1 + 0.6137n)]/n. \tag{3.17}$$

All results are drawn in Fig. 4 which shows a good agreement between the present result and that of FLECK *et al.* [2]. Note here the strain-rate sensitivity exponent n is a reciprocal of the hardening exponent used by McClintock and Fleck. Equations (3.14) – (3.17) give the same exact expression for $n = 1$: $\chi = \lambda$. For $n = 0$ and the large void growth rate λ Eq. (3.14) becomes (see Eq. (B.10))

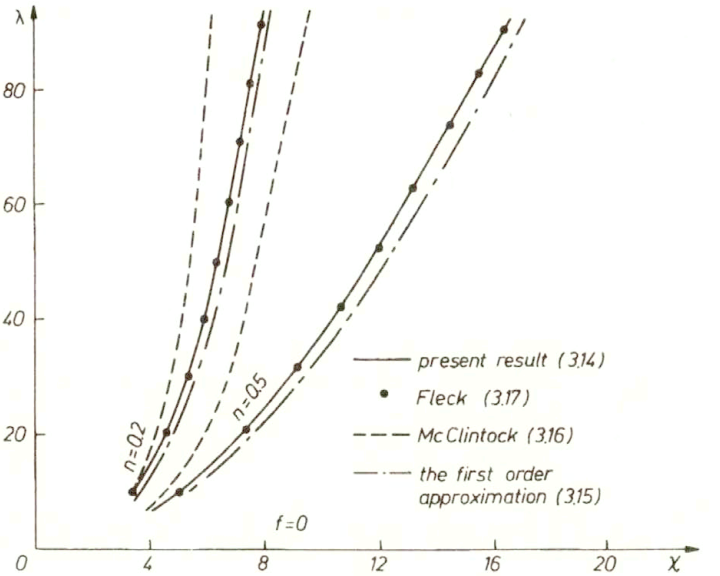

FIG. 4. Comparison of present results with those of McClintock and Fleck in an infinite medium ($f = 0$).

(3.18) $$\chi = \ln(2\lambda) - 0.61/2 \qquad \text{or} \qquad \lambda = 0.68 \exp(\chi).$$

In this case, Eqs. (3.16) and (3.17) can also be simply expressed as $\lambda = 0.50 \exp(\chi)$ and $\lambda = 0.68 \exp(\chi)$, respectively. The latter has the same form as Eq. (3.18), though they result from different approaches.

4. Conclusions

This paper presents the analysis of the circular cylindrical void growth in a shear band using a macroscopic potential function and the corresponding constitutive relation. The analysis is based on a finite unit cell model. The effects of void volume fraction and strain rate sensitivity exponent on the void growth rate were considered. For the infinite matrix material, the present result can be reduced to the models of McClintock *et al.* and Fleck and Hutchinson. Further modifications of the present model may be needed to include the effects of strain hardening and of the shape of the voids.

The author would like to thank Prof. Z.P. HUANG and Dr. J. FANG for their support and help offered during his employment in the BeijingUniversity.

Appendix A. Numerical scheme for the potential function Φ_1 in Eq. (2.7)

The potential function Φ_1 in Eq. (2.7) can be expressed as a function of macroscopic strain rate $\dot{E}_{ij}$ and parameters A_{ks} and B_{ks}, which should be chosen to

minimize the function Φ_1. However, the expression of Φ_1 is so complicated that the parameters have to be determined by means of the numerical method. The steepest descent algorithm (which can be found in many books on numerical methods) is available for determining the parameters and the corresponding function Φ_1. Φ_1 can be expressed in terms of $\dot{\varepsilon}_e$ which is defined in Eq. (2.6). When $k = 0, 2$ and $s = -1, 0, 1$, $\dot{\varepsilon}^*_{rr}$ and $\dot{\varepsilon}^*_{r\theta}$ can be expressed by Eq. (2.5) in non-dimensional form:

$$\dot{\varepsilon}^*_{rr} = 2(\dot{E}'/\dot{\Gamma})\left[\sum_1^3 c_i q_i(x)\cos 2\theta - \sum_4^6 c_i q_i(x)\sin 2\theta\right],$$

(A.1)

$$\dot{\varepsilon}^*_{r\theta} = \frac{1}{2}(\dot{E}'/\dot{\Gamma})\left[\sum_1^3 c_i q'_i(x)\sin 2\theta + \sum_4^6 c_i q'_i(x)\cos 2\theta + \sum_7^9 c_i q_i(x)\right],$$

where, for convenient calculation, the following substitutions have been made,

$$x = b^2/r^2,$$

$$c_1 = B_{2,-1}/b, \quad c_2 = B_{2,0}, \quad c_3 = B_{2,1}b, \quad c_4 = A_{2,-1}/b, \quad c_5 = A_{2,0},$$

$$c_6 = A_{2,1}b, \quad c_7 = A_{0,-1}/b, \quad c_8 = A_{0,0}, \quad c_9 = A_{0,1}b,$$

(A.2)

$$q_1 = q_4 = 2x(\sqrt{x}-1), \quad q_2 = q_5 = x-1, \quad q_3 = q_6 = 2(1-1/\sqrt{x}),$$

$$q_7 = \sqrt{x}(3x-1), \quad q_8 = 2\sqrt{x}, \quad q_9 = (3-x)/\sqrt{x},$$

$$q'_1 = q'_4 = 4(1-\sqrt{x})^2 + 3x - 1, \quad q'_2 = q'_5 = 4(1-\sqrt{x})^2 + 2\sqrt{x},$$

$$q'_3 = q'_6 = [4(1-\sqrt{x})^2 - x + 3]/\sqrt{x}.$$

Under the above conditions, Φ_1 can be rewritten as

(A.3)
$$\bar{\Phi}_1 = \Phi_1/\Phi_0 = \frac{2}{\pi}\int_0^{\pi}\int_1^{1/f}\left[(2\dot{\Gamma}/\sqrt{3}\dot{\varepsilon}_0)^{(n+1)}\frac{1}{(n+1)}H^{(n+1)/2}\right]x^{-2}\,dx\,d\theta,$$

where

$$H \equiv H(\dot{\mathbf{E}}, x, \theta, c_i) = H_1(\dot{\mathbf{E}}, x, \theta) + H_2(\dot{\mathbf{E}}, x, \theta, c_i),$$

$$H_1(\dot{\mathbf{E}}, x, \theta) = \frac{1}{4} + \frac{3}{4}(\dot{E}_3/\dot{\Gamma})^2 + (x\dot{E}/\dot{\Gamma})^2 + (\dot{E}'/\dot{\Gamma})^2 + 2x(\dot{E}\dot{E}'/\dot{\Gamma}^2)\cos(2\theta) - x(\dot{E}/\dot{\Gamma})\sin(2\theta),$$

$$H_2(\dot{\mathbf{E}}, x, \theta, c_i) = 2\dot{\varepsilon}\dot{\varepsilon}^*_{rr} + 2\dot{\varepsilon}^0_{r\theta}\dot{\varepsilon}^*_{r\theta} + \dot{\varepsilon}^{*2}_{rr} + \dot{\varepsilon}^{*2}_{r\theta},$$

$$\Phi_0 = \sigma_0\dot{\varepsilon}_0, \quad \dot{\varepsilon} = \frac{1}{2}\sin 2\theta - (\dot{E}'/\dot{\Gamma})\cos 2\theta - x\dot{E}/\dot{\Gamma}, \quad \dot{\varepsilon}^0_{r\theta} = \frac{1}{2}\cos 2\theta + (\dot{E}'/\dot{\Gamma})\sin 2\theta.$$

Thus $\bar{\Phi}_1 = \bar{\Phi}_1(\dot{E}_3/\dot{\Gamma}, \dot{E}/\dot{\Gamma}, \dot{E}'/\dot{\Gamma}, c_i)$ for given f, n and ratio $\dot{\Gamma}/\dot{\varepsilon}_0$.

The program of the steepest descent algorithm requires the knowledge of Φ_1 and its derivatives with respect to c_i, which are given by

$$\partial\bar{\Phi}_1/\partial c_i = \frac{1}{\pi}(2\dot{\Gamma}/\sqrt{3}\,\dot{\varepsilon}_0)^{(n+1)} \int_0^{\pi}\int_1^{1/f}\left[H^{(n-1)/2}\right] H_{2,\,i}\, x^{-2}\, dx\, d\theta, \tag{A.4}$$

where

$$H_{2,\,i} = \partial H_2/\partial c_i = 2(\dot{\varepsilon}^0_{rr} + \dot{\varepsilon}^*_{rr})(\partial\dot{\varepsilon}^*_{rr}/\partial c_i + 2(\dot{\varepsilon}^0_{r\theta} + \dot{\varepsilon}^*_{r\theta})(\partial\dot{\varepsilon}^*_{r\theta}/\partial c_i).$$

The components of $\partial\dot{\varepsilon}^*_{rr}/\partial c_i$ and $\partial\dot{\varepsilon}^*_{r\theta}/\partial c_i$ can be determined by (A.1) and (A.2), which gives,

$$\begin{aligned}
\partial\dot{\varepsilon}^*_{rr}/\partial c_i &= 2(\dot{E}'/\dot{\Gamma})\, c_i\, q_i(x)\cos 2\theta \qquad \text{for} \qquad i = 1, 2, 3,\\
&= -2(\dot{E}'/\dot{\Gamma})\, c_i\, q_i(x)\sin 2\theta \qquad \text{for} \qquad i = 4, 5, 6; \qquad \text{(A.5)}
\end{aligned}$$

and

$$\begin{aligned}
\partial\dot{\varepsilon}^*_{r\theta}/\partial c_i &= \frac{1}{2}(\dot{E}'/\dot{\Gamma})\, c_i\, q_i'(x)\sin 2\theta \qquad \text{for} \qquad i = 1, 2, 3,\\
&= \frac{1}{2}(\dot{E}'/\dot{\Gamma})\, c_i\, q_i'(x)\cos 2\theta \qquad \text{for} \qquad i = 4, 5, 6,\\
&= \frac{1}{2}(\dot{E}'/\dot{\Gamma})\, c_i\, q_i(x) \qquad \text{for} \qquad i = 7, 8, 9.
\end{aligned}$$

The integrations in Eqs. (A.3) and (A.4) are performed by means of the Simpson double integration formulae. On substituting (A.3)–(A.5) into the program of the steepest descent algorithm, the value of $\bar{\Phi}_1$ can be computed numericallly. The results and the values of the computation are given in Table 1.

Appendix B. Expressions of F_m and G_m in Eq. (3.7)

In terms of the series (3.4), the triaxiality χ in Eq. (3.3) can be expressed as

$$\chi = \int_0^{2\pi}\int_{\omega}^{\omega/f}\left\{P^{(n-1)/2}\left[1 + L_k\left(\frac{2t}{P}h\right)^k\right]\right\}(1 - h/t)\, dt\, d\theta \Bigg/ \int_0^{2\pi}\int_{\omega}^{\omega/f}\left\{P^{(n-1)/2}\left[1 + L_k\left(\frac{2t}{P}h\right)^k\right]\right\}(1 - ht)\, t^{-2}\,\omega\, dt\, d\theta, \tag{B.1}$$

where

$$P = 1 + t^2, \qquad h = \sin 2\theta, \qquad L_k = \sum_{k=1}^{\infty}\frac{(2k - 1 - n)!!}{(2k)!!}.$$

The integral

$$\int_0^{2\pi} h^k \, d\theta \qquad \text{or} \qquad \int_0^{2\pi} h^{k+1} \, d\theta$$

can be expressed in terms of the special functions $\beta(x, y)$ and $\Gamma(m)$

$$\text{(B.2)} \quad \int_0^{2\pi} \sin^k 2\theta \, d\theta = \frac{1}{2} \int_{-2\pi}^{2\pi} \sin^k u \, du = 2\beta\left(\frac{1}{2}, \frac{2m+1}{2}\right) = \frac{2(2m-1)!!}{(2m)!!}\pi \qquad \text{for } k = 2m,$$

where the following properties of β-function and Γ-function are employed

$$\Gamma(m) = (m-1)!, \quad \Gamma(m+\frac{1}{2}) = 1 \cdot 3 \ldots (2m-1)\sqrt{\pi}/2^m,$$

$$\beta(x, y) = \Gamma(x)\Gamma(y)/\Gamma(x+y).$$

Then, (B.1) gives

$$\text{(B.3)} \quad \chi = \int_{\lambda f}^{\lambda} \left[2P^{(n-1)/2} + F_m\right] dt \Big/ \int_{\lambda f}^{\lambda} \left[2P^{(n-1)/2} + G_m\right] t^{-2} \lambda f \, dt,$$

where

$$F_m = \sum_{m=1}^{\infty} \left[\frac{(4m-1-n)!!}{(4m)!!} - \frac{(4m-3-n)!!}{(4m-2)!!} \frac{P}{2} t^{-2}\right] \frac{2(2m-1)!!}{(2m)!!} (2t)^{2m} P^{-(1-n+4m)/2},$$

(B.4)

$$G_m = \sum_{m=1}^{\infty} \left[\frac{(4m-1-n)!!}{(4m)!!} - \frac{(4m-3-n)!!}{(4m-2)!!} \frac{P}{2}\right] \frac{2(2m-1)!!}{(2m)!!} (2t)^{2m} P^{-(1-n+4m)/2}.$$

F_{0m} and G_{0m} can be obtained by

$$F_{0m} = F_m \mid_{n=0} \qquad \text{and} \qquad G_{0m} = G_m \mid_{n=0}.$$

In the numerical computation, let us take m = 5. For the infinite matrix material, the following recurrence formulae are considered:

$$\int_0^{\lambda} t^{2m}(1+t^2)^{-(1+4m)/2} \, dt = \frac{1}{4m-1} \lambda^{2m+1}(1+\lambda^2)^{(1-4m)/2} + \frac{2m-2}{4m-1} \int_0^{\lambda} t^{2m}(1+t^2)^{(1-4m)/2} \, dt,$$

(B.5)

$$\int_0^{\lambda} t^{2m}(1+t^2)^{(1-4m)/2} \, dt = \frac{-1}{2m-2} \lambda^{2m-1}(1+\lambda^2)^{(3-4m)/2} + \frac{2m-1}{2m-2} \int_0^{\lambda} t^{2m-2}(1+t^2)^{(1-4m)/2} \, dt.$$

For large void growth rate λ (corresponding to high triaxiality) and $m > 1$, (B.5) becomes

$$\int_0^\lambda t^{2m}(1+t^2)^{-(1+4m)/2}\,dt = \frac{2m-2}{4m-1}\int_0^\lambda t^{2m}(1+t^2)^{(1-4m)/2}\,dt,$$

(B.6)

$$\int_0^\lambda t^{2m}(1+t^2)^{(1-4m)/2}\,dt = \frac{2m-1}{2m-2}\int_0^\lambda t^{2m-2}(1+t^2)^{(1-4m)/2}\,dt.$$

Using these results and performing some lengthy manipulations, the following result can be obtained for $n = 0$:

$$\text{(B.7)}\quad \int_0^\lambda F_{0m}\,dt = \int_0^\lambda \left(\frac{1}{2}P^{-3/2} - \frac{3}{2}P^{-5/2}\right)dt + \sum_{m=2}^{\infty}\left\{\left[\frac{4m-1)!!}{(4m)!!}\frac{2m-1}{4m-1} - \frac{(4m-3)!!}{2(4m-2)!!}\right]\right.$$

$$\left.\times\frac{(2m-1)!!}{(2m)!!}2^{2m+1}\prod_{J=3}^{k}\left(\frac{2m-2J+3}{2m+2J-6}\right)\int_0^\lambda\left[P^{(3-4m)/2} - P^{(1-4m)/2}\right]dt\right\}.$$

Then, for large λ,

$$\int_0^\lambda P^{(-3)/2}dt = 1,$$

$$\text{(B.8)}\quad \int_0^\lambda P^{(3-4m)/2}\,dt = \sum_{I=0}^{2m-2}\frac{(-1)^I(2m-3)!}{I!(2m-I-3)!}\frac{1}{(2I+1)},$$

$$\int_0^\lambda P^{(1-4m)/2}\,dt = \sum_{I=0}^{2m-2}\frac{(-1)^I(2m-2)!}{I!(2m-I-1)!}\frac{1}{(2I+1)}.$$

The computed results of (B.7) are listed below for $m = 8$

$m = 1$	Eq. (B.7) $= -0.50$,	$m = 5$	Eq. (B.7) $= -0.60$,
2	-0.56,	6	-0.60,
3	-0.58,	7	-0.61,
4	-0.59,	8	-0.61.

When $n \neq 0$, similar results can be obtained. Thus for the infinite matrix material, the expression (3.14) can be derived from Eq. (B.3) with the limitation (3.13). For $n = 0$, Eq. (3.14) gives

$$\chi = \int_0^{\lambda} \left[P^{-1/2} + F_{0m}/2 \right] dt. \tag{B.9}$$

For large λ and using the above table, (B.9) becomes

$$\chi = \ln \left[\lambda + \sqrt{(\lambda^2 + 1)} \right] - 0.61/2 \simeq \ln (2\lambda) - 0.305.$$

Thus

$$\lambda = 0.68 \exp (\chi), \tag{B.10}$$

which is identical with Eq. (3.18).

References

1. F.A. McClintock, S. M. Kaplan, C.A. Burg, *Ductile fracture by hole growth in shear bands*, Int. J. Fracture Mech., **2**, 614 – 627, 1966.
2. N.A. Fleck, J. W. Hutchinson, *Void growth in shear*, Proc. Roy. Soc. Lond., A, 407, 435 – 458, 1986.
3. P. Gilormini, C. Licht, P. Suquet, *Growth of void in a ductile matrix: a review*, Arch. Mech., **40**, 43 – 80, 1988.
4. D. M. Tracey, *Strain hardening and interaction on the growth of voids in ductile fracture*, Eng. Fract. Mech., 3, 301 – 316, 1971.
5. A. Needleman, *Void growth in an elastic plastic medium*, J. Appl. Mech., **39**, 964 – 970, 1972.
6. A. L. Gurson, *Continuum theory of ductile rupture by void nucleation and growth. I. Yield criteria and flow rules for porous ductile media*, J. Eng. Mater. Tech., Trans. ASME, **99**, 2 – 15, 1977.
7. A. Needleman, J. R. Rice, [in:] Mechanics of Sheet Metal Forming, [Ed.] Koistinen and Wang, 237 – 265, Plenum Publ. Co., 1978.
8. V. Tvergaard *Influence of voids on shear band instability under plane strain conditions*, Int. J. Fract., **17**, 389 – 407, 1981.
9. J. Koplik, A. Needleman, *Void growth and coalescence in porous plastic solids*, Int. J. Solids Struct., **24**, 835 – 853, 1988.
10. M. E. Mear, *On the plastic yielding of porous metals*, Mech. Mater., **9**, 33 – 48, 1990.
11. J. M. Duva, *A constitutive description of nonlinear materials containing void*, Mech. Mater., 5, 137 – 144, 1986.
12. C. Licht, P. Suquet, *Growth of cylindrical voids in nonlinear viscous material at arbitrary void volume fractions: a simple model*, Arch. Mech., **40**, 741 – 757, 1988.
13. M. J. Worswick, R. J. Pick, *Void growth and constitutive softening in a periodically voided solid*, J. Mech. Phys. Solids, **38**, 601 – 625, 1990.

14. K.L. PAN, Z. P. HUANG, *A cylindrical void growth model in viscoplastic materials*, Int. J. of Damage Mech., **3**, 1994.
15. R. HILL, *The essential structure of constitutive laws for metal composites and polycrystals*, J. Mech. Phys. Solids, **15**, 79 – 95, 1967.

DEPARTMENT OF ENGINEERING MECHANICS
TONGJI UNIVERSITY, SHANGHAI, P.R. CHINA.

Received June 20, 1993.

Arch. Mech., 45, 5, pp. 527-535, Warszawa 1993

Singular solutions to a Hamilton–Jacobi equation

B. KAŹMIERCZAK (WARSZAWA)

SOLUTIONS of a certain Hamilton – Jacobi equation in two dimensions are analyzed locally. This equation arises in asymptotic theory of laser-sustained plasma. The main tool of the analysis is the implicit function theorem.

1. Introduction

REACTION-DIFFUSION equations (see e.g. [1, 2]) are widely used in biology, medicine, chemistry, nuclear reactor theory, physics etc. For example, energy phenomena in stationary plasma sustained by laser radiation may be well described by a single reaction-diffusion equation of the following kind:

$$\varepsilon^2 \Delta u + f(\underline{\mathbf{x}}, u) = \varepsilon \mathbf{v} \nabla u, \qquad \underline{\mathbf{x}} \in \Omega \subset \mathbb{R}^3. \tag{1.1}$$

Here T is plasma temperature, $\mathbf{v}$ its scaled convectional velocity, $\underline{\mathbf{x}}$ – spatial variable, f is a reaction term responsible for energy balance in plasma – its absorption from the laser beam and its losses through radiation; ε^2 is a dimensionless parameter being a mean ratio of scaled heat conduction coefficient and the reaction term (see [3, 4]).

It is assumed that for every $\underline{\mathbf{x}}$ the equation $f(\underline{\mathbf{x}}, T) = 0$ has two solutions: $T_L(\underline{\mathbf{x}})$ and $T_h(\underline{\mathbf{x}})$ which are stable, i.e. $f_T(\underline{\mathbf{x}}, T_L(\underline{\mathbf{x}})) < 0, f_T(\underline{\mathbf{x}}, T_h(\underline{\mathbf{x}})) < 0$. These two solutions obviously correspond to low temperature gas and (partially ionized) plasma of relatively high temperature ($1.5 \cdot 10^4$ K). In most experiments ε is small. Thus it is interesting to see what happens when $\varepsilon \to 0$. It is proved in [5] that, in this limit, asymptotic solutions can be constructed by "gluing up" local equilibrium states $T_L(\underline{\mathbf{x}})$ and $T_h(\underline{\mathbf{x}})$ with the help of transition layers. To be more precise, let $\underline{\mathbf{x}}$ in $f(\underline{\mathbf{x}}, T)$ be fixed for a moment, that means $\underline{\mathbf{x}} = X$. Then, let us assume the solution in the form

$$u = \phi(\mathbf{n}(X) \cdot \mathbf{y}),$$

where

$$\mathbf{y} := \varepsilon^{-1}(\underline{\mathbf{x}} - X), \qquad (\mathbf{n}(X))^2 = 1.$$

This leads to the following family of ordinary differential equations depending on the parameter (!) X:

$$\phi'' + f(X, \phi) = \phi'(\mathbf{v} \cdot \mathbf{n})(X), \tag{1.2}$$

where $' := d/d\xi$ and $\xi := \mathbf{n} \cdot \mathbf{y}$. We demand that

$$\phi(-\infty, X) = T_L(X), \qquad \phi(\infty, X) = T_h(X), \qquad \phi(0, X) = \frac{1}{2}(T_L(X) + T_h(X))$$

and that

$$\phi'(-\infty, X) = \phi'(\infty, X) = 0.$$

It is known (see e.g. [1]) that due to the assumptions made for any $X \in \mathbb{R}^3$ there could be only one value $(\mathbf{v} \cdot \mathbf{n})(X)$ such that the solution to Eq. (1.2) exists. Thus we obtain a well defined relation

$$\mathbf{v}(X) \cdot \mathbf{n}(X) - F(X) = 0, \tag{1.3}$$

where F is known. It is shown in [5] that, if we have a hypersurface $\Omega(x) = 0$, such that $\mathbf{n}(X)$ being a properly defined normal to it satisfies Eq. (1.3), then by appropriate sewing of the equilibrium states $T_L(\underline{\mathbf{x}})$, $T_h(\underline{\mathbf{x}})$ and the transition layers $\phi(\cdot, X)$ (where $\Omega(X) = 0$), we can construct asymptotic solution to Eq. (1.1). (Moreover, by the method of sub- and supersolutions these functions can be used to prove the existence of real solution to Eq. (1.1) for $\varepsilon > 0$). Finally, let us note that in the $\underline{\mathbf{x}}$-units the width of the transition layers is of the order $0(\varepsilon)$, and so it vanishes as $\varepsilon \to 0$. Thus in the limit the asymptotic solution is completely characterized by the hypersurface $\Omega(X) = 0$.

2. Setting of the problem and main assumptions

Thus tha main difficulty consists in finding adequate hypersurfaces satisfying the relation (1.3) which, as a matter of fact, is a kind of Hamilton – Jacobi equation. In a special axially symmetric case the problem becomes effectively two-dimensional. Thus in this case we have to find closed curves $\chi:[0, 1] \to \mathbb{R}^2$ satisfying the relation

$$H(\mathbf{n}(s), \underline{\mathbf{x}}(s)) := \mathbf{v}(\underline{\mathbf{x}}(s)) \cdot \mathbf{n}(\underline{\mathbf{x}}(s)) - F(\underline{\mathbf{x}}(s)) = 0, \tag{2.1}$$

where $\mathbf{n}(s)$ is a unit vector normal to the curve χ at a point $\underline{\mathbf{x}}$ (cf. [5]). Now, suppose that $\mathbf{v} \neq 0$ at some point $\underline{\mathbf{x}} = \mathbf{x}_0$. Let us introduce a Cartesian system of coordinates (x, y) with the point $(0, 0)$ at $\mathbf{x}_0$ and with its y-axis antiparallel to $\mathbf{v}(\mathbf{x}_0)$. Suppose that in these coordinates a curve satisfying Eq. (2.1) and passing through $\mathbf{x}_0$ can be described by a smooth function $y(x)$, i. e. it is a set of points $(x, y(x))$. If $z: y_{,x}$ and $\mathbf{n}(\mathbf{x}) = [z, -1](1 + z^2)^{-1/2}$, then from Eq. (2.1) we obtain the relation

$$y_{,x} = (v_1^2 - F^2)^{-1}(v_1 v_2 \pm F\sqrt{v^2 - F^2}). \tag{2.2}$$

Two things are obvious. First, in the region, where $v^2 < F^2$, there are no real solutions for any of these equations, whereas in the region, where $v^2 < F^2$ through every point passes (locally) exactly one C^1-solution curve for Eq. $(2.2)_1$ and exactly one for Eq. $(2.2)_2$. The question arises, what happens to these trajectories when we are approaching a point where $v^2 = F^2$. If it fulfils certain additional assumption, then it is

called critical. It is suggested in [5], that the construction of the curves should be started at such a point.

DEFINITION (cf. [5]). *Let* $\mathscr{R}$ be an open connected component of the set of points at which $|\mathbf{v}| < F$. *Let* $\mathscr{G}$ *denote its boundary. A point* $\mathbf{x}_0 \in \mathscr{G}$ *is called critical, if* $\mathscr{G}$ *is* C^2 *at* $\mathbf{x}_0$ *and* $\mathbf{v}(\mathbf{x}_0) \neq 0$ *is perpendicular to* $\mathscr{G}$. ■

Let $\mathscr{E}$ *denote the line through* $\mathbf{x}_0$ *perpendicular to the vector field* $\mathbf{v}$.

The objective of this paper is to analyze the trajectories of (2.2) starting from a critical point $\mathbf{x}_0$. Near this point Eqs. (2.2) may be written as

$$(2.3)_1 \qquad y' = (\underline{v}_1^2 - \underline{F}^2)^{-1}(\underline{v}_1\underline{v}_2 + \underline{F}\sqrt{1 - \underline{F}^2}),$$

$$(2.3)_2 \qquad y' = (\underline{v}_1^2 - \underline{F}^2)^{-1}(\underline{v}_1\underline{v}_2 - \underline{F}\sqrt{1 - \underline{F}^2}),$$

where

$$' := (\ )_{,x}, \qquad \underline{\mathbf{v}}(\mathbf{x}) := \mathbf{v}(\mathbf{x})\ |\mathbf{v}(\mathbf{x})|^{-1} \quad \text{and} \quad \underline{F}(\mathbf{x}) := F(\mathbf{x})\ |\mathbf{v}(\mathbf{x})|^{-1}.$$

Thus $\underline{\mathbf{v}}$ is normed to 1 near x_0 and $\underline{F}$ is normed to 1 at $\mathbf{x}_0$.

ASSUMPTION. Let us assume:

1. Near $\mathbf{x}_0$ the line $\mathscr{E}$ lies outside the region $\mathscr{R}$.
2. $\underline{\mathbf{v}}$ and $\underline{F}$ are smooth, $\underline{F}$ has nonvanishing gradient and $\underline{F}_{,xx}(\mathbf{x}_0) \neq 0$. ■

Below, for the sake of simplicity, we will omit the bars in $\underline{\mathbf{v}}$ *and* $\underline{F}$.

3. Main result

The main result of the paper is comprised in the following

THEOREM. *Suppose that Assumption is true. Then there exists exactly one* C^1*-trajectory passing through* (0, 0) *satisfying Eq.* $(2.3)_1$, *and exactly one satisfying Eq.* $(2.3)_2$. *For* $|x| \to 0$ *these trajectories form two parabolas, one of them lying above and the other lying below.* ■

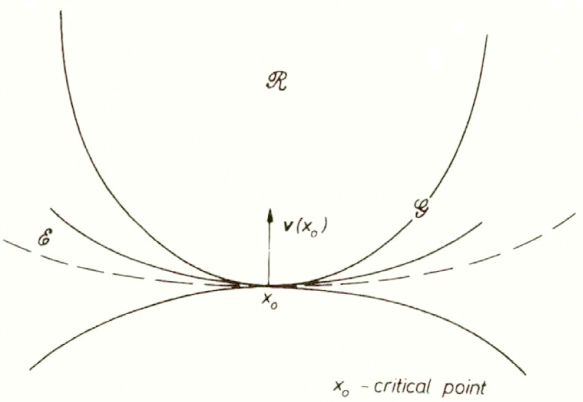

FIG. 1.

This theorem is visualized in Fig. 1.

4. Proof of the Theorem

The plan of the proof is the following. First, we will find solutions to appropriate equations with constant coefficients. Then, by means of the implicit function theorem, we will prove local existence of solutions to the "full" equations. Finally we will show uniqueness for the constant coefficient case.

4.1. Constant coefficient case

First, we will find solutions to constant coefficient equations. Then, by using the implicit function theorem in appropriate Banach spaces, we will obtain all smooth solutions of Eqs. $(2.3)_{1,2}$. So, we start from the equations:

$$y' = v_{l,x}(\mathbf{x}_0)\,x \pm \sqrt{-2F_{,y}(\mathbf{x}_0)y - 2F_{,xx}(\mathbf{x}_0)\,x^2}, \qquad y(0) = 0.$$

By the linear change of variables: $\Psi = ay$, $\bar{x} = sx$, these equations may be replaced by the following ones:

$$\Psi' = \{Ca\bar{x}s^{-2} \pm \sqrt{\Psi aDs^{-2} + a^2 s^{-4} E\bar{x}^2}\},$$

with the obvious meaning of the constants C, D and E. Let us demand $s^{-2}\,aD = 1$. Then the coefficient of $\bar{x}$ is equal to $\mu = CD^{-1}$ and the coefficient of $\bar{x}^2$ (under the square root) is equal to $b = ED^{-2}$. Thus b and μ do not depend on the above scaling. As a consequence we arrive at the problem:

$$\Psi' = \mu\bar{x} \pm \sqrt{\Psi + b\bar{x}^2}, \qquad \Psi(0) = 0.$$

Let

$$\bar{y} = \Psi - 2^{-1}\mu\bar{x}^2.$$

Then, if

$$B := D^{-1}(ED^{-1} + C),$$

we obtain the problem:

$$\begin{aligned} &\bar{y}' = \sqrt{\bar{y} + B\bar{x}^2}, && \bar{y}(0) = 0, \\ &\bar{y}' = -\sqrt{\bar{y} + B\bar{x}^2}, && \bar{y}(0) = 0. \end{aligned} \tag{4.1}$$

Near x_0 the points on $\mathscr{E}$ fulfil the equation $y = 2^{-1}C_{\mathscr{E}}(x)\,x^2$ with $C_{\mathscr{E}}(x) \underset{x\to 0}{\longrightarrow} -C$ and $\mathscr{G}$ is given by the equation $y = -ED^{-1}\,C_{\mathscr{G}}(x)\,x^2$ with $C_{\mathscr{G}}(x) \underset{x\to 0}{\longrightarrow} 1$. Thus, from the Assumption we infer that $B > 0$.

Below in this proof, for simplicity, we will write x and y instead of $\bar{x}$ and $\bar{y}$.

Let us make the ansatz: $y = kx^2$. Then, k has to fulfil the equation $4k^2 = k + B$, i. e. $k_\pm = 8^{-1}\{1 \pm \sqrt{1 + 16B}\}$. Equations (4.1) have, respectively, the following solutions:

$$y_+(x) = \begin{cases} k_+ x^2, & x > 0, \\ k_- x^2, & x < 0, \end{cases}$$

and

$$y_-(x) = \begin{cases} k_- x^2, & x > 0, \\ k_+ x^2, & x < 0, \end{cases}$$

4.2. Use of the implicit function theorem

Now, Eqs. (2.3) may be written in the following equivalent form:

$$y' - P_1(x, y) \pm (1 + P_2(x, y))\sqrt{y + Bx^2 + dxy + ey^2 + cwr(x^2, y^2, xy)} = 0,$$

(4.2)

$$y(0) = 0,$$

where

$$P_1(x, y) = fy + cwr(x, y), \qquad P_2(x, y) = gx + hy + cwr(x, y), \qquad d, e, f, g, h \in \mathbb{R}^1,$$

P_1 and P_2 are smooth and $cwr(x, y)$ ($cwr(x^2, y^2, xy)$) denotes expressions of the order less than x or y (x^2, y^2 or xy, respectively). Let us remind that the term μx has been just taken into account while writing Eqs. $(4.1)_{1,2}$.

LEMMA. If $y \in C^1$ $(0, a)$, $|a| > 0$, is a solution to the problem (2.3), then $y(x) = O(x^2)$ for $x \to 0$.

P r o o f . Assume by contradiction that the lemma is false. Then, for $|x| > 0$ sufficiently small, the function y has a constant sign; to be precise it is not equal to 0. For, if it were not so, then considering the equation in the sequence $\{x_n\}$ of extremum points, we would conclude that $y(x_n) = O(x_n^2)$. Dividing Eq. (2.3) by $\beta(x) := \sqrt{|y(x)|}$ and integrating over $(0, x)$ ($|x|$ sufficiently small) we obtain the relation

$$\beta(x) = |x| \beta(\xi)(f + o(1)) + |x| (1 + O(1))\sqrt{1 + o(1)}, \qquad \xi \in (0, x).$$

Consequently, it would be $y(x) = O(x^2)$ in contradiction with the supposition. This proves the lemma. ■

According to Lemma for each of the intervals $(0, m)$ and $(-m, 0)$ ($|m|$ sufficiently small) it makes sense to substitute $y(x, m) = x^2 \Phi(x, m)$. First, let us consider the case of positive x and perturbations of $y = k_+ x^2$. For fixed $m > 0$ Eq. (2.3) is equivalent to the equation

$$(x^2 \Phi(x))' = mxS_1(x, y) + x(1 + mS_2(x, y))\sqrt{\Phi(x) + B + mS_3(x, y)},$$

where $C^0([0, m]^2)$ norm of S_i remains finite as $m \to 0$. This equation can be considered as an equation of the type $K(\lambda, \Phi) = 0$, where

$$K:(\lambda, \Phi) \to \Phi - x^{-2} \int_0^x \{\lambda S_1(\Phi) + \sqrt{\Phi + B + \lambda S_3(\Phi)}\,(1 + \lambda S_2(\Phi)\}\, s\, ds. \tag{4.3}$$

Let $K:(\mathbb{R}^1, \mathbb{Q}) \to \mathbb{Q}$, where $\mathbb{Q} = C^0([0, m])$. Then, in some open neighbourhood of $(0, \Phi = k_+)$ this mapping is continuously Frechet differentiable with respect to Φ. We have

$$D_\Phi K(0, k_+):\delta\Phi \to \delta\Phi - x^{-2} \int_0^x (4(k_+ + B))^{-\frac{1}{2}}\, \delta\Phi(s) s\, ds.$$

For $B > 0$ (even for $B > -16^{-1}$), using the contraction principle we conclude that the equation $D_\Phi(0, k_+)\delta\Phi = j \in \mathbb{Q}$ has a unique solution $\delta\Phi \in \mathbb{Q}$. We just analyze the following mapping

$$\delta\Phi \to x^{-2} \int_0^x (4(k + B))^{-\frac{1}{2}}\, \delta\Phi(s)\, s\, ds + j.$$

Then, by means of the implicit function theorem we infer that for $|\lambda|$ sufficiently small, the equation $K(\lambda, \Phi) = 0$ has a unique C^0 solution. Identifying λ with m we conclude that for sufficiently small $m > 0$ Eq. $(2.3)_1$ has a unique C^1 solution, which is near to $k_+ x^2$ in $C^0([0, m])$.

REMARK. It is interesting that $|\Phi'(x)|$ is also bounded. Getting rid of m we can write square root in Eq. (4.3) as

$$s\,(\sqrt{\Phi + B} + mS_4(s, y)) = s(\sqrt{\Phi + B} + sP_4(s, y)),$$

where P_4 is bounded in C^0. Differentiating the equation $K\Phi = 0$ we infer that $|\Phi'(x)| < C < \infty$ for all $x \in [0, m]$, due to the fact that singular terms of the order x^{-1} cancel.

Now, we consider the perturbations of $y = k_- x^2$ (still for $x > 0$). Thus, let

$$\mathbf{G}(m) := \{y \in C^1([0, m]): \sup_{x \in (0, m)} (|y(x)x^{-2}| + |y'(x)x^{-1}|) < \infty\},$$

$$\mathbf{P}(m) := \{y \in C^0([0, m]): \sup_{x \in (0, m)} (|f(x)x^{-1}|) < \infty\}.$$

G and **P** become Banach spaces, if

$$\| y \|_{\mathbf{G}(m)} = \sup_{x \in (0,\, m)} \{ | y(x) x^{-2} | + | y'(x) x^{-1} | \}$$

and

$$\| f \|_{\mathbf{P}(m)} = \sup_{x \in (0,\, m)} \{ | f(x) x^{-1} | \}.$$

This time let

$$K(\lambda, y) y' + \lambda x S_1(x, y) + (1 + \lambda S_2(x, y)) \sqrt{y + Bx^2 + \lambda S_3(x, y)}.$$

K is continously Frechet differentiable mapping from $\mathbf{G}(m)$ to $\mathbf{P}$ in a certain open neighbourhood of $y = k_- x^2$. If $D_y K$ denotes its Frechet derivative at this point, then the equation $(D_y K) y = f, f \in \mathbf{P}$, is of the following form:

$$y' + \alpha y x^{-1} = f, \tag{4.4}$$

where $\alpha = (4(k_- + B))^{-\frac{1}{2}} > 0$. For $f = 0$ Eq. (4.4) has no solutions in $\mathbf{G}(m)$, as it is fulfilled only by the family of functions $y = \tau x^{-\alpha}$, $\tau \in \mathbb{R}^1$. For $f \in \mathbf{P}$, Eq. (4.4) has a uniquely determined solution given by the expression

$$y(x) = (x^{-\alpha}) \int_0^x (s^{\alpha}) f(s)\, ds.$$

Thus, according to the implicit function theorm, for all sufficiently small $| \lambda |$ there exists precisely one $y(\lambda, x) \in \mathbf{G}(\lambda)$ satisfying the equation $Ky = 0$ such that $y(0, x) = k_- x^2$.

Identifying λ with m we conclude that for all sufficiently small $m > 0$ Eq. $(2.3)_2$ has precisely one solution in $\mathbf{G}(m)$, which is near to $k_- x^2$. In the same way we analyze the case $x < 0$. The solution of Eq. (4.4) reads then

$$y(x) = (-x^{-\alpha}) \int_0^x (-s^{\alpha}) f(s)\, ds.$$

The last assertion of the Theorem is obtained by returning to the initial coordinates.

4.3. Uniqueness

To complete the proof of the Theorem we will prove that for $B \geqslant 0$ the functions $k_+ x^2$ and $k_- x^2$ are the unique solutions of Eqs. $(4.1)_1$ and $(4.1)_2$.

For $y \in C^1$ satisfying Eq. $(4.1)_1$ or Eq. $(4.1)_2$ let us denote

$$h(x) = \pm x(\sqrt{y(x) + Bx^2})^{-1}. \tag{4.5}$$

In both cases we obtain the equation

$$h' = x^{-1}h(-Bh^2 - 2^{-1}h + 1). \tag{4.6}$$

It is easy to note that the roots of the equation $(-Bh^2 - 2^{-1}h + 1 = 0)$ and the roots of the equation $(4k^2 - k - B = 0)$ are connected by the following relation: $h_i = (2k_i)^{-1}$, $i = 1, 2$. On the other hand, if we put $y = x^2\Phi(x)$ (cf. Lemma), then for $|x|$ sufficiently small the relation

$$x^2\Phi(x) = \pm \int_0^x s\sqrt{\Phi(s) + B}\, ds$$

implies that $\Phi(x) = \pm 2^{-1}\sqrt{(\Phi(\xi) + B)}$, for a certain $\xi \in (\min(x, 0), \max(x, 0))$. Hence for $x \to 0$, $\Phi(0) + B = 4\Phi^2(0)$ and consequently for $B \in (-16^{-1}, \infty)$ we have

$$0 < |h(0)| < \infty. \tag{4.7}$$

For $B = 0$ the equations may be solved explicitly, so it is easy to verify the assertion. So, let $B > 0$. Due to the obvious change of variables we may assume, according to Eqs. (4.5) and (4.6) that $x > 0$. Then $h' = x^{-1}(E(h))$, where

$$E(h) = \begin{cases} > 0 & \text{for} \quad h \in (-\infty, h_1) \cup (0, h_2), \\ < 0 & \text{for} \quad h \in (h_1, 0) \cup (h_2, \infty). \end{cases}$$

Suppose that for certain $\eta > 0$: $h(\eta) > h_2$. Now, if we move from η toward 0, then $h(x)$ increases to ∞ (at least logarithmically). Similarly, let $h(\xi) < h_1$ for certain $\xi > 0$. If we move from ξ toward 0, then $h(x)$ decreases to $-\infty$ (at least logarithmically). Analogously, if $h(\xi) \in (0, h_2)$, then $h(x)$ would decrease for $x \to 0$. But then we would have $h(0) = 0$, which is impossible due to Eq. (4.7). Similarly $h(x) \to 0$ for $x \to 0$, if $h(\xi) \in (h_1, 0)$, which is impossible. Thus the only solutions from $C^1((0, X))$, $X > 0$, are $k_+ x^2$, and $k_- x^2$. Thus, the proof of the Theorem is completed.

Acknowledgements

The author expresses his gratitude to Prof. Z. PERADZYŃSKI for pointing out the problem and many helpful suggestions.

This work was supported by the grant KBN No. PB 20480-90-1.

References

1. P. FIFE, *Mathematical aspects of reacting and diffusing system*, Lect. Notes in Biomathem., 28, Springer, 1979.
2. J. SMOLLER, *Shock waves and reaction-diffusion systems*, Springer-Verlag, 1983.
3. W. ECKHAUS, A. HARTEN and Z. PERADZYŃSKI, *Plasma produced by a laser in a medium with convection and free surface satisfying a Hamilton—Jacobi equation*, Physica, **27D**, 90—112, 1987.
4. W. ECKHAUS, A. HARTEN and Z. PERADZYŃSKI, *A singularly perturbed free boundary problem describing a laser sustained plasma*, SIAM J. Appl. Math., **45**, 1, 1985.
5. Z. PERADZYŃSKI, *On propagation of the transition layers in solutions to nonlinear partial differential equations* [in]: Lecture Notes in Physics, 249, Springer, 1985.

POLISH ACADEMY OF SCIENCES
INSTITUTE OF FUNDAMENTAL TECHNOLOGICAL RESEARCH.

Received June 18, 1993.

Arch. Mech., 45, 5, pp. 537-562, Warszawa 1993

Random walk with finite speed as a model of pollution transport in turbulent atmosphere

Z. KOTULSKI (WARSZAWA)

IN THE PAPER we apply the model of random walk with finite speed to the description of the pollution transport in the atmosphere. We consider one, two and three-dimensional models. We obtain the systems of equations for the conditional probability distribution functions of particle's locations in space and time. They are convenient to describe the evolution of the probability distribution of the range of the pollutant emitted from the source, its distribution over the earth surface and its spatial distribution. The sedimentation (absorption of the particles on earth's surface) is taken into account in the models.

1. Introduction

THE PROBLEM of the pollution transport and its modeling is, at present, one of the most important tasks of the physics of atmosphere. This phenomenon is a very complicated physical process, depending on a number of factors, not always comletely identified [8]. These factors can be of very different nature. First of all, the final distribution of the pollutant depends of the kind of its source (temporal or permanent, concentrated or distributed, more or less intensive). Secondly, the properties of the motion of air transporting the pollutant particles (both large-scale, laminar and local, turbulent) have a strong effect on their concentration in space and time. Also physical and chemical properties of the pollutant particles, such as their possible coagulation, absorption by vapors or rains, sedimentation facility or chemical reactions, can affect the transport process. Finally, the properties of the earth surface have an influence on the sedimentation of the particles and should be taken into accaunt. Studying the transport process in turbulent atmosphere we must realize all these facts, in spite of our limited abilities of including them into the mathematical models.

Considering the process of the pollution transport in the atmosphere, we are interested in obtaining some equations describing the mass transfer on a large scale. However, to obtain such global equations we must start the considerations from the small-scale behavior of the particles. Unfortunately, we are not able to take into account all really existing physical phenomena that take place in interparticle influences. Therefore we must treat the problem in a statistical way, assuming certain reactions of particles with some probability and, eventually, identifying particular probabilities in the model and comparing the resulting equations of the mass transfer with experimental results.

The description of the neutral particle flowing through and interacting with some environmental materials needs, at any time t, the knowledge of sixvariables: three position variables and three momentum variables. In the statistical model we should know the probability distributions of these variables (see [7]). Sometimes it is more convenient to replace the momentum variable with three equivalent variables: kinetic energy of the particle and two angular variables specifying the velocity direction vector. Such a description implicitly permits the particles to have different masses and velocities and freely change the travel direction.

One of the possible small-scale methods of description of particle motion is a random-walk concept (see [9]). In the literature many different random-walk models have been proposed to describe the dispersion of particles in inhomogeneous or unsteady turbulence. In most of them it is assumed that the flowing particles have equal masses. Moreover, some restrictive conditions on their possible velocities and the movement directions are assumed. For such simplified models the position variables are sufficient to describe the transport process.

Among the proposed random walk models there are more or less suitable ones to describe the process of transport of the pollutant particles. Selecting one of them we need some a priori criteria to distinguish good models from the bad ones.

Several authors apply such criteria to verify their models of random walk. These quality measures are often very intuitive and sound quite different, but in mathematical formulation they give the same results (cf. [10]). Choosing the random walk model we postulate its good large-scale and small-scale behavior. In the large scale we require the well-mixing condition; that is, if the particles are initially well mixed, they will remain well-mixed during the diffusion process. In small scale, we postulate that random walk should reduce to a diffusion-equation model as the Lagrangian time scale tends to zero.

In many problems the diffusion equation is sufficient to describe the polution transport process (e.g. the global mass transport or large-scale changes of the pollutant concentration – see e.g. [5, 6]). However, in some problems we must know the instant of time at which the pollutant reaches a certain area; in such a case the widely used diffusion equation is not sufficient – one needs models where the velocity of particles is taken into account. The random walk processes make it possible to consider also this parameter in the global transport equation.

Let us remark that, in modeling of the real physical phenomena, the final correctness criterion is the compliance of the results deduced from the mathematical model with experimental observations.

Modeling the process of pollution transport we know that it takes place in a three-dimensional physical space. Nevertheless, we often use one- or two-dimensional models to describe such a phenomenon. Applied to real transport process, such simplified models need some interpretation: the one-dimensional model can describe a distance of the pollutant particle from the source, and the two-dimensional model – the distribution of the particles around the source. Only three-dimensional models can give real traces of the particles and their actual location in space.

In this paper we consider all these models: one, two and three-dimensional. All of them are based on the model of random walk process proposed by G. I. Taylor and S. Goldstein where the possibility of sedimentation of the particle (its death) has been included. Identifying the probabilities of jumps in any direction or imprisoning the particle at a given point, we can describe the transport process by means of the models proposed.

2. The model of one-dimensional random walk with finite speed

Our considerations are a generalization of the one-dimensional model of random walk proposed by G. I. Taylor and S. Goldstein and presented in a transparent way in KAC'S lecture notes [2]. In this section we introduce the problem following their reasoning.

Assume that we have one particle moving to the left and to the right along a straight line. It starts at time $t = 0$ and goes from point $x = 0$ in a fixed direction. In time Δt it covers the distance Δx,

$$\Delta x = v\Delta t, \tag{2.1}$$

where parameter v plays the role of finite velocity of the particle. After the jump, the particle changes its direction to the opposite one with probability $a\Delta t$ or continues its motion in the same direction with probability $1 - a\Delta t$. The location on the line, of the particle starting from 0, after n steps (that is after the time $n\Delta t$), is S_n.

To describe this model mathematically we must introduce a specific notation. Let $\varphi(x)$ be an arbitrary function. We are interested in the evolution of the function $<\varphi(x + S_n)>$ in time (symbol $<\cdot>$ denotes the mathematical expectation of a random variable).

Define the random variable ε in the following way:

$$\varepsilon = \begin{cases} 1 \text{ with probability } & 1 - a\Delta t, \\ -1 \text{ with probability } & a\Delta t. \end{cases} \tag{2.2}$$

Consider the following sequence of independent random variables with identical distributions, defined above:

$$\varepsilon_1, \varepsilon_2, \varepsilon_3, \ldots, \varepsilon_{n-1}. \tag{2.3}$$

Assume that the particle starts from point x in the positive direction. Then the change of location of the particle after n steps is

$$S_n^+ = v\Delta t(1 + \varepsilon_1 + \varepsilon_2\varepsilon_1 + \ldots + \varepsilon_{n-1}\varepsilon_{n-2}, \ldots, \varepsilon_2\varepsilon_1). \tag{2.4}$$

If the particle starts in negative direction, the analogous variable is

$$S_n^- = -v\Delta t(1 + \varepsilon_1 + \varepsilon_2\varepsilon_1 + \ldots + \varepsilon_{n-1}\varepsilon_{n-2}, \ldots, \varepsilon_2\varepsilon_1) = -S_n^+. \tag{2.5}$$

We investigate two following functions:

(2.6) $$F_n^+(x) = <\varphi(x + S_n^+>$$

and

(2.7) $$F_n^-(x) = <\varphi(x - S_n^+)>.$$

Writing explicitly, $F_n^+(x)$ is

(2.8) $$F_n^+(x) = <\varphi(x + v\Delta t(1 + \varepsilon_1 + \varepsilon_2\varepsilon_1 + \ldots + \varepsilon_{n-1}\varepsilon_{n-2}, \ldots, \varepsilon_2\varepsilon_1))>$$

or

(2.9) $$F_n^+(x) = <\varphi(x + v\Delta t + v\Delta t(1 + \varepsilon_2 + \ldots + \varepsilon_{n-1}\varepsilon_{n-2}, \ldots, \varepsilon_2)\varepsilon_1>.$$

We calculate the conditional expectation of the formula (2.9) with respect to ε_1:

(2.10) $$F_n^+(x) = a\Delta t <\varphi(x + v\Delta t - v\Delta t(1 + \varepsilon_2 + \ldots + \varepsilon_{n-1}\varepsilon_{n-2}, \ldots, \varepsilon_2))> + (1 - a\Delta t) <\varphi(x + v\Delta t + v\Delta t(1 + \varepsilon_2 + \ldots + \varepsilon_{n-1}\varepsilon_{n-2}, \ldots, \varepsilon_2))>,$$

or, in a recurrent way,

(2.11) $$F_n^+(x) = a\Delta t\, F_{n-1}^-(x + v\Delta t) + (1 - a\Delta t) F_{n-1}^+(x + v\Delta t).$$

Making the analogous operation for the particle starting in the negative direction we obtain:

(2.12) $$F_n^-(x) = a\Delta t\, F_{n-1}^+(x - v\Delta t) + (1 - a\Delta t) F_{n-1}^-(x - v\Delta t),$$

what, together with the relationship (2.11), gives the system of difference equations for $F_n^+(x)$ and $F_n^-(x)$.

From Eq. (2.11) we obtain

(2.13) $$\frac{F_n^+(x) - F_{n-1}^+(x)}{\Delta t} = \frac{v(F_{n-1}^+(x + v\Delta t) - F_{n-1}^+(x))}{v\Delta t} + aF_{n-1}^-(x + v\Delta t) - aF_{n-1}^+(x + v\Delta t)$$

and, going to the limit for $n \to \infty$, $\Delta t \to 0$, $t = n\Delta t = \text{const}$, the following differential equation:

(2.14) $$\frac{\partial F^+}{\partial t} = v\frac{\partial F^+}{\partial x} + aF^- - aF^+.$$

Analogously, for F^- we have from Eq. (2.12)

(2.15) $$\frac{F_n^-(x) - F_{n-1}^-(x)}{\Delta t} = \frac{-v(F_{n-1}^-(x + v\Delta t) - F_{n-1}^-(x))}{-v\Delta t} + aF_{n-1}^+(x - v\Delta t) - aF_{n-1}^-(x - v\Delta t)$$

and

(2.16) $$\frac{\partial F^-}{\partial t} = -v\frac{\partial F^-}{\partial x} + aF^+ - aF^-.$$

We introduce new functions F and G, defined by

$$F = \frac{1}{2}(F^+ + F^-), \qquad G = \frac{1}{2}(F^+ - F^-). \tag{2.17}$$

Function F can represent the probability density function that particle at time t is located at point x provided that it started from point $x = 0$ in the positive or the negative directions with the same probability equal to 1/2.

Adding Eqs. (2.14) and (2.16) results in the following equation:

$$\frac{\partial F}{\partial t} = v\frac{\partial G}{\partial x}; \tag{2.18}$$

analogously, subtraction of Eq. (2.14) from Eq. (2.16) gives a supplementary partial differential equation

$$\frac{\partial G}{\partial t} = v\frac{\partial F}{\partial x} - 2aG. \tag{2.19}$$

By eliminating G from Eqs. (2.18) and (2.19) we obtain

$$\frac{1}{v}\frac{\partial^2 F}{\partial t^2} = v\frac{\partial^2 F}{\partial x^2} - \frac{2a}{v}\frac{\partial F}{\partial t} \tag{2.20}$$

– the telegrapher's equation (or, the string equation with damping); this is the equation for the probability density function which describes the distribution of the particles starting from point $x = 0$ at time $t = 0$ in a symmetric way and travelling along the line with the finite speed v changing the direction in the manner defined in Eq. (2.2).

To solve the problem of particles diffusion on the line, we must complete equation (2.20) with the initial conditions

$$F(x, 0) = \varphi(x), \qquad \left[\frac{\partial F}{\partial t}\right]_{t=0} = 0, \tag{2.21}$$

describing the initial location of diffusing particles.

To consider the limiting case in Eq. (2.20), we assume: $a \to \infty$, $v \to \infty$, but $2a/v^2$ remains constant (the particle makes more and more small, quick jumps):

$$\frac{2a}{v^2} = \frac{1}{D}. \tag{2.22}$$

In the limit we obtain the well-known parabolic diffusion equation:

$$\frac{1}{D}\frac{\partial F}{\partial t} = \frac{\partial^2 F}{\partial x^2}. \tag{2.23}$$

This means that the random walk with finite speed defined in this section satisfies one of the required correctness conditions, and the present random walk process can be regarded as a good model of the transport process of pollutant particles.

3. The one-dimensional model of the transport with sedimentation

To make the description of the particles diffusion more realistic, let us assume that after some travel time the particle is absorbed by the environment and stops the diffusion. In the model of random walk this fact can also be taken into account. Let us assume that the particle starts from point $x = 0$, as in the previous section, goes in a fixed direction (to the right or to the left) or remains at that point never leaving it. At time Δt it has covered the distance Δx, where

$$\Delta x = v\Delta t. \tag{3.1}$$

After the jump the particle changes its direction to the opposite one with probability $a\,\Delta t$, sediments at its new location with probability $b\,\Delta t$ or continues the motion in the previous direction with probability $1 - (a + b)\,\Delta t$.

Similarly to the previous section, to describe this model mathematically we introduce the following notation. Let S_n be the location of the particle after n steps (that is after the time $n\Delta t$). Let $\varphi(x)$ be an arbitrary function. We are interested in the evolution of the averaged function φ, $<\varphi(x + S_n)>$. If $\varphi(x)$ is the Dirac delta function, then $<\varphi(x + S_n)>$ represents the probability density function of location of the diffusing particle.

Define the random variable ε in the following way:

$$\varepsilon = \begin{cases} 1 & \text{with probability} \quad 1 - (a + b)\Delta t, \\ -1 & \text{with probability} \quad a\Delta t, \\ 0 & \text{with probability} \quad b\Delta t. \end{cases} \tag{3.2}$$

To describe the walk of the particle let us consider the sequence of independent, identically distributed random variables with the distribution defined in Eq. (3.2),

$$\varepsilon_1, \varepsilon_2, \varepsilon_3, \ldots, \varepsilon_{n-1}. \tag{3.3}$$

Assume that the particle starts from point x in the positive direction. Then the change of location of the particle after n steps is

$$S_n^+ = v\Delta t(1 + \varepsilon_1 + \varepsilon_2\varepsilon_1 + \ldots + \varepsilon_{n-1}\varepsilon_{n-2}, \ldots, \varepsilon_2\varepsilon_1). \tag{3.4}$$

When the particle starts into the negative direction, the analogous variable is

$$S_n^- = -v\Delta t(1 + \varepsilon_1 + \varepsilon_2\varepsilon_1 + \ldots + \varepsilon_{n-1}\varepsilon_{n-2}, \ldots, \varepsilon_2\varepsilon_1) = -S_n^+. \tag{3.5}$$

The last possible solution, the particle remains in the starting point, gives the variable describing its location in the following form:

$$S_n^0 = 0. \tag{3.6}$$

Substituting the three expressions for the location of the particle, we obtain the following versions of $<\varphi(x + S_n)>$:

$$F_n^+(x) = \langle \varphi(x + S_n^+) \rangle, \tag{3.7}$$

$$F_n^-(x) = \langle \varphi(x + S_n^-) \rangle = \langle \varphi(x - S_n^+) \rangle, \tag{3.8}$$

$$F_n^0(x) = \langle \varphi(x + S_n^0) \rangle = \langle \varphi(x) \rangle. \tag{3.9}$$

Explicitly, $F_n^+(x)$ is

$$F_n^+(x) = \langle \varphi(x + v\Delta t(1 + \varepsilon_1 + \varepsilon_2\varepsilon_1 + \ldots + \varepsilon_{n-1}\varepsilon_{n-2}, \ldots, \varepsilon_2\varepsilon_1)) \rangle, \tag{3.10}$$

or

$$F_n^+(x) = \langle \varphi(x + v\Delta t + v\Delta t(1 + \varepsilon_2 + \ldots + \varepsilon_{n-1}\varepsilon_{n-2}, \ldots, \varepsilon_2)\varepsilon_1) \rangle. \tag{3.11}$$

Calculating the conditional expectation of the formula (3.11) for $F_n^+(x)$ with respect to ε_1, we obtain

$$\begin{aligned} F_n^+(x) = a\Delta t \langle \varphi(x + v\Delta t - v\Delta t(1 + \varepsilon_2 + \ldots + \varepsilon_{n-1}\varepsilon_{n-2}, \ldots, \varepsilon_2)) \rangle \\ + (1 - (a+b)\Delta t) \langle \varphi(x + v\Delta t + v\Delta t(1 + \varepsilon_2 + \ldots + \varepsilon_{n-1}\varepsilon_{n-2} \ldots \varepsilon_2)) \rangle \\ + b\Delta t \langle \varphi(x + v\Delta t) \rangle, \end{aligned} \tag{3.12}$$

or, in a recurrent way,

$$\begin{aligned} F_n^+(x) = a\Delta t F_{n-1}^-(x + v\Delta t) + (1 - (a + b)\Delta t) F_{n-1}^+(x + v\Delta t) \\ + b\Delta t F_n^0(x + v\Delta t). \end{aligned} \tag{3.13}$$

Performing this operation for the particle starting in the negative direction we obtain the recurrent equation for $F_n^-(x)$,

$$\begin{aligned} F_n^-(x) = a\Delta t F_{n-1}^+(x - v\Delta t) + (1 - (a + b)\Delta t) F_{n-1}^-(x - v\Delta t) \\ + b\Delta t F_n^0(x - v\Delta t). \end{aligned} \tag{3.14}$$

Analogously, the recurrent equation for the function $F_n^0(x)$ describing the behavior of the sedimented particle is

$$F_n^0(x) = F_{n-1}^0(x). \tag{3.15}$$

These three formulae constitute the system of difference equations and give a complete characteristics of the diffusion process (random walk).

Analogously to the considerations of the previous section, we can consider the continuous version of the equations for $F_n^+(x)$, $F_n^-(x)$ and $F_n^0(x)$ (the conditional probability density functions). From Eq. (3.13) we obtain

$$\begin{aligned} \frac{F_n^+(x) - F_{n-1}^+(x)}{\Delta t} = \frac{v(F_{n-1}^+(x + v\Delta t) - F_{n-1}^+(x))}{v\Delta t} + aF_{n-1}^-(x + v\Delta t) \\ - (a + b)F_{n-1}^+(x + v\Delta t) + bF_n^0(x + v\Delta t). \end{aligned} \tag{3.16}$$

Going to the limit for $n \to \infty$, $\Delta t \to 0$, $t = n\Delta t = \text{const}$, we obtain the following differential equation:

$$\frac{\partial F^+}{\partial t} = v\frac{\partial F^+}{\partial x} + aF^- - (a+b)F^+ + bF^0. \tag{3.17}$$

Repeating the procedure for F^- we obtain from Eq. (3.14)

$$\frac{F^-_n(x) - F^-_{n-1}(x)}{\Delta t} = \frac{-v(F^-_{n-1}(x - v\Delta t) - F^-_{n-1}(x))}{-v\Delta t} + aF^+_{n-1}(x - v\Delta t) - (a+b)F^-_{n-1}(x - v\Delta t) + bF^0_n(x - v\Delta t) \tag{3.18}$$

and, in the limit,

$$\frac{\partial F^-}{\partial t} = -v\frac{\partial F^-}{\partial x} + aF^+ - (a+b)F^- + bF^0. \tag{3.19}$$

The supplementary equation for F^0 obtained from the difference equation (3.15) takes the following form:

$$\frac{\partial F^0}{\partial t} = 0. \tag{3.20}$$

To obtain the equation for probability density function F of the location of the particle (under the condition that it left the point $x = 0$ equiprobably in both directions), we introduce new variables:

$$F = \frac{1}{2}(F^+ + F^-), \qquad G = \frac{1}{2}(F^+ - F^-). \tag{3.21}$$

Adding Eqs. (3.17) and (3.19) we obtain

$$\frac{\partial F}{\partial t} = v\frac{\partial G}{\partial x} - bF + bF^0; \tag{3.22}$$

subtraction of Eq. (3.19) from Eq. (3.17) gives

$$\frac{\partial G}{\partial t} = v\frac{\partial F}{\partial x} - (2a+b)G. \tag{3.23}$$

Eliminating G from Eqs. (3.22) and (3.23) we obtain the equation for the probability density function F,

$$\frac{1}{v}\frac{\partial^2 F}{\partial t^2} = v\frac{\partial^2 F}{\partial x^2} - \frac{2(a+b)}{v}\frac{\partial F}{\partial t} + \frac{(2a+b)b}{v}F - \frac{(2a+b)b}{v}F^0, \tag{3.24}$$

where Eq. (3.20) has been also taken into account.

To consider the limit (diffusion) case let us transform Eq. (3.24) to a more convenient form:

$$\frac{1}{v^2}\frac{\partial^2 F}{\partial t^2} = \frac{\partial^2 F}{\partial x^2} - \left[\frac{2a}{v^2} + \frac{2b}{v^2}\right]\frac{\partial F}{\partial t} + \left[\frac{2ab}{v^2} + \frac{2b^2}{v^2}\right][F - F^0]. \tag{3.25}$$

Similarly to Sec. 2, consider such a limiting case of Eq. (3.25), where $a \to \infty$, $v \to \infty$ but $2a/v^2$ remains constant:

$$\frac{2a}{v^2} = \frac{1}{D}; \tag{3.26}$$

moreover, the constant b is assumed to be a finite number. Then Eq. (3.25) takes the form

$$\frac{1}{D}\frac{\partial F}{\partial t} = \frac{\partial^2 F}{\partial x^2} + \frac{b}{D}[F - F^0]. \tag{3.27}$$

It is seen that the resulting equation is the diffusion equation with annihilation terms. Also in this case the limiting equation is of a diffusive character, so the preliminary condition of correctness of the random walk model as a description of the transport process is satisfied.

4. The case of two-dimensional models

The one-dimensional model makes it possible to describe the pollution transport phenomenon only in a limited way. To take into account the spatial distribution of the particles around the source, we should consider a two-dimensional model. For this purpose we can apply the models of random walk being a certain generalization of the random walk defined in Sec. 2 and the random walk with absorption defined in Sec.3.

4.1. The random walk without sedimentation

Consider the motion of a particle in the plane, analogous to the one presented in Sec.2. The particle staying at an instant of time t_0 at point $x = (x_1, x_2)$ covers during the time period Δt the distance $\Delta x = v\Delta t$, possibly changing its direction. The trajectories of the particle lie piecewise on the straight lines parallel to the axes of the coordinate system x_1, x_2. Moving, the particle can choose one of the four possible directions (follow the previous one, turn to the left or right or go back). This process can be written mathematically similarly to the previous case with application of the matrix-vector notation.

Assume that the particle goes to the left with probability $a\Delta t$, goes back with probability $b\Delta t$, goes to the right with probability $c\Delta t$ and continues its way in the previous direction with probability $1 - (a + b + c)\Delta t$. This means that the particle moves from the initial point along one of the vectors:

$$\mathbf{a} = \begin{bmatrix} 0 \\ 1 \end{bmatrix}, \quad \mathbf{b} = \begin{bmatrix} -1 \\ 0 \end{bmatrix}, \quad \mathbf{c} = \begin{bmatrix} 0 \\ -1 \end{bmatrix}, \quad \mathbf{d} = \begin{bmatrix} 1 \\ 0 \end{bmatrix}, \tag{4.1}$$

with some probability, dependent on the previous direction of particle's motion.

We can introduce the matrix of rotation of the particle's velocity vector, which is random and takes the values according to our assumptions concerning the model. The matrix of rotation $\mathbf{E}(\omega)$ takes the following values:

$$\mathbf{E}(\omega) = \mathbf{A} = \begin{bmatrix} 0 & -1 \\ 1 & 0 \end{bmatrix} \quad \text{with probability } a\Delta t, \tag{4.2}$$

$$\mathbf{E}(\omega) = \mathbf{B} = \begin{bmatrix} -1 & 0 \\ 0 & -1 \end{bmatrix} \quad \text{with probability } b\Delta t, \tag{4.3}$$

$$\mathbf{E}(\omega) = \mathbf{C} = \begin{bmatrix} 0 & 1 \\ -1 & 0 \end{bmatrix} \quad \text{with probability } c\Delta t, \tag{4.4}$$

$$\mathbf{E}(\omega) = \mathbf{D} = \begin{bmatrix} 1 & 0 \\ 0 & 1 \end{bmatrix} \quad \text{with probability } 1 - (a + b + c)\Delta t. \tag{4.5}$$

The rotation matrices act on the direction vectors on the following way:

$$\mathbf{Ad} = \mathbf{a}, \quad \mathbf{Bd} = \mathbf{b}, \quad \mathbf{Cd} = \mathbf{c}, \quad \mathbf{Dd} = \mathbf{d}, \tag{4.6}$$

$$\mathbf{Aa} = \mathbf{b}, \quad \mathbf{Ba} = \mathbf{c}, \quad \mathbf{Ca} = \mathbf{d}, \quad \mathbf{Da} = \mathbf{a}, \tag{4.7}$$

$$\mathbf{Ab} = \mathbf{c}, \quad \mathbf{Bb} = \mathbf{d}, \quad \mathbf{Cb} = \mathbf{a}, \quad \mathbf{Db} = \mathbf{b}, \tag{4.8}$$

$$\mathbf{Ac} = \mathbf{d}, \quad \mathbf{Bc} = \mathbf{a}, \quad \mathbf{Cc} = \mathbf{b}, \quad \mathbf{Dc} = \mathbf{c}. \tag{4.9}$$

The change of location of the particle in n steps is

$$\mathbf{S}_n^{\mathbf{r}} = v\Delta t(\mathbf{Id} + \mathbf{E}_1 + \mathbf{E}_2\mathbf{E}_1 + \ \ldots\ + \mathbf{E}_{n-1}\mathbf{E}_{n-2}, \ldots, \mathbf{E}_2\mathbf{E}_1)\,\mathbf{r}, \tag{4.10}$$

where $\mathbf{r}$ is the initial direction of particle's motion and takes one of four values: $\mathbf{r} = \mathbf{a}$, $\mathbf{r} = \mathbf{b}$, $\mathbf{r} = \mathbf{c}$, or $\mathbf{r} = \mathbf{d}$.

Consider an arbitrary real-valued function on $\mathbb{R}^2$, $\varphi(\mathbf{x})$, and the function being its average value:

$$F_n^{\mathbf{r}}(\mathbf{x}) = <\varphi(\mathbf{x} + \mathbf{S}_n^{\mathbf{r}})>. \tag{4.11}$$

Written down in an explicit form, function $F_n^{\mathbf{r}}(\mathbf{x})$ is

$$F_n^{\mathbf{r}}(\mathbf{x}) = <\varphi(\mathbf{x} + v\Delta t\ \mathbf{r} + v\Delta t(\mathbf{E}_1 + \mathbf{E}_2\mathbf{E}_1 + \ \ldots\ + \mathbf{E}_{n-1}\mathbf{E}_{n-2}, \ldots, \mathbf{E}_2\mathbf{E}_1)\,\mathbf{r})>. \tag{4.12}$$

Like in the one-dimensional model, we can calculate the conditional mean value of this expression with respect to the random transition matrix $\mathbf{E}_1$. We obtain

$$\begin{aligned} F_n^{\mathbf{r}}(\mathbf{x}) = {} & a\Delta t\, F_{n-1}^{\mathbf{Ar}}(\mathbf{x} + v\Delta t\,\mathbf{r}) + b\Delta t\, F_{n-1}^{\mathbf{Br}}(\mathbf{x} + v\Delta t\,\mathbf{r}) \\ & + c\Delta t\, F_{n-1}^{\mathbf{Cr}}(\mathbf{x} + v\Delta t\,\mathbf{r}) + (1 - (a + b + c)\Delta t)\, F_{n-1}^{\mathbf{Dr}}(\mathbf{x} + v\Delta t\,\mathbf{r}), \end{aligned} \tag{4.13}$$

or, since $\mathbf{Dr} = \mathbf{r}$,

$$(4.14)\quad F^{\mathbf{r}}_n(\mathbf{x}) = a\Delta t\, F^{\mathbf{Ar}}_{n-1}(\mathbf{x} + v\Delta t\,\mathbf{r}) + b\Delta t\, F^{\mathbf{Br}}_{n-1}(\mathbf{x} + v\Delta t\,\mathbf{r}) + c\Delta t\, F^{\mathbf{Cr}}_{n-1}(\mathbf{x} + v\Delta t\,\mathbf{r}) + (1 - (a+b+c)\Delta t)\, F^{\mathbf{r}}_{n-1}(\mathbf{x} + v\Delta t\,\mathbf{r}).$$

The difference equations (4.14) for $\mathbf{r} = \mathbf{a}, \mathbf{b}, \mathbf{c}, \mathbf{d}$ can be written in the following form:

$$(4.15)\quad \frac{F^{\mathbf{r}}_n(\mathbf{x}) - F^{\mathbf{r}}_{n-1}(\mathbf{x})}{\Delta t} = \frac{v(F^{\mathbf{r}}_{n-1}(\mathbf{x} + v\Delta t\,\mathbf{r}) - F^{\mathbf{r}}_{n-1}(\mathbf{x}))}{v\Delta t} + aF^{\mathbf{Ar}}_{n-1}(\mathbf{x} + v\Delta t\,\mathbf{r}) + bF^{\mathbf{Br}}_{n-1}(\mathbf{x} + v\Delta t\,\mathbf{r}) + cF^{\mathbf{Cr}}_{n-1}(\mathbf{x} + v\Delta t\,\mathbf{r}) + (a+b+c)F^{\mathbf{r}}_{n-1}(\mathbf{x} + v\Delta t\,\mathbf{r}).$$

Passing to the limit ($\Delta t \to 0$) we obtain the system of partial differential equations for the conditional probability density functions $F^{\mathbf{r}}$, $\mathbf{r} = \mathbf{a}, \mathbf{b}, \mathbf{c}, \mathbf{d}$:

$$(4.16)\quad \frac{\partial F^{\mathbf{r}}}{\partial t} = v\mathbf{r}\nabla F^{\mathbf{r}}(\mathbf{x}) + aF^{\mathbf{Ar}}(\mathbf{x}) + bF^{\mathbf{Br}}(\mathbf{x}) + cF^{\mathbf{Cr}}(\mathbf{x}) - (a+b+c)F^{\mathbf{r}}(\mathbf{x}).$$

Taking successively $\mathbf{r} = \mathbf{a}, \mathbf{b}, \mathbf{c}, \mathbf{d}$, we obtain the system of equations in an explicit form:

$$(4.17)\quad \frac{\partial}{\partial t}\begin{bmatrix} F^{\mathbf{a}} \\ F^{\mathbf{b}} \\ F^{\mathbf{c}} \\ F^{\mathbf{d}} \end{bmatrix} - v\begin{bmatrix} \frac{\partial}{\partial x_2} & 0 & 0 & 0 \\ 0 & -\frac{\partial}{\partial x_1} & 0 & 0 \\ 0 & 0 & -\frac{\partial}{\partial x_2} & 0 \\ 0 & 0 & 0 & \frac{\partial}{\partial x_1} \end{bmatrix}\begin{bmatrix} F^{\mathbf{a}} \\ F^{\mathbf{b}} \\ F^{\mathbf{c}} \\ F^{\mathbf{d}} \end{bmatrix} = \begin{bmatrix} -(a+b+c) & a & b & c \\ c & -(a+b+c) & a & b \\ b & c & -(a+b+c) & a \\ a & b & c & -(a+b+c) \end{bmatrix}\begin{bmatrix} F^{\mathbf{a}} \\ F^{\mathbf{b}} \\ F^{\mathbf{c}} \\ F^{\mathbf{d}} \end{bmatrix}.$$

Introducing new unknown functions P, R, Q, T, defined by

$$(4.18)\quad P = F^{\mathbf{a}} + F^{\mathbf{c}}, \qquad Q = F^{\mathbf{a}} - F^{\mathbf{c}},$$

$$(4.19)\quad R = F^{\mathbf{b}} + F^{\mathbf{d}}, \qquad T = F^{\mathbf{b}} - F^{\mathbf{d}},$$

we obtain the new system of equations

$$\frac{\partial}{\partial t}P - v\frac{\partial}{\partial x_2}Q = -(a+c)P + (a+c)R, \tag{4.20}$$

$$\frac{\partial}{\partial t}Q - v\frac{\partial}{\partial x_2}P = -(a+2b+c)Q + (a-c)T, \tag{4.21}$$

$$\frac{\partial}{\partial t}R + v\frac{\partial}{\partial x_1}T = -(a+c)R + (a+c)P, \tag{4.22}$$

$$\frac{\partial}{\partial t}T + v\frac{\partial}{\partial x_1}R = -(a+2b+c)T - (a-c)Q. \tag{4.23}$$

To obtain the equation for the unconditional probability density function, let us introduce two new functions:

$$U = P + R = F^a + F^c + F^b + F^d, \tag{4.24}$$

$$S = P - R = F^a + F^c - F^b - F^d. \tag{4.25}$$

Now, the function F, defined as

$$F = \frac{1}{4}U, \tag{4.26}$$

represents the probability density function of the event that the pollutant particle reaches a certain area, independently of its initial direction. The above substitution and differentiation with respect to spatial variables transforms the equations to the following form:

$$\frac{\partial}{\partial t}P - v\frac{\partial}{\partial x_2}Q = -(a+c)S, \tag{4.27}$$

$$\frac{\partial}{\partial x_1}\frac{\partial}{\partial t}Q - v\frac{\partial}{\partial x_1}\frac{\partial}{\partial x_2}P = -(a+2b+c)\frac{\partial}{\partial x_1}Q + (a-c)\frac{\partial}{\partial x_1}T, \tag{4.28}$$

$$\frac{\partial}{\partial t}R + v\frac{\partial}{\partial x_1}T = (a+c)S, \tag{4.29}$$

$$\frac{\partial}{\partial x_2}\frac{\partial}{\partial t}T + v\frac{\partial}{\partial x_2}\frac{\partial}{\partial x_1}R = -(a+2b+c)\frac{\partial}{\partial x_2}T - (a-c)\frac{\partial}{\partial x_2}Q. \tag{4.30}$$

Addition and subtraction of the pairs of the equations gives the following system of partial differential equations for four functions U, S, T, Q:

$$\frac{\partial}{\partial t}U - v\frac{\partial}{\partial x_2}Q + v\frac{\partial}{\partial x_1}T = 0, \tag{4.31}$$

$$\frac{\partial^2}{\partial t \partial x_1} Q + \frac{\partial^2}{\partial t \partial x_2} T - v \frac{\partial^2}{\partial x_1 \partial x_2} U = -(a+2b+c)\left[\frac{\partial}{\partial x_1} Q + \frac{\partial}{\partial x_2} T\right] + (a-c)\left[\frac{\partial}{\partial x_1} T - \frac{\partial}{\partial x_2} Q\right], \tag{4.32}$$

$$\frac{\partial}{\partial t} S - v \frac{\partial}{\partial x_2} Q - v \frac{\partial}{\partial x_1} T = -2(a+c) S, \tag{4.33}$$

$$\frac{\partial^2}{\partial t \partial x_1} Q - \frac{\partial^2}{\partial t \partial x_2} T - v \frac{\partial^2}{\partial x_1 \partial x_2} S = -(a+2b+c)\left[\frac{\partial}{\partial x_1} Q + \frac{\partial}{\partial x_2} T\right] + (a-c)\left[\frac{\partial}{\partial x_1} T + \frac{\partial}{\partial x_2} Q\right]. \tag{4.34}$$

The system of equations obtained can be used for the calculation of the probability density U describing the unconditional location of the particle. Elimination of the functions S, T, Q from Eqs. (4.31) – (4.34) is too complicated and, moreover, it would change the class of the function sought; therefore, we leave this system of equations in its present form.

4.2. Random walk with sedimentation

Modeling the two-dimensional diffusion process we can also take into account the possibility of the sedimentation of the particles in the environment. Then, analogously to Sec. 3, the particle can either move in one of the four possible directions:

$$\mathbf{a} = \begin{bmatrix} 0 \\ 1 \end{bmatrix}, \quad \mathbf{b} = \begin{bmatrix} -1 \\ 0 \end{bmatrix}, \quad \mathbf{c} = \begin{bmatrix} 0 \\ -1 \end{bmatrix}, \quad \mathbf{d} = \begin{bmatrix} 1 \\ 0 \end{bmatrix}, \tag{4.35}$$

with probability dependent on the previous direction of the particle's motion, or remain at the point of its present location, what can be represented by a zero vector of motion

$$\mathbf{g} = \begin{bmatrix} 0 \\ 0 \end{bmatrix}. \tag{4.36}$$

We can also introduce the matrix of rotation (or annihilation) of the particle's velocity vector, which is random and takes the values according to our assumptions concerning the model. The matrix of rotation $\mathbf{E}(\omega)$ takes the following values:

$$\mathbf{E}(\omega) = \mathbf{A} = \begin{bmatrix} 0 & -1 \\ 1 & 0 \end{bmatrix} \quad \text{with probability } a\Delta t, \tag{4.37}$$

$$\mathbf{E}(\omega) = \mathbf{B} = \begin{bmatrix} -1 & 0 \\ 0 & -1 \end{bmatrix} \quad \text{with probability } b\Delta t, \tag{4.38}$$

$$\mathbf{E}(\omega) = \mathbf{C} = \begin{bmatrix} 0 & 1 \\ -1 & 0 \end{bmatrix} \quad \text{with probability } c\Delta t, \tag{4.39}$$

$$\mathbf{E}(\omega) = \mathbf{G} = \begin{bmatrix} 0 & 0 \\ 0 & 0 \end{bmatrix} \quad \text{with probability } g\Delta t, \tag{4.40}$$

$$\mathbf{E}(\omega) = \mathbf{D} = \begin{bmatrix} 1 & 0 \\ 0 & 1 \end{bmatrix} \quad \text{with probability } 1 - (a + b + c + g)\Delta t. \tag{4.41}$$

The rotation matrices defined above act on the velocity direction vectors in the following way:

$$\mathbf{Ad} = \mathbf{a}, \quad \mathbf{Bd} = \mathbf{b}, \quad \mathbf{Cd} = \mathbf{d}, \quad \mathbf{Dd} = \mathbf{d}, \quad \mathbf{Gd} = \mathbf{g}, \tag{4.42}$$

$$\mathbf{Aa} = \mathbf{b}, \quad \mathbf{Ba} = \mathbf{c}, \quad \mathbf{Ca} = \mathbf{a}, \quad \mathbf{Da} = \mathbf{a}, \quad \mathbf{Ga} = \mathbf{g}, \tag{4.43}$$

$$\mathbf{Ab} = \mathbf{c}, \quad \mathbf{Bb} = \mathbf{d}, \quad \mathbf{Cb} = \mathbf{a}, \quad \mathbf{Db} = \mathbf{b}, \quad \mathbf{Gb} = \mathbf{g}, \tag{4.44}$$

$$\mathbf{Ac} = \mathbf{d}, \quad \mathbf{Bc} = \mathbf{a}, \quad \mathbf{Cc} = \mathbf{b}, \quad \mathbf{Dc} = \mathbf{c}, \quad \mathbf{Gc} = \mathbf{g}, \tag{4.45}$$

$$\mathbf{Ag} = \mathbf{g}, \quad \mathbf{Bg} = \mathbf{g}, \quad \mathbf{Cg} = \mathbf{g}, \quad \mathbf{Dg} = \mathbf{g}, \quad \mathbf{Gg} = \mathbf{g}. \tag{4.46}$$

The change of location of the particle in n steps (under the condition that the particle has really left the starting point) is

$$\mathbf{S}_n^{\mathbf{r}} = v\Delta t(\mathbf{Id} + \mathbf{E}_1 + \mathbf{E}_2\mathbf{E}_1 + \ldots + \mathbf{E}_{n-1}\mathbf{E}_{n-2}, \ldots, \mathbf{E}_2\mathbf{E}_1)\,\mathbf{r}, \tag{4.47}$$

where $\mathbf{r}$ is the initial direction of particle's motion, that is $\mathbf{r} = \mathbf{a}$, $\mathbf{r} = \mathbf{b}$, $\mathbf{r} = \mathbf{c}$, or $\mathbf{r} = \mathbf{d}$; in the case of not leaving the point, the motion vector can be written as

$$\mathbf{S}_n^{\mathbf{g}} = \mathbf{g}. \tag{4.48}$$

Consider an arbitrary real-valued function $\varphi(\mathbf{x})$ defined on $\mathbb{R}^2$, and its conditional average values (under the conditions of all possible initial directions of the walking particle) $<\varphi(\mathbf{x} + \mathbf{S}_n^{\mathbf{r}})>$, $\mathbf{r} = \mathbf{a}, \mathbf{b}, \mathbf{c}, \mathbf{d}, \mathbf{g}$. Performing the reasoning analogous to the one made in the non-sedimentation case, we obtain the system of equations for the conditional probability density functions $F^{\mathbf{r}}$, $\mathbf{r} = \mathbf{a}, \mathbf{b}, \mathbf{c}, \mathbf{d}, \mathbf{g}$:

$$\frac{\partial F^{\mathbf{r}}}{\partial t} = v\mathbf{r} \cdot \nabla F^{\mathbf{r}}(\mathbf{x}) + aF^{\mathbf{Ar}}(\mathbf{x}) + bF^{\mathbf{Br}}(\mathbf{x}) + cF^{\mathbf{Cr}}(\mathbf{x}) \tag{4.49}$$

$$- (a + b + c + g)F^{\mathbf{r}}(\mathbf{x}) + gF^{\mathbf{g}}(\mathbf{x}),$$

for $\mathbf{r} = \mathbf{a}, \mathbf{b}, \mathbf{c}, \mathbf{d}$ and

$$\frac{\partial F^{\mathbf{g}}}{\partial t} = 0. \tag{4.50}$$

The system of equations (4.49) can be written in the vector form

$$\frac{\partial}{\partial t}\begin{bmatrix} F^{\mathbf{a}} \\ F^{\mathbf{b}} \\ F^{\mathbf{c}} \\ F^{\mathbf{d}} \\ F^{\mathbf{g}} \end{bmatrix} - v\begin{bmatrix} \frac{\partial}{\partial x_2} & 0 & 0 & 0 & 0 \\ 0 & -\frac{\partial}{\partial x_1} & 0 & 0 & 0 \\ 0 & 0 & -\frac{\partial}{\partial x_2} & 0 & 0 \\ 0 & 0 & 0 & \frac{\partial}{\partial x_1} & 0 \\ 0 & 0 & 0 & 0 & 0 \end{bmatrix}\begin{bmatrix} F^{\mathbf{a}} \\ F^{\mathbf{b}} \\ F^{\mathbf{c}} \\ F^{\mathbf{d}} \\ F^{\mathbf{g}} \end{bmatrix} \tag{4.51}$$

$$= \begin{bmatrix} -(a+b+c+g) & a & b & c & g \\ c & -(a+b+c+g) & a & b & g \\ b & c & -(a+b+c+g) & a & g \\ a & b & c & -(a+b+c+g) & g \\ 0 & 0 & 0 & 0 & 0 \end{bmatrix}\begin{bmatrix} F^{\mathbf{a}} \\ F^{\mathbf{b}} \\ F^{\mathbf{c}} \\ F^{\mathbf{d}} \\ F^{\mathbf{g}} \end{bmatrix}.$$

Similarly to the model without sedimentation, assuming that the probabilities of the initial directions of the pollutant particles are equal, we can obtain the system of equations where the probability density function of the actual location of the particle is one of the functions sought for. Repeating the calculations in the way analogous to the previous case of non-sedimenting particles, we can obtain the system of equations for the following sets of functions

$$P = F^{\mathbf{a}} + F^{\mathbf{c}}, \qquad Q = F^{\mathbf{a}} - F^{\mathbf{c}}, \tag{4.52}$$

$$R = F^{\mathbf{b}} + F^{\mathbf{d}}, \qquad T = F^{\mathbf{b}} - F^{\mathbf{d}} \qquad \text{and } F^{\mathbf{g}}, \tag{4.53}$$

or alternatively,

$$U = F^{\mathbf{a}} + F^{\mathbf{c}} + F^{\mathbf{b}} + F^{\mathbf{d}}, \qquad Q = F^{\mathbf{a}} - F^{\mathbf{c}}, \tag{4.54}$$

(4.55) $$S = F^a + F^c - F^b - F^d, \qquad T = F^b - F^d \qquad \text{and } F^g.$$

In the first case the system of equations is

(4.56) $$\frac{\partial}{\partial t} P - \nu \frac{\partial}{\partial x_2} Q = -(a + c + g) P + (a + c) R + 2g F^g,$$

(4.57) $$\frac{\partial}{\partial t} Q - \nu \frac{\partial}{\partial x_2} P = -(a + 2b + c + g) Q + (a - c) T,$$

(4.58) $$\frac{\partial}{\partial t} R + \nu \frac{\partial}{\partial x_1} T = -(a + c + g) R + (a + c) P + 2g F^g,$$

(4.59) $$\frac{\partial}{\partial t} T + \nu \frac{\partial}{\partial x_1} R = -(a + 2b + c + g) T - (a - c) Q,$$

(4.60) $$\frac{\partial F^g}{\partial t} = 0,$$

while in the second case we obtain

(4.61) $$\frac{\partial}{\partial t} U - \nu \frac{\partial}{\partial x_2} Q + \nu \frac{\partial}{\partial x_1} T = -gU + 4g F^g,$$

(4.62) $$\frac{\partial^2}{\partial t \partial x_1} Q + \frac{\partial^2}{\partial t \partial x_2} T - \nu \frac{\partial^2}{\partial x_1 \partial x_2} U$$

$$= -(a + 2b + c + g) \left[\frac{\partial}{\partial x_1} Q + \frac{\partial}{\partial x_2} T \right] + (a - c) \left[\frac{\partial}{\partial x_1} T - \frac{\partial}{\partial x_2} Q \right],$$

(4.63) $$\frac{\partial}{\partial t} S - \nu \frac{\partial}{\partial x_2} Q - \nu \frac{\partial}{\partial x_1} T = -2(a + c) S - gS,$$

(4.64) $$\frac{\partial^2}{\partial t \partial x_1} Q - \frac{\partial^2}{\partial t \partial x_2} T - \nu \frac{\partial^2}{\partial x_1 \partial x_2} S$$

$$= -(a + 2b + c + g) \left[\frac{\partial}{\partial x_1} Q - \frac{\partial}{\partial x_2} T \right] + (a - c) \left[\frac{\partial}{\partial x_1} T + \frac{\partial}{\partial x_2} Q \right],$$

(4.65) $$\frac{\partial F^g}{\partial t} = 0.$$

5. The model of pollution transport with sedimentation in three-dimensional space

Modeling the pollution transport in three-dimensional space, we can also use the random walk process. In such a case we can describe the flow of particles in a much more realistic way than in the one- or two-dimensional cases. At present the phenomenon of sedimentation of the particles doesn't require to introduce the probability of annihilation of the particle. In order to describe it, we can simply assume that the particle reaches a certain surface (ground surface) which is an absorbing boundary, characterized by an appropriate boundary condition for the probability density function (see [11]). We can alternatively assume that the boundary reflects the particle, what is expressed mathematically by vanishing of the particles flux on the surface (expressed in terms of the probability density function), see [11]. Obviously, the boundary can also partially reflect and partially absorb the particles. In such a situation the boundary condition is a certain combination of the conditions for the reflecting and absorbing boundary.

Let us consider a random walk in a three-dimensional space. We define the source point $\mathbf{x}_0$ and the sedimentation plane $\mathscr{Z}$ $(x-y)$, described in the three-dimensional Euclidean space coordinates in such a way that

$$\text{(5.1)} \qquad \mathbf{x}_0 = \begin{bmatrix} 0 \\ 0 \\ z_0 \end{bmatrix} \quad \text{and} \quad \mathscr{Z}(x-y) = \left[\mathbf{x} = \begin{bmatrix} x \\ y \\ 0 \end{bmatrix}, \quad x \in \mathrm{R},\ y \in \mathrm{R} \right].$$

The particle starting from the source point can walk in one of the six possible directions, parallel to the coordinate axes of the space; staying at any point at a given instant of time, it also can continue its walk in one of six possible directions with probability dependent on the direction of its previous step. The direction vectors of possible particle's steps in a three-dimensional space are:

$$\text{(5.2)} \qquad \mathbf{a} = \begin{bmatrix} 0 \\ 1 \\ 0 \end{bmatrix}, \quad \mathbf{b} = \begin{bmatrix} -1 \\ 1 \\ 0 \end{bmatrix}, \quad \mathbf{c} = \begin{bmatrix} 0 \\ -1 \\ 0 \end{bmatrix}, \quad \mathbf{d} = \begin{bmatrix} 1 \\ 0 \\ 0 \end{bmatrix}, \quad \mathbf{e} = \begin{bmatrix} 0 \\ 0 \\ 1 \end{bmatrix}, \quad \mathbf{f} = \begin{bmatrix} 0 \\ 0 \\ -1 \end{bmatrix},$$

where **a**, **b**, **c**, **d**, represent the possible directions of transport, **e** – the direction of convection and **f** – the direction of sedimentation. Reaching the sedimentation plane $\{\mathbf{x} = (x, y, 0)^T, \quad x, y \in \mathbb{R}\}$ the particle stops and is excluded from the balance of mass of the travelling particles.

Change of direction is governed by some rotation matrix **A**, depending on the initial direction (direction of the previous step). To define the random walk we assume the probabilities of changes of the direction of particle's motion and, consequently, the probability that the rotation matrix **A** takes a given value.

To model the transport process we assume that the rotation matrix takes its value depending not only on the rotation angle but also on the initial and final direction of particle's velocity.

In the transport plane $x - y$ transformations of the velocity vector are the rotations around the axis **e**, and they are described by the following matrices:

- turning to the left (**a** ⇒ **b**, **b** ⇒ **c**, **c** ⇒ d, **d** ⇒ **a**)

$$\mathbf{A} = \begin{bmatrix} 0 & -1 & 0 \\ 1 & 0 & 0 \\ 0 & 0 & 1 \end{bmatrix} \quad \text{with probability } \alpha_1 \Delta t; \tag{5.3}$$

- reflecting (**a** ⇒ **c**, **b** ⇒ **d**, **c** ⇒ **a**, **d** ⇒ **b**)

$$\mathbf{A} = \begin{bmatrix} -1 & 0 & 0 \\ 1 & -1 & 0 \\ 0 & 0 & 1 \end{bmatrix} \quad \text{with probability } \beta \Delta t; \tag{5.4}$$

- turning to the right (**a** ⇒ **d**, **b** ⇒ **a**, **c** ⇒ **b**, **d** ⇒ **c**)

$$\mathbf{A} = \begin{bmatrix} 0 & 1 & 0 \\ -1 & 0 & 0 \\ 0 & 0 & 1 \end{bmatrix} \quad \text{with probability } \alpha_2 \Delta t. \tag{5.5}$$

The matrices describing changes from the transport process in plane $x - y$ to the convection (that is the walk with the velocity vector **e**) have the following form:

for the transformation **a** ⇒ **e**

$$\mathbf{A} = \begin{bmatrix} 1 & 0 & 0 \\ 0 & 0 & -1 \\ 0 & 1 & 0 \end{bmatrix}; \tag{5.6}$$

for the transformation **b** ⇒ **e**

$$\mathbf{A} = \begin{bmatrix} 0 & 0 & 1 \\ 0 & 1 & 0 \\ -1 & 0 & 0 \end{bmatrix}; \tag{5.7}$$

for the transformation **c** ⇒ **e**

$$\mathbf{A} = \begin{bmatrix} 1 & 0 & 0 \\ 0 & 0 & 1 \\ 0 & -1 & 0 \end{bmatrix}; \tag{5.8}$$

for the transformation $\mathbf{d} \Rightarrow \mathbf{e}$

$$\mathbf{A} = \begin{bmatrix} 0 & 0 & -1 \\ 0 & 1 & 0 \\ 1 & 0 & 0 \end{bmatrix}; \tag{5.9}$$

all with the probability $\kappa \Delta t$, and

for the transformation $\mathbf{f} \Rightarrow \mathbf{e}$

$$\mathbf{A} = \begin{bmatrix} 1 & 0 & 0 \\ 0 & 1 & 0 \\ 0 & 0 & -1 \end{bmatrix} \quad \text{with probability } \psi \Delta t. \tag{5.10}$$

Similarly, the change from the transport to sedimentation (the walk with velocity **f**) is described by the following matrices:

for the transformation $\mathbf{a} \Rightarrow \mathbf{f}$

$$\mathbf{A} = \begin{bmatrix} 1 & 0 & 0 \\ 0 & 0 & 1 \\ 0 & -1 & 0 \end{bmatrix}; \tag{5.11}$$

for the transformation $\mathbf{b} \Rightarrow \mathbf{f}$

$$\mathbf{A} = \begin{bmatrix} 1 & 0 & -1 \\ 0 & 1 & 0 \\ 1 & 0 & 0 \end{bmatrix}; \tag{5.12}$$

for the transformation $\mathbf{c} \Rightarrow \mathbf{f}$

$$\mathbf{A} = \begin{bmatrix} 1 & 0 & 0 \\ 0 & 1 & -1 \\ 0 & 1 & 0 \end{bmatrix}; \tag{5.13}$$

for the transformation $\mathbf{d} \Rightarrow \mathbf{f}$

(5.14) $$\mathbf{A} = \begin{bmatrix} 0 & 0 & 1 \\ 0 & 1 & 0 \\ -1 & 0 & 0 \end{bmatrix};$$

all with probability $\gamma \Delta t$, and

for the transformation $\mathbf{e} \Rightarrow \mathbf{f}$

(5.15) $$\mathbf{A} = \begin{bmatrix} 1 & 0 & 0 \\ 0 & 1 & 0 \\ 0 & 0 & -1 \end{bmatrix}$$ with probability $\varepsilon \Delta t$.

The last possible changes of the direction of the particle velocity are the changes from convection to transport:

for the transformation $\mathbf{e} \Rightarrow \mathbf{a}$

(5.16) $$\mathbf{A} = \begin{bmatrix} 1 & 0 & 0 \\ 0 & 0 & 1 \\ 0 & -1 & 0 \end{bmatrix};$$

for the transformation $\mathbf{e} \Rightarrow \mathbf{b}$

(5.17) $$\mathbf{A} = \begin{bmatrix} 0 & 0 & -1 \\ 0 & 1 & 0 \\ 1 & 0 & 0 \end{bmatrix};$$

for the transformation $\mathbf{e} \Rightarrow \mathbf{c}$

(5.18) $$\mathbf{A} = \begin{bmatrix} 1 & 0 & 0 \\ 0 & 0 & -1 \\ 0 & 1 & 0 \end{bmatrix};$$

for the transformation $\mathbf{e} \Rightarrow \mathbf{d}$

(5.19) $$\mathbf{A} = \begin{bmatrix} 0 & 0 & 1 \\ 0 & 1 & 0 \\ -1 & 0 & 0 \end{bmatrix},$$

all with probability $\delta \Delta t$, and from sedimentation to transport:

for the transformation $\mathbf{f} \Rightarrow \mathbf{a}$

(5.20) $$\mathbf{A} = \begin{bmatrix} 1 & 0 & 0 \\ 0 & 0 & -1 \\ 0 & 1 & 0 \end{bmatrix};$$

for the transformation $\mathbf{f} \Rightarrow \mathbf{b}$

$$\mathbf{A} = \begin{bmatrix} 0 & 0 & 1 \\ 0 & 1 & 0 \\ -1 & 0 & 0 \end{bmatrix}; \tag{5.21}$$

for the transformation $\mathbf{f} \Rightarrow \mathbf{c}$

$$\mathbf{A} = \begin{bmatrix} 1 & 0 & 0 \\ 0 & 0 & 1 \\ 0 & -1 & 0 \end{bmatrix}; \tag{5.22}$$

for the transformation $\mathbf{f} \Rightarrow \mathbf{d}$

$$\mathbf{A} = \begin{bmatrix} 0 & 0 & -1 \\ 0 & 1 & 0 \\ 1 & 0 & 0 \end{bmatrix}, \tag{5.23}$$

with probability $\varphi \Delta t$.

To derive the equations for the probability of the location of the walking particle we repeat the procedure applied in the two-dimensional model. Let us assume that $\mathbf{w}$ is the initial velocity vector of the particle (taking the value **a**, **b**, **c**, **d**, **e** or **f**), while $\mathbf{x} = (x_1, x_2, x_3)$ is the starting point (at initial time $t = 0$). Then the change of location of the particle after n time steps is

$$S_n^{\mathbf{w}} = v\Delta t[\mathbf{w} + \mathbf{A}_1\mathbf{w} + \mathbf{A}_2\mathbf{A}_1\mathbf{w} + \ \dots \ + \mathbf{A}_{n-1}\mathbf{A}_{n-2}, \dots, \mathbf{A}_1\mathbf{w}]. \tag{5.24}$$

We consider the function of the actual location of the particle defined as

$$F_n^{\mathbf{w}}(\mathbf{x}) = <\Phi[\mathbf{x} + S_n^{\mathbf{w}}]>. \tag{5.25}$$

Writing $S_n^{\mathbf{w}}$ explicitly we obtain

$$F_n^{\mathbf{w}}(\mathbf{x}) = <\Phi\left[\mathbf{x} + v\Delta t\left[\mathbf{w} + \mathbf{A}_1\mathbf{w} + \mathbf{A}_2\mathbf{A}_1\mathbf{w} + \ \dots \ + \mathbf{A}_{n-1}\mathbf{A}_{n-2}, \dots, \mathbf{A}_1\mathbf{w}\right]\right]>. \tag{5.26}$$

The conditional expectation of the function $F_n^{\mathbf{w}}(\mathbf{x})$ with respect to matrix $\mathbf{A}_1$ (under the condition that $\mathbf{w}$ is equal, respectively, to **a**, **b**, **c**, **d**, **e**, and **f**) is the following:

$$\begin{aligned} F_n^{\mathbf{a}}(\mathbf{x}) = {} & \alpha_1 \Delta t F_{n-1}^{\mathbf{b}}(\mathbf{x} + v\Delta t\,\mathbf{a}) + \alpha_2 \Delta t F_{n-1}^{\mathbf{d}}(\mathbf{x} + v\Delta t\,\mathbf{a}) \\ & + \beta \Delta t F_{n-1}^{\mathbf{c}}(\mathbf{x} + v\Delta t\,\mathbf{a}) + \kappa \Delta t F_{n-1}^{\mathbf{e}}(\mathbf{x} + v\Delta t\,\mathbf{a}) + \gamma \Delta t F_{n-1}^{\mathbf{f}}(\mathbf{x} + v\Delta t\,\mathbf{a}) \\ & + (1 - (\alpha_1 + \alpha_2 + \beta + \kappa + \gamma)\,\Delta t) F_{n-1}^{\mathbf{a}}(\mathbf{x} + v\Delta t\mathbf{a}), \end{aligned} \tag{5.27}$$

$$F_n^{\mathbf{b}}(\mathbf{x}) = \alpha_1 \Delta t F_{n-1}^{\mathbf{c}}(\mathbf{x} + v\Delta t\,\mathbf{b}) + \alpha_2 \Delta t F_{n-1}^{\mathbf{a}}(\mathbf{x} + v\Delta t\,\mathbf{b}) \tag{5.28}$$
$$+ \beta \Delta t F_{n-1}^{\mathbf{d}}(\mathbf{x} + v\Delta t\,\mathbf{b}) + \kappa \Delta t F_{n-1}^{\mathbf{e}}(\mathbf{x} + v\Delta t\,\mathbf{b}) + \gamma \Delta t F_{n-1}^{\mathbf{f}}(\mathbf{x} + v\Delta t\,\mathbf{b})$$
$$+ (1 - (\alpha_1 + \alpha_2 + \beta + \kappa + \gamma)\Delta t) F_{n-1}^{\mathbf{b}}(\mathbf{x} + v\Delta t\,\mathbf{b}),$$

$$F_n^{\mathbf{c}}(\mathbf{x}) = \alpha_1 \Delta t F_{n-1}^{\mathbf{d}}(\mathbf{x} + v\Delta t\,\mathbf{c}) + \alpha_2 \Delta t F_{n-1}^{\mathbf{b}}(\mathbf{x} + v\Delta t\,\mathbf{c}) \tag{5.29}$$
$$+ \beta \Delta t F_{n-1}^{\mathbf{a}}(\mathbf{x} + v\Delta t\,\mathbf{c}) + \kappa \Delta t F_{n-1}^{\mathbf{e}}(\mathbf{x} + v\Delta t\,\mathbf{c}) + \gamma \Delta t F_{n-1}^{\mathbf{f}}(\mathbf{x} + v\Delta t\,\mathbf{c})$$
$$+ (1 - (\alpha_1 + \alpha_2 + \beta + \kappa + \gamma)\Delta t) F_{n-1}^{\mathbf{c}}(\mathbf{x} + v\Delta t\,\mathbf{c}),$$

$$F_n^{\mathbf{d}}(\mathbf{x}) = \alpha_1 \Delta t F_{n-1}^{\mathbf{a}}(\mathbf{x} + v\Delta t\,\mathbf{d}) + \alpha_2 \Delta t F_{n-1}^{\mathbf{c}}(\mathbf{x} + v\Delta t\,\mathbf{d}) \tag{5.30}$$
$$+ \beta \Delta t F_{n-1}^{\mathbf{b}}(\mathbf{x} + v\Delta t\,\mathbf{d}) + \kappa \Delta t F_{n-1}^{\mathbf{e}}(\mathbf{x} + v\Delta t\,\mathbf{d}) + \gamma \Delta t F_{n-1}^{\mathbf{f}}(\mathbf{x} + v\Delta t\,\mathbf{d})$$
$$+ (1 - (\alpha_1 + \alpha_2 + \beta + \kappa + \gamma)\Delta t) F_{n-1}^{\mathbf{d}}(\mathbf{x} + v\Delta t\,\mathbf{d}),$$

$$F_n^{\mathbf{e}}(\mathbf{x}) = \delta \Delta t \big[F_{n-1}^{\mathbf{a}}(\mathbf{x} + v\Delta t\,\mathbf{e}) + F_{n-1}^{\mathbf{b}}(\mathbf{x} + v\Delta t\,\mathbf{e}) \tag{5.31}$$
$$+ F_{n-1}^{\mathbf{c}}(\mathbf{x} + v\Delta t\,\mathbf{e}) + F_{n-1}^{\mathbf{d}}(\mathbf{x} + v\Delta t\,\mathbf{e})\big]$$
$$+ \varepsilon \Delta t F_{n-1}^{\mathbf{f}}(\mathbf{x} + v\Delta t\,\mathbf{e}) + (1 - (4\delta + \varepsilon)\Delta t) F_{n-1}^{\mathbf{e}}(\mathbf{x} + v\Delta t\,\mathbf{e}),$$

$$F_n^{\mathbf{f}}(\mathbf{x}) = \varphi \Delta t \big[F_{n-1}^{\mathbf{a}}(\mathbf{x} + v\Delta t\,\mathbf{f}) + F_{n-1}^{\mathbf{b}}(\mathbf{x} + v\Delta t\,\mathbf{f}) \tag{5.32}$$
$$+ F_{n-1}^{\mathbf{c}}(\mathbf{x} + v\Delta t\,\mathbf{f}) + F_{n-1}^{\mathbf{d}}(\mathbf{x} + v\Delta t\,\mathbf{f})\big]$$
$$+ \psi \Delta t F_{n-1}^{\mathbf{e}}(\mathbf{x} + v\Delta t\,\mathbf{f}) + (1 - (4\varphi + \psi)\Delta t) F_{n-1}^{\mathbf{f}}(\mathbf{x} + v\Delta t\,\mathbf{f}).$$

Passing to the limit in the difference equations (5.27)–(5.32), as in the previous cases, we obtain the following system of partial differential equations for the conditional probability density functions:

$$\frac{\partial F^{\mathbf{a}}(t,\mathbf{x})}{\partial t} = \alpha_1 F^{\mathbf{b}}(t,\mathbf{x}) + \alpha_2 F^{\mathbf{d}}(t,\mathbf{x}) + \beta F^{\mathbf{c}}(t,\mathbf{x}) + \kappa F^{\mathbf{e}}(t,\mathbf{x}) + \gamma F^{\mathbf{f}}(t,\mathbf{x}) \tag{5.33}$$
$$- (\alpha_1 + \alpha_2 + \beta + \kappa + \gamma) F^{\mathbf{a}}(t,\mathbf{x}) + v\mathbf{a}\cdot\nabla F^{\mathbf{a}}(t,\mathbf{x}),$$

$$\frac{\partial F^{\mathbf{b}}(t,\mathbf{x})}{\partial t} = \alpha_1 F^{\mathbf{c}}(t,\mathbf{x}) + \alpha_2 F^{\mathbf{a}}(t,\mathbf{x}) + \beta F^{\mathbf{d}}(t,\mathbf{x}) + \kappa F^{\mathbf{e}}(t,\mathbf{x}) + \gamma F^{\mathbf{f}}(t,\mathbf{x}) \tag{5.34}$$
$$- (\alpha_1 + \alpha_2 + \beta + \kappa + \gamma) F^{\mathbf{b}}(t,\mathbf{x}) + v\mathbf{b}\cdot\nabla F^{\mathbf{b}}(t,\mathbf{x}),$$

$$\frac{\partial F^{\mathbf{c}}(t,\mathbf{x})}{\partial t} = \alpha_1 F^{\mathbf{d}}(t,\mathbf{x}) + \alpha_2 F^{\mathbf{b}}(t,\mathbf{x}) + \beta F^{\mathbf{a}}(t,\mathbf{x}) + \kappa F^{\mathbf{e}}(t,\mathbf{x}) + \gamma F^{\mathbf{f}}(t,\mathbf{x}) \tag{5.35}$$
$$- (\alpha_1 + \alpha_2 + \beta + \kappa + \gamma) F^{\mathbf{c}}(t,\mathbf{x}) + v\mathbf{c}\cdot\nabla F^{\mathbf{c}}(t,\mathbf{x}),$$

$$\frac{\partial F^{d}(t,\mathbf{x})}{\partial t} = \alpha_1 F^{a}(t,\mathbf{x}) + \alpha_2 F^{c}(t,\mathbf{x}) + \beta F^{b}(t,\mathbf{x}) + \kappa F^{e}(t,\mathbf{x}) + \gamma F^{f}(t,\mathbf{x}) - (\alpha_1 + \alpha_2 + \beta + \kappa + \gamma) F^{d}(t,\mathbf{x}) + v\mathbf{d}\cdot\nabla F^{d}(t,\mathbf{x}), \tag{5.36}$$

$$\frac{\partial F^{e}(t,\mathbf{x})}{\partial t} = \delta\left[F^{a}(t,\mathbf{x}) + F^{b}(t,\mathbf{x}) + F^{c}(t,\mathbf{x}) + F^{d}(t,\mathbf{x})\right] + \varepsilon F^{f}(t,\mathbf{x}) - (4\delta + \varepsilon) F^{e}(t,\mathbf{x}) + v\mathbf{e}\cdot\nabla F^{e}(t,\mathbf{x}), \tag{5.37}$$

$$\frac{\partial F^{f}(t,\mathbf{x})}{\partial t} = \psi\left[F^{a}(t,\mathbf{x}) + F^{b}(t,\mathbf{x}) + F^{c}(t,\mathbf{x}) + F^{d}(t,\mathbf{x})\right] + \psi F^{e}(t,\mathbf{x}) - (4\varphi + \psi) F^{f}(t,\mathbf{x}) + v\mathbf{f}\cdot\nabla F^{f}(t,\mathbf{x}), \tag{5.38}$$

where symbol "·" denotes the inner product of vectors and ∇ is the symbol of gradient.

In the matrix form the system of equations takes the form

$$\frac{\partial}{\partial t}\begin{bmatrix} F^{a} \\ F^{b} \\ F^{c} \\ F^{d} \\ F^{e} \\ F^{f} \end{bmatrix} = \begin{bmatrix} -\Omega & \alpha_1 & \beta & \alpha_2 & \kappa & \gamma \\ \alpha_2 & -\Omega & \alpha_1 & \beta & \kappa & \gamma \\ \beta & \alpha_2 & -\Omega & \alpha_1 & \kappa & \gamma \\ \alpha_1 & \beta & \alpha_2 & -\Omega & \kappa & \gamma \\ \delta & \delta & \delta & \delta & -(4\delta + \varepsilon) & \varepsilon \\ \varphi & \varphi & \varphi & \varphi & \psi & -(4\varphi + \psi) \end{bmatrix} \begin{bmatrix} F^{a} \\ F^{b} \\ F^{c} \\ F^{d} \\ F^{e} \\ F^{f} \end{bmatrix} + v \begin{bmatrix} \frac{\partial}{\partial x_2} & 0 & 0 & 0 & 0 & 0 \\ 0 & -\frac{\partial}{\partial x_1} & 0 & 0 & 0 & 0 \\ 0 & 0 & -\frac{\partial}{\partial x_2} & 0 & 0 & 0 \\ 0 & 0 & 0 & \frac{\partial}{\partial x_1} & 0 & 0 \\ 0 & 0 & 0 & 0 & \frac{\partial}{\partial x_3} & 0 \\ 0 & 0 & 0 & 0 & 0 & -\frac{\partial}{\partial x_3} \end{bmatrix} \begin{bmatrix} F^{a} \\ F^{b} \\ F^{c} \\ F^{d} \\ F^{e} \\ F^{f} \end{bmatrix}, \tag{5.39}$$

where $\Omega = (\alpha_1 + \alpha_2 + \beta + \kappa + \gamma)$.

To complete the mathematical description of the transport phenomenon we must assume the initial and boundary conditions for the probability density (or in another interpretation: the pollutant concentration density) functions sought for. As we have assumed, the plane $\{\mathbf{x} = (x, y, 0)^T, x, y \in \mathbb{R}\}$ is the absorbing boundary. This causes the vanishing of all the conditional probability density functions (see [11]):

$$F^{a}(t,x,y,0) = F^{b}(t,x,y,0) = F^{c}(t,x,y,0) = F^{d}(t,x,y,0) = F^{e}(t,x,y,0) = F^{f}(t,x,y,0) = 0. \tag{5.40}$$

In our interpretation of the functions $F^{\mathbf{w}}$, $\mathbf{w} = \mathbf{a}, \mathbf{b}, \mathbf{c}, \mathbf{d}, \mathbf{e}, \mathbf{f}$, the initial condition represents the initial location of the fractions of the pollutant particles initiating their walk in a given direction. Since we have assumed the point source of the particles, the initial functions are three-dimensional Dirac delta-functions concentrated at point $(0, 0, z_0)^T$,

$$F^{a}(0,x,y,z) = a_0\delta(x)\,\delta(y)\,\delta(z - z_0), \tag{5.41}$$

$$F^{b}(0,x,y,z) = b_0\delta(x)\,\delta(y)\,\delta(z - z_0), \tag{5.42}$$

$$F^{c}(0,x,y,z) = c_0\delta(x)\,\delta(y)\,\delta(z - z_0), \tag{5.43}$$

$$F^{d}(0,x,y,z) = d_0\delta(x)\,\delta(y)\,\delta(z - z_0), \tag{5.44}$$

$$F^{e}(0,x,y,z) = e_0\delta(x)\,\delta(y)\,\delta(z - z_0), \tag{5.45}$$

$$F^{f}(0,x,y,z) = f_0\delta(x)\,\delta(y)\,\delta(z - z_0), \tag{5.46}$$

where the sum of all intensities equals one,

$$a_0 + b_0 + c_0 + d_0 + e_0 + f_0 = 1. \tag{5.47}$$

Certainly, one can consider some more general problem in which the boundary absorbing condition is given on a more complicated surface, or the initial condition is distributed over the space in a different manner.

6. Concluding remarks

In this paper we have proposed several models of the random walk process occurring with a finite speed, useful for the description of transport of the particles. The models are not very restrictive. They can be easily adopted to describe the transport process in many physical environments: turbulent atmosphere, soil or water, depending on the selection of the parameters.

In our considerations, starting from the law of motion of the particle, we have derived the global transport equations for the probability density functions of particle location (or the equations for the pollutant concentration). The obtained equations constitute the system of linear partial differential equations with constant coefficients. The problem of existence and uniqueness of the solutions to such equations has been

already solved. Since we assume that the solutions of the equations are probability density functions, we are looking for the solutions in the class of functions integrable with some polynomial weights (functions with finite moments). It is proved (see [1]) that if the initial conditions and possible excitations (sources) have this property, then the solution will exist, will be unique and also (locally) integrable with a polynomial weight.

The equations obtained can be used for a quantitative analysis of the modeled transport processes. The simplest way of doing this is based on their numerical solution. This is quite natural since they are obtained as the limit of the difference equations, directly applicable for computational analysis. Some conclusions concerning the transport process can be also drawn analytically. Since the transport equations are hyperbolic, we can estimate the effective velocity of the pollutant front from the source.

The proposed random walk process can be studied not only globally, by the analysis of the transport equation. Another possible approach is the investigation of the trajectory equation (2.4) and its multi-dimensional generalizations. It necessitates the application of the random matrix methods (see [4]); in such a manner we can obtain another kind of information concerning the diffusion particles – the areas of concentration, eventual attraction curves, etc.

Application of the proposed models for the description of real transport problems requires identification of the parameters characterizing the probability intensities of the velocity direction jumps, as well as the absolute values of the velocity.

Studying the pollutant particles structure we can try to estimate the probability intensities (e.g. large particle rather sediments than convects, etc.), but complete identification of the model needs some well-prepared experimental data to estimate the parameters of the model. The measurements in the experiment must be performed in a specific way to make them useful for the identification of our model (see [3]). Design of such an experiment and estimation of the parameters is a very important task to solve in modeling of the pollution transport in turbulent atmosphere with the use of random walk process.

References

1. L. HÖRMANDER *The analysis of linear partial differential operators. II. Differential operators with constant coefficients*, Springer 1983.
2. M. KAC, *Some stochastic problems in physics and mathematics*, Magnolia Petroleum Co., 1956.
3. P. KAZIMIERCZYK, Z. KOTULSKI, *On the optimal sensors' location* [in Polish], IFTR Reports, 42/87, pp. 1–123, 1987.
4. H. KESTEN, *Random difference equations and renewal theory for products of random matrices*, Acta Mathematica, 131, 207–248, 1973.
5. Z. KOTULSKI, *On the Markovian model of turbulent diffusion*, Reports on Math. Phys., 24, 1, 129–140,
6. Z. KOTULSKI, K. SOBCZYK, *Non-local description of pollution transport in random medium*, IFTR Reports, 34, 1992 (also, Modeling and Scientific Computing, 1, 1, 142–152, 1993).

7. G. C. POMRANING, *Linear kinetic theory and particle transport in stochastic mixtures*, World Scientific, Singapore 1991.
8. Z. SORBIAN, *Turbulence and diffusion in the lower atmosphere* [in Polish], PWN, Warsaw 1983.
19. H. SPOHN, *Large scale dynamics of interacting particles*, Springer, Berlin 1991.
10. D.J. THOMSON, *Criteria for selection of stochastic models of particle trajectories in turbulent flows*, J. Fluid Mech., 180, 529–556, 1987.
11. V. I. TIKHONOV, M.A. MIRNOV, *Markov processes*, Soviet. Radio Editors , Moscow 1977.

POLISH ACADEMY OF SCIENCES
INSTITUTE OF FUNDAMENTAL TECHNOLOGICAL RESEARCH.

Received June 25, 1993.

Arch. Mech., 45, 5, pp. 563-573, Warszawa 1993

Hodograph method in steady plane MHD micropolar fluid flows

I. ADLURI (WHEELING) and A.M.S. EL KARAMANY (TRIPOLI)

EQUATIONS of motion of a steady plane MHD micropolar fluid flow are transformed to the hodograph plane by means of the Legendre transform function of the stream-function. Results are summarized in the form a theorem, some flow problems of physical importance are investigated as applications of this theorem and exact solutions and geometry of the flow are obtained in each case.

1. Introduction

IN RECENT YEARS, the flow of micropolar fluids has been studied by many investigators using the theory and constitutive equations first given and developed by ERINGEN [1, 2]. He presented the theory which is the generalization of the theory of viscous fluids by taking into account the local microrotations and microinertia. The mathematical model underlying micropolar fluid may represent liquid crystals, suspensions, animal blood and fluids consisting of dumb-bell molecules. The problem of finding exact solutions of governing equations of micropolar fluid flows presents insurmountable mathematical difficulties due to the fact that these equations are nonlinear. However, exact solutions have been obtained by many researchers in certain particular cases, mostly when the nonlinear convective terms vanish in a natural way.

The present study deals with the application of hodograph transformation to obtain exact solutions of the governing equations of a steady plane flow of an electrically conducting micropolar fluid in the presence of a transverse magnetic field. CHANDNA *et al.* [3–9] have used hodograph and Legendre transformations to investigate steady plane viscous flows, non-Newtonian flows, and constantly aligned, transverse and orthogonal MHD non-Newtonian flows. Recently, ADLURI [10, 11] has applied hodograph method to obtain some exact solutions of the flow equations of steady plane micropolar fluid and orthogonal MHD non-Newtonian fluid.

First, the equations of the flow are transformed to the hodograph plane interchanging the role of independent variables x, y and the velocity components u, v; then, introducing a Legendre transform function of the stream-function, all equations in the hodograph plane are expressed in terms of this transform function. These results are put together as a theorem and some interesting flow problems of both physical and geometrical importance are discussed as applications of this theorem. It is observed that radial and spiral flows cannot exist in a micropolar fluid whether fluid is conducting or nonconducting.

2. Equations of motion

The equations governing the steady plane MHD polar fluid flow in the presence of a transverse magnetic field, in the absence of body forces and body couples, are given by

$$\frac{\partial u}{\partial y}+\frac{\partial v}{\partial y}=0, \tag{2.1}$$

$$\frac{\partial h}{\partial x}=\rho v\omega+k\frac{\partial v}{\partial y}-(\mu+k)\frac{\partial \omega}{\partial y}, \tag{2.2}$$

$$\frac{\partial h}{\partial y}=-\rho u\omega-k\frac{\partial v}{\partial x}+(\mu+k)\frac{\partial \omega}{\partial x}, \tag{2.3}$$

$$\rho j\left(u\frac{\partial v}{\partial x}+v\frac{\partial v}{\partial y}\right)=-2kv+k\omega+\gamma\left(\frac{\partial^2 v}{\partial x^2}+\frac{\partial^2 v}{\partial y^2}\right), \tag{2.4}$$

$$\frac{u\partial H}{\partial x}+\frac{v\partial H}{\partial y}=\frac{1}{\mu_e\sigma}\left(\frac{\partial^2 H}{\partial x^2}+\frac{\partial^2 H}{\partial y^2}\right), \tag{2.5}$$

$$\omega=\frac{\partial v}{\partial x}-\frac{\partial u}{\partial y}, \tag{2.6}$$

$$h=\frac{1}{2}\rho(u^2+v^2)+p+\frac{1}{2}\mu_e H^2, \tag{2.7}$$

where $(u(x, y), v(x, y), 0)$ represents the velocity vector field, $(0, 0, H(x, y))$ is the magnetic field, $(0, 0, v(x, y))$ is the micropolar field, ω is the vorticity, p is the pressure, ρ is the density, μ_e is the constant magnetic permeability, σ is electrical conductivity, j is the microinertia and μ, k, γ are the material constans.

Eliminating h between Eqs. (2.2) and (2.3), we get

$$\rho\left(u\frac{\partial \omega}{\partial x}+v\frac{\partial \omega}{\partial y}\right)=-k\left(\frac{\partial^2 v}{\partial x^2}+\frac{\partial^2 v}{\partial y^2}\right)+(\mu+k)\left(\frac{\partial^2 \omega}{\partial x^2}+\frac{\partial^2 \omega}{\partial y^2}\right). \tag{2.8}$$

3. Equations in the hodograph plane

Let the flow variables $u(x, y)$, $v(x, y)$ be such that, in the region of flow, the Jacobian

$$J(x, y)=\frac{\partial(u, v)}{\partial(x, y)}\neq 0.$$

Considering x, y as functions of u and v, we can derive the following relations:

$$\frac{\partial u}{\partial x} = J\frac{\partial y}{\partial v}, \quad \frac{\partial u}{\partial y} = -J\frac{\partial x}{\partial v}, \quad \frac{\partial v}{\partial x} = -J\frac{\partial y}{\partial u}, \quad \frac{\partial v}{\partial y} = J\frac{\partial x}{\partial u}, \tag{3.1}$$

$$J(x, y) = \frac{\partial(u, v)}{\partial(x, y)} = \left[\frac{\partial(x, y)}{\partial(u, v)}\right]^{-1} = \bar{J}(u, v), \tag{3.2}$$

$$\frac{\partial f}{\partial x} = \frac{\partial(f, y)}{\partial(x, y)} = J\frac{\partial(\bar{f}, y)}{\partial(u, v)} = \bar{J}\frac{\partial(\bar{f}, y)}{\partial(u, v)}, \tag{3.3}$$

$$\frac{\partial f}{\partial y} = -\frac{\partial(f, x)}{\partial(x, y)} = J\frac{\partial(x, \bar{f})}{\partial(u, v)} = \bar{J}\frac{\partial(x, \bar{f})}{\partial(u, v)}, \tag{3.4}$$

where $f(x, y) = f(x(u, v), y(u, v) = f(u, v)$ is any continuously differentiable function.

Using the above relations, we can transform Eqs. (2.1), (2.8), (2.4) and (2.5), respectively, into the following equations:

$$\frac{\partial x}{\partial u} + \frac{\partial y}{\partial v} = 0, \tag{3.5}$$

$$\rho(vP_1 + uP_2) = -k\left\{\frac{\partial(x, \bar{J}Q_1)}{\partial(u, v)} + \frac{\partial(\bar{J}Q_2, y)}{\partial(u, v)}\right\} + (\mu + k)\left\{\frac{\partial(x, \bar{J}P_1)}{\partial(u, v)} + \frac{\partial(\bar{J}P_2, y)}{\partial(u, v)}\right\}, \tag{3.6}$$

$$\rho jJ(vQ_1 + uQ_2) = -2k\bar{v} + k\bar{\omega} + \gamma\bar{J}\left\{\frac{\partial(x, \bar{J}Q_1}{\partial(u, v)} + \frac{\partial(\bar{J}Q_2, y)}{\partial(u, v)}\right\}, \tag{3.7}$$

$$(vR_1 + uR_2) = \frac{1}{\mu_e\sigma}\left\{\frac{\partial(x, \bar{J}R_1)}{\partial(u, v)} + \frac{\partial(\bar{J}R_2, y)}{\partial(u, v)}\right\}, \tag{3.8}$$

where

$$\begin{aligned} \omega(x, y) &= \omega(x(u, v), y(u, v)) = \bar{\omega}(u, v), \\ v(x, y) &= v(x(u, v), y(u, v)) = \bar{v}(u, v), \\ H(x, y) &= H(x(u, v), y(u, v)) = \bar{H}(u, v); \end{aligned} \tag{3.9}$$

$$\begin{aligned} P_1 = P_1(u, v) &= \frac{\partial(x, \bar{\omega})}{\partial(u, v)}, \qquad P_2 = P_2(u, v) = \frac{\partial(\bar{\omega}, y)}{\partial(u, v)}, \\ Q_1 = Q_1(u, v) &= \frac{\partial(x, \bar{v})}{\partial(u, v)}, \qquad Q_2 = Q_2(u, v) = \frac{\partial(\bar{v}, y)}{\partial(u, v)}, \\ R_1 = R_1(u, v) &= \frac{\partial(x, \bar{H})}{\partial(u, v)}, \qquad R_2 = R_2(u, v) = \frac{\partial(\bar{H}, y)}{\partial(u, v)}. \end{aligned} \tag{3.10}$$

Equations (3.5) – (3.8) constitute a system of four equations for four unknown functions $x(u, v)$, $y(u, v)$, $\bar{v}(u, v)$ and $\bar{H}(u, v)$. Once this system is solved for these functions, we can determine $u(x, y)$, $v(x, y)$, $v(x, y)$, $\omega(x, y)$, $H(x, y)$ and $p(x, y)$ for the

system of equations (2.1) – (2.6) governing the steady plane flow of a MHD micropolar fluid under the influence of a transverse magnetic field.

4. Equations in Legendre transform function — $\bar{v}(u, v)$ and $\overline{H}(u, v)$

Equation of continuity (2.1) implies the existence of a stream-function $\psi(x, y)$ such that

$$d\psi = -v\,dx + u\,dy \quad \text{or} \quad \frac{\partial \psi}{\partial x} = -v, \quad \frac{\partial \psi}{\partial y} = u \tag{4.1}$$

and Eq. (3.5) implies the existence of a function $L(u, v)$ called a Legendre transform function of the stream-function $\psi(x, y)$, so that

$$dL = -y\,du + x\,dv \quad \text{or} \quad \frac{\partial L}{\partial u} = -y, \quad \frac{\partial L}{\partial v} = x. \tag{4.2}$$

Functions $\psi(x, y)$ and $L(u, v)$ are related by

$$L(u,v) = vx - uy + \psi(x, y). \tag{4.3}$$

Using Eq. (4.2), Eqs. (3.5)–(3.10) can be transformed into the following equations:

$$\rho(vP_1 + uP_2) = -k\left\{\frac{\partial(\partial L/\partial v,\ \bar{J}Q_1)}{\partial(u,\ v)} + \frac{\partial(\partial L/\partial u,\ \bar{J}Q_2)}{\partial(u,\ v)}\right\} + (\mu + k)\left\{\frac{\partial(\partial L/\partial v,\ \bar{J}P_1)}{\partial(u,\ v)} + \frac{\partial(\partial L/\partial u,\ \bar{J}P_2)}{\partial(u,\ v)}\right\}, \tag{4.4}$$

$$\rho j\bar{J}(vQ_1 + uQ_2) = -2k\bar{v} + k\bar{\omega} + \gamma\bar{J}\left\{\frac{\partial(\partial L/\partial v,\ \bar{J}Q_1)}{\partial(u,\ v)} + \frac{\partial(\partial L/\partial u,\ \bar{J}Q_2)}{\partial(u,\ v)}\right\}, \tag{4.5}$$

$$(vR_1 + uR_2) = \frac{1}{\mu_e \sigma}\left\{\frac{\partial(\partial L/\partial v,\ \bar{J}R_1)}{\partial(u,\ v)} + \frac{\partial(\partial L/\partial u,\ \bar{J}R_2)}{\partial(u,\ v)}\right\}, \tag{4.6}$$

$$P_1 = \frac{\partial(\partial L/\partial v,\ \bar{\omega})}{\partial(u,\ v)}, \qquad P_2 = \frac{\partial(\partial L/\partial u,\ \bar{\omega})}{\partial(u,\ v)},$$

$$Q_1 = \frac{\partial(\partial L/\partial v,\ \bar{v})}{\partial(u,\ v)}, \qquad Q_2 = \frac{\partial(\partial L/\partial u,\ \bar{v})}{\partial(u,\ v)}, \tag{4.7}$$

$$R_1 = \frac{\partial(\partial L/\partial v,\ \overline{H})}{\partial(u,\ v)}, \qquad R_2 = \frac{\partial(\partial L/\partial u,\ \overline{H})}{\partial(u,\ v)},$$

where

$$\bar{J} = \left[\frac{\partial^2 L}{\partial u^2}\cdot\frac{\partial^2 L}{\partial v^2}+\left(\frac{\partial^2 L}{\partial u\partial v}\right)^2\right]^{-1}, \tag{4.8}$$

$$\bar{\omega} = \bar{J}\left(\frac{\partial^2 L}{\partial u^2}-\frac{\partial^2 L}{\partial v^2}\right). \tag{4.9}$$

From Eqs. (4.4)–(4.9), we have the following theorem:

THEOREM. *If $L(u, v)$ is the Legendre transform function of a stream-function of a steady plane flow of a MHD micropolar fluid in the presence of a transverse magnetic field, and $\bar{v}(u, v)$ and $\bar{H}(u, v)$ are transformed components of microrotation and magnetic field, then $L(u, v)$, $\bar{v}(u, v)$ and $\bar{H}(u, v)$ must satisfy Eqs.* (4.4)–(4.6), *where $\bar{\omega}(u, v)$, $\bar{J}(u, v)$, $P_1(u, v)$, $P_2(u, v)$, $Q_1(u, v)$, $Q_2(u, v)$, $R_1(u, v)$ and $R_2(u, v)$ are given by Eq.* (4.7)–(4.9).

5. Applications

To reveal the implications of the results obtained in the previous section, we shall investigate some flow problems of physical interest as application of the theorem.

APPLICATION I

Let

$$L(u, v) = Au^2+Bv^2 \tag{5.1}$$

be the Legendre transformed function, A and B are nonzero constants.

Substituting Eq. (5.1) in Eqs. (4.4)–(4.9), we get

$$\bar{J} = \frac{1}{4AB}, \quad \bar{\omega} = \frac{A+B}{2AB}, \quad P_1 = 0, \quad P_2 = 0, \tag{5.2}$$

$$Q_1 = -\frac{2B\partial\bar{v}}{\partial u}, \quad Q_2 = \frac{2A\partial\bar{v}}{\partial v}, \quad R_1 = -\frac{2B\partial\bar{H}}{\partial u}, \quad R_2 = \frac{2A\partial\bar{H}}{\partial v}, \tag{5.3}$$

$$B^2\frac{\partial^2\bar{v}}{\partial u^2}+A^2\frac{\partial^2\bar{v}}{\partial v^2} = 0, \tag{5.4}$$

$$\frac{\rho j}{2AB}\left(Au\frac{\partial\bar{v}}{\partial v}-Bv\frac{\partial\bar{v}}{\partial u}\right) = -2k\bar{v}+k\frac{(A+B)}{2AB}, \tag{5.5}$$

$$2AB\left(Au\frac{\partial\bar{H}}{\partial v}-Bv\frac{\partial\bar{H}}{\partial u}\right) = \frac{1}{\mu_e\sigma}\left(B^2\frac{\partial^2\bar{H}}{\partial u^2}+A^2\frac{\partial^2\bar{H}}{\partial v^2}\right). \tag{5.6}$$

Solving Eqs. (5.4) and (5.5) for $\bar{v}(u, v)$, we get

$$\bar{v} = c_1\left(u-\frac{4Bkv}{\rho j}\right)+\frac{(A+B)}{4AB} \tag{5.7}$$

provided

$$AB = -\frac{\rho^2 j^2}{16k^2}, \tag{5.8}$$

where c_1 is an arbitrary constant.

Solving Eq. (5.6), we obtain

$$\overline{H}(u, v) = H_0 \tag{5.9}$$

where H_0 is a constant. Condition (5.8) implies that both A and B are nonzero, unequal and have opposite signs. Since $A \neq B$, it follows that a steady plane flow of a micropolar fluid cannot be a vortex flow whether the fluid is conducting or nonconducting.

Using Eq. (5.1) in Eqs. (4.2) and (5.7), we get

$$u(x, y) = -\frac{y}{2A}, \quad v(x, y) = \frac{x}{2B} \tag{5.10}$$

$$v(x, y) = -\frac{c_1}{2A\rho j}(4kAx + \rho j y) + \frac{A+B}{4AB}. \tag{5.11}$$

Substituting Eqs. (5.10) and (5.11) in Eqs. (2.2) and (2.3) and integrating the resulting equations, one can obtain

$$h(x, y) = \frac{\rho(A+B)}{8AB}\left(\frac{x^2}{B} + \frac{y^2}{A}\right) - \frac{kc_1}{2A}x + \frac{2c_1}{\rho j}k^2 y + \frac{\mu_e}{2}H_0^2 + \text{const}$$

which, on using in Eq. (2.7), yields

$$p(x, y) = \frac{\rho}{8AB}(x^2 + y^2) - \frac{kc_1}{2A}x + \frac{2c_1}{\rho j}k^2 y + \frac{\mu_e}{2}H_0^2 + \pi_1 \tag{5.12}$$

where π_1 is an arbitrary constant.

From Eqs. (4.3), (5.1) and (5.10) we get

$$\psi(x, y) = \frac{x^2}{4B} + \frac{y^2}{4A}, \tag{5.13}$$

where A and B are unequal and have opposite signs.

If $L(u, v) = Au^2 + Bv^2$ is the Legendre transform function of a steady plane flow of a MHD micropolar fluid of finite electrical conductivity in the presence of a transverse magnetic field $(0, 0, H_0)$, then the flow in the physical plane is a flow with hyperbolic stream-lines and the flow variables are given by Eqs. (5.9)–(5.13).

In case of infinitely conducting fluid, i.e. for $\sigma \to \infty$, the diffusion equation (5.6) simplifies to

$$Au\frac{\partial \overline{H}}{\partial v} - Bv\frac{\partial \overline{H}}{\partial u} = 0. \tag{5.14}$$

Solving this equation, we have

$$\bar{H}(u, v) = F\left(\frac{Au^2}{2}+\frac{Bv^2}{2}\right), \tag{5.15}$$

where F is an arbitrary function of its argument.

Proceeding as in the previous case, $H(x, y)$ and $p(x, y)$ can be found in the following form:

$$H(x, y) = F\left(\frac{x^2}{8B}+\frac{y^2}{8A}\right), \tag{5.16}$$

$$p(x, y) = \frac{\rho}{8AB}(x^2+y^2) - \frac{kc_1}{2A}x+\frac{2c_1k^2}{\rho j}y+\frac{\mu_e}{2}\left\{F\left(\frac{x^2}{8B}+\frac{y^2}{8A}\right)\right\}^2+\pi_2 \tag{5.17}$$

where π_2 is an arbitrary constant.

APPLICATION II

Let

$$L(u, v) = (A_1u+B_1)v+C_1u^2+D_1u+E_1 \tag{5.18}$$

be the Legendre transform function, where $A_1 \neq 0$, B_1, C_1, D_1, E_1 are arbitrary constants.

Proceeding as in the previous application, we can obtain

$$\bar{J} = -\frac{1}{A_1^2}, \quad \bar{\omega} = -\frac{2C_1}{A_1^2}, \quad P_1 = 0, \quad P_2 = 0, \tag{5.19}$$

$$Q_1 = A_1\frac{\partial \bar{v}}{\partial v}, \quad Q_2 = 2C_1\frac{\partial \bar{v}}{\partial v} - A_1\frac{\partial \bar{v}}{\partial u}, \quad R_1 = A_1\frac{\partial \bar{H}}{\partial v}, \quad R_2 = 2C_1\frac{\partial \bar{H}}{\partial v} - A_1\frac{\partial \bar{H}}{\partial u}.$$

Using Eqs. (5.18) and (5.19), (4.4)–(4.6) can be simplified, respectively, to

$$\frac{\partial^2 \bar{v}}{\partial u^2} - \frac{4C_1}{A_1}\frac{\partial^2 \bar{v}}{\partial u \partial v}+\left(1+\frac{4C_1^2}{A_1^2}\right)\frac{\partial^2 \bar{v}}{\partial v^2} = 0, \tag{5.20}$$

$$\frac{\rho j}{A_1^2}\left\{(A_1v+2C_1u)\frac{\partial \bar{v}}{\partial v} - A_1u\frac{\partial \bar{v}}{\partial u}\right\} = 2k\bar{v}+\frac{2kC_1}{A_1^2}, \tag{5.21}$$

$$\left\{(A_1v+2C_1u)\frac{\partial \bar{H}}{\partial v} - A_1u\frac{\partial \bar{H}}{\partial u}\right\} = \frac{1}{\mu_e\sigma}\left\{\frac{4C_1}{A_1}\frac{\partial^2 \bar{H}}{\partial u \partial v}-\left(1+\frac{4C_1^2}{A_1^2}\right)\frac{\partial^2 \bar{H}}{\partial v^2} - \frac{\partial^2 \bar{H}}{\partial u^2}\right\}. \tag{5.22}$$

Solving the system of equations (5.20)–(5.22), we get

$$\bar{v}(u, v) = c_2\left(u+\frac{A_1}{C_1}v\right) - \frac{C_1}{A_1^2}, \tag{5.23}$$

$$\overline{H}(u, v) = \lambda_1 \int \left[\exp\left(\frac{1}{2} A_1 \mu_e \sigma u^2 \right) \right] du + \lambda_2 , \tag{5.24}$$

$$A_1 = \frac{\rho j}{2k}, \tag{5.25}$$

where c_2, λ_1, λ_2 are arbitrary constants.

Employing the previous technique, we obtain the flow variables as

$$u(x, y) = \frac{(x - B_1)}{A_1}, \quad v(x, y) = -\frac{(2C_1 x + A_1 y - 2B_1 C_1 + A_1 D_1)}{A_1^2}, \tag{5.26}$$

$$\bar{v}(x, y) = -C_2 \left\{ \frac{(x - B_1)}{A_1} + \frac{(y + D_1)}{C_1} \right\} - \frac{C_1}{A_1^2}, \tag{5.27}$$

$$H(x, y) = \frac{\lambda_1}{A_1} \int \left[\exp\left\{ \frac{\mu_e \sigma}{2A_1} (x - B_1)^2 \right\} \right] dx + \lambda_2 , \tag{5.28}$$

$$p(x, y) = \frac{2C_1 \rho}{A} \{ C_1 x^2 + (A_1 D_1 - 2B_1 C_1) x + A_1 y (x - B_1) \} - \frac{\rho}{2} \left\{ \frac{(x - B_1)^2}{A_1^2} + \frac{(2C_1 x + A_1 y - 2B_1 C_1 + A_1 D_1)^2}{A_1^4} \right\} - \frac{\mu_e}{2} \left\{ \frac{\lambda_1}{A_1} \int \left[\exp\left\{ \frac{\mu_e \sigma}{2A_1} (x - B_1)^2 \right\} \right] dx + \lambda_2 \right\}^2 + \pi_3 , \tag{5.29}$$

$$\psi(x, y) = C_1 \frac{(x - B_1)}{A_1} \left\{ \frac{(x - B_1)}{A_1} + \frac{(y + D_1)}{C_1} \right\} + E_1 , \tag{5.30}$$

where π_3 is an arbitrary constant.

If $L(u, v) = (A_1(u + B_1)v + C_1 u^2 + D_1 u + E_1$ is the Legendre transform function of a stream-function of a steady plane flow of a finitely conducting micropolar fluid in the presence of a transverse magnetic field, then the flow variables are given by Eqs. (5.26)–(5.30) when $A_1 = \rho j/2k$, and the flow in the physical plane is:

a) a flow with $C_1 x^2 + A_1 xy - A_1 B_1 y + (A_1 D_1 - 2B_1 C_1) x =$ constant as stream-lines when $C_1 \neq 0$ in $L(u, v)$,

b) a flow with rectangular hyperbolas $(x - B_1)(y + D_1) =$ constant as stream-lines when $C_1 = 0$ in $L(u, v)$. In case of infinitely conducting fluid, Eq. (5.20) and (5.21) remain unaltered whereas the diffusion equation (5.22) reduces to

$$(A_1 v + 2C_1 u) \frac{\partial \overline{H}}{\partial v} - A_1 u \frac{\partial \overline{H}}{\partial u} = 0 . \tag{5.31}$$

Solving this, we get

$$\bar{H}(u, v) = G(C_1u^2 + A_1uv), \tag{5.32}$$

where G is an arbitrary function of its argument.

Using Eq. (5.25), $H(x, y)$ can be obtained as

$$H(x, y) = G\left[\frac{-C_1(x-B_1)^2 - A_1(x-B_1)(y+D_1)}{A_1^2}\right]. \tag{5.33}$$

The pressure function, in this case, is given by

$$p(x, y) = \frac{2C_1\rho}{A_1^4}\{C_1x^2 + (A_1D_1 - 2B_1C_1)x + A_1y(x - B_1)\} \tag{5.34}$$

$$-\frac{\rho}{2}\left\{\frac{(x-B_1)^2}{A_1^2} + \frac{(2C_1x + A_1y + A_1D_1 - 2B_1C_1)^2}{A_1^4}\right\}$$

$$+kc_2\left(\frac{x}{C_1} - \frac{y}{A_1}\right) - \frac{\mu_e}{2}\{G(x, y)\}^2 + \pi_4,$$

where π_4 is an arbitrary constant.

The flow variables of a steady plane micropolar fluid of infinite electrical conductivity are given by Eqs. (5.26), (5.27), (5.33) and (5.34).

APPLICATION III (Radial flow)

Letting

$$L(u, v) = A_2 \tan^{-1}(v/u) + B_2, \quad A_2 \neq 0, \tag{5.35}$$

and employing the procedure used in the previous applications, we get

$$\bar{J} = -\frac{(u^2+v^2)^2}{A_2^2}, \quad \bar{\omega} = 0, \quad P_1 = 0, \quad P_2 = 0, \tag{5.36}$$

$$\frac{\partial^2\bar{v}}{\partial u^2} + \frac{\partial^2\bar{v}}{\partial v^2} = 0, \tag{5.37}$$

$$u\frac{\partial\bar{v}}{\partial u} + v\frac{\partial\bar{v}}{\partial v} = \frac{2kA_2\bar{v}}{\rho j(u^2+v^2)}, \tag{5.38}$$

$$\frac{A_2}{(u^2+v^2)}\left(u\frac{\partial\bar{H}}{\partial u} + v\frac{\partial\bar{H}}{\partial v}\right) + \frac{1}{\mu_e\sigma}\left(\frac{\partial^2\bar{H}}{\partial u^2} + \frac{\partial^2\bar{H}}{\partial v^2}\right) = 0. \tag{5.39}$$

Solving Eqs. (5.37) and (5.38), we have

$$\bar{v}(u, v) = 0, \tag{5.40}$$

which is a trivial solution. Therefore, in a steady plane micropolar fluid a radial flow cannot exist whether the fluid is conducting or nonconducting.

APPLICATION IV (Spiral flow)
Let

$$L(u, v) = \frac{1}{2} A_3 \ln(u^2+v^2) + B_3 \tan^{-1}(v/u), \tag{5.41}$$

where $A_3 \neq 0$, $B_3 \neq 0$.

Using Eq. (5.41) in Eqs. (4.4)–(4.9), we obtain

$$\bar{J} = -\frac{(u^2+v^2)^2}{(A_3^2+B_3^2)}, \quad \bar{\omega} = 0, \quad P_1 = 0, \quad P_2 = 0, \tag{5.42}$$

$$\frac{\partial^2 \bar{v}}{\partial u^2} + \frac{\partial^2 \bar{v}}{\partial v^2} = 0, \tag{5.43}$$

$$\frac{\rho j (u^2+v^2)}{A_3^2+B_3^2} \left\{ (B_3 v - A_3 u) \frac{\partial \bar{v}}{\partial v} + (B_3 u - A_3 v) \frac{\partial \bar{v}}{\partial u} \right\} = 2k\bar{v}, \tag{5.44}$$

$$\frac{(B_3 - A_3 u)}{(u^2+v^2)} \frac{\partial \bar{H}}{\partial v} + \frac{(B_3 u + A_3 v)}{(u^2+v^2)} \frac{\partial \bar{H}}{\partial u} + \frac{1}{\mu_e \sigma} \left(\frac{\partial^2 \bar{H}}{\partial u^2} + \frac{\partial^2 \bar{H}}{\partial v^2} \right) = 0. \tag{5.45}$$

Solution of Eqs. (5.43) and (5.44) is given by

$$\bar{v}(u, v) = 0, \tag{5.46}$$

which is again a trivial solution. From Eq. (5.46) it follows that in a steady plane micropolar fluid a spiral flow is not possible whether or not the fluid is conducting.

References

1. A.C. ERINGEN, *Simple micro-fluids*, Int. J. Engng. Sci., **2**, 205–217, 1964.
2. A.C. ERINGEN, *Theory of micropolar fluids*, J. Math. Mech., **16**, 1–18, 1966.
3. O.P. CHANDNA, R.M. BARRON and A.C. SMITH, *Rotation plane steady flow of viscous fluid*, SIAM J. Appl. Math., **42**, 1323–1336, 1982.
4. A.M. SIDDIQUI, Q.M. KALONI and O.P. CHANDNA, *Hodograph transformation methods in non--Newtonian fluid flows*, J. Engng. Math., **19**, 203–216, 1985.
5. O.P. CHANDNA and P.V. NGUYEN, *Hodograph method in non-Newtonian MHD transverse fluid flows*, J. Engng. Math., **23**, 119–139, 1989.
6. P.V. NGUYEN and O.P. CHANDNA, *Hodograph study of non-Newtonian MHD aligned steady plane flows*, Int. J. Math. and Math. Sci., **13**, 93–114, 1990.
7. O.P. CHANDNA and P.V. NGUYEN, *Hodograph transformation method and solution in aligned MHD plane flows*, Int. J. Engng. Sci., **28**, 973–987, 1990.
8. O.P. CHANDNA and P.V. NGUYEN, *Hodographic study of MHD constantly inclined flows*, Int. J. Engng. Sci., **30**, 69–82, 1992.

9. P.V. NGUYEN and O.P. CHANDNA, *Hodograph method in MHD orthogonal fluid flows*, Int. J. Math. and Math. Sci., **15**, 149–160, 1992.
10. I. ADLURI, *Hodographic study of plane micropolar fluid flows*, Int. J. Math. and Math. Sci., 1993 (to appear).
11. I. ADLURI, *Hodograph method in plane MHD non-Newtonian fluid flows*, Arch. Mech., **45**, 121–133, 1992.

DEPARTMENT OF MATHEMATICS
WHEELING JESUIT COLLEGE, WHEELING, USA
and
DEPARTMENT OF MATHEMATICS
ALFATEH UNIVERSITY, TRIPOLI, LIBYA.

Received August 12, 1993.

Arch. Mech., 45, 5, pp. 575-593, Warszawa 1993

On dynamics of systems modelling continuous and periodic guideways (*)

R. BOGACZ, T. KRZYŻYŃSKI (WARSZAWA) and K. POPP (HANNOVER)

THE PAPER DEALS with the dynamics of a class of mechanical systems which are referred to as periodic systems in the literature. A periodic system consists of a number of identical elements which are coupled in an identical way to form the complete system. The guideways for the Maglev vehicle are usually frames which are composed of repetitive elements. Here, the dynamical analysis leads to the investigation of continuous periodic structures. The aim of the paper is the determination of the dynamic response of the guideway to the action of a travelling disturbance source. The structure is modelled as a continuous Bernoulli – Euler beam which is made periodic system by the attachment of equally spaced supports. In the present paper the steady-state response is obtained in the form of a superposition of travelling waves. Also the problem of free wave propagation is briefly discussed. The method is based on Floquet's theorem and consists in a direct solution of the differential equation for the continuous beam, which allows to determine the displacement field in any cell of the periodic system.

1. Introduction

THE PAPER DEALS with the dynamics of a class of mechanical systems which are referred to as periodic systems in the literature. The periodic system consists of a number of identical elements which are coupled in an identical way to form the complete system. It may be constructed either by real assembling together the identical elements or by subdividing an uniform structure. The theory of periodic systems is well known in solid state physics and electrical engineering, cf. [1]. The development of mechanical continuous periodic systems is relatively new, and the papers like [2, 3, 4] constitute an important contribution both to the theory and to its applications. The intensive studies in this area are forced by the design and development of such modern systems like large space structures [5], ground pipelines [6] or elevated guideways for high-speed magnetically levitated vehicles (Maglev), cf. [7, 8, 9]. The guideways for Maglev systems are usually frames which are composed of repetitive elements and their dynamical analysis leads to the analysis of continuous periodic structures. Since Maglev systems are designed to connect large distances, the investigation of steady-state dynamics of the guideways under travelling disturbance sources is needed.

(*) Investigations supported by the KBN grant No 309389101 and the Alexander von Humboldt Foundation.

The major objective of the paper is to determine the dynamical response of the periodic structures modelling the guideways for high-speed vehicles. Two models of continuous periodic structure are considered. The first model (A) consists of an infinite Bernoulli – Euler beam resting on a viscoelastic Winkler-type foundation, cf. Fig. 1.

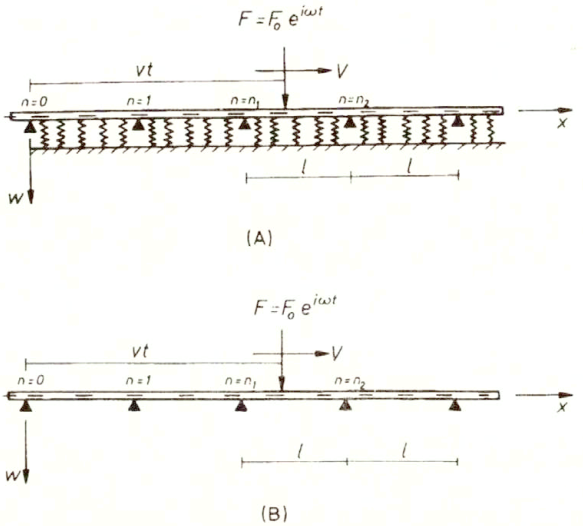

FIG. 1. System models.

The second model (B) differs from the first one in the absence of the foundation. The detailed analytical treatment presented in this paper concers mainly model (A), but the problems are formulated in such a way that most of the obtained expressions can be applied to both models. In order to compare some effects derived for models (A) and (B) with those for continuous but not periodic systems, we refer to model (C). The last one is either a beam on elastic foundation or a simple prismatic beam, in both cases without periodic supports. Thus, model (C) is a continuous system which is derived from the corresponding periodic one. The numerical results presented for models (A) and (B) have been obtained for the case of rigid periodic supports and pure elastic systems.

The investigation of forced vibrations follows the analysis of travelling waves propagation in the unloaded systems, which is presented in the next section of the paper. This analysis is needed for illustrating the fundamental properties of the periodic systems considered. In the case of forced steady-state vibrations, the disturbance source is taken in the form of a travelling harmonic force. Such a disturbance source enables us to examine all effects which are inseparably related to the dispersive systems, cf. [10, 11]. Additionally, the solution for the continuous periodic system under a travelling harmonic force makes it possible to study the dynamic interaction between a vehicle and the guideway by means of the way proposed in paper [12]. The case of a constant magnitude force travelling over an

infinite periodic structure has been studied in papers [7, 13]. One of the methods presented in [7] consists in an integral transformation of the displacement function and a numerical retransformation. The method presented in [13] is based on expanding the periodic interaction between flexible supports and the continuous beam into Fourier series. In the present paper the integral transform approach is developed for the case of a travelling harmonic force, and the retransformation is carried out by means of analytical methods.

2. Propagation of travelling waves in continuous periodic structures

2.1. Formulation of the problem

The equation of motion of the Bernoulli–Euler beam on a viscoelastic foundation, subjected to the load $\bar{p} = \bar{p}(x, t)$ is taken in the following form:

$$EI\frac{\partial^4 w}{\partial x^4} + \mu\frac{\partial^2 w}{\partial t^2} + \eta\frac{\partial w}{\partial t} + qw = \bar{p}(x, t), \tag{2.1}$$

where $w = w(x, t)$ is the displacement function of spatial variable x and time t. In Eq. (2.1) EI, μ, q and η denote the beam flexural stiffness, the beam mass per unit length, the foundation elasticity coefficient and the viscosity coefficient, respectively. To solve the dynamic problem for the periodic structure we follow the way proposed by MEAD [4] and consider the continuous beam under the action of an infinite array of concetrated forces which are the reaction forces exerted by the supports. In case of steady-state harmonic motion, the force magnitude p_{n+1} can be expressed as $p_{n+1} = p_n \cdot \exp(i\bar{\lambda} l)$, where $\bar{\lambda}$ is a complex number, and the load function $\bar{p}(x, t)$ takes the following form:

$$\bar{p}(x, t) = \sum_{-\infty}^{\infty} p_0 \cdot \delta(x - nl) \cdot e^{i(n\bar{\lambda} l + \omega t)}, \tag{2.2}$$

where p_0 is the magnitude of the reaction force at the support number $n = 0$, l is the spacing of the supports and ω is the frequency. In Eq. (2.2) the term $\delta(x - nl)$ denotes the Dirac-delta function.

The analysis which follows is carried out by means of non-dimensional quantities:

(A)

$X = xa_0$ space variable $(a_0 = \sqrt[4]{q/4EI})$,
$\tau = t\omega_0$ time $(\omega_0 = \sqrt{q/\mu})$,
$W(X, \tau)$ displacement of the beam, $W = w/w_0$, $(w_0 = p_0/(8EIa_0^3))$,
$\Omega = \omega/\omega_0$ frequency,
$N = \eta/\eta_0$ viscosity coefficient $(\eta_0 = 2\sqrt{q\mu})$,
$V = v/v_0$ velocity of the disturbance source $(v_0 = \omega_0/a_0,\ v_0 = \sqrt[4]{4qEI/\mu^2})$,
$L = la_0$ support spacing,
$\lambda = \bar{\lambda}/a_0$ wavenumber.

The non-dimensional equation of motion for model (A) obtained by means of the relations (A) can be expressed as

$$\frac{\partial^4 W}{\partial X^4}+4\frac{\partial^2 W}{\partial \tau^2}+8N\frac{\partial W}{\partial \tau}+4W=8\sum_{-\infty}^{\infty}\delta(X-nL)\cdot e^{i(n\lambda L+\Omega\tau)}. \tag{2.3}$$

In case of a beam resting on the periodic supports only, the foundation coefficient q vanishes in Eq. (2.1). The non-dimensional equation of motion for model (B) can be written in a form similar to Eq. (2.2),

$$\frac{\partial^4 W}{\partial X^4}+4\frac{\partial^2 W}{\partial \tau^2}+8N\frac{\partial W}{\partial \tau}=8\sum_{-\infty}^{\infty}\delta(X-nL)\cdot e^{i(n\lambda L+\Omega\tau)}. \tag{2.4}$$

The non-dimensional quantities can also be expressed by relations (A), but the characteristic values a_0, ω_0, η_0 and v_0 take the following form for model (B):

$$\text{(B)} \qquad a_0=\sqrt[4]{1/4I},\quad \omega_0=\sqrt{E/\mu},\quad \eta_0=2\sqrt{\mu E},\quad v_0=\omega_0/a_0=\sqrt[4]{4E^2I/\mu^2},$$

where E is Young's modulus for the beam and I is the moment of inertia of the beam cross-section.

The expressions for the function $W=W(X,\tau)$ presented in the paper follow from examination of case (A). The appropriate use of the relations (A) makes it possible to obtain the results for case (B).

2.2. Passing and stopping bands for elastic systems

The steady-state solution of Eq. (2.3)

$$W(X,\tau)=\overline{W}(X)\cdot\exp(i\Omega\tau), \tag{2.5}$$

can be obtained by means of the following Fourier transform technique:

$$\overline{W}^*(S)=\int_{-\infty}^{\infty}\overline{W}(X)\cdot e^{-iSX}\,dX,\qquad \overline{W}(X)=\frac{1}{2\pi}\int_{-\infty}^{\infty}\overline{W}^*(S)\cdot e^{-iSX}\,dS. \tag{2.6}$$

The displacement of the beam resulting from the application of Eqs. (2.5) and (2.6) to Eq. (2.3) can be expressed as

$$W(X,\tau)=8i\left[\sum_{j=1}^{2}A_j\cdot\left(\sum_{-\infty}^{n=n_1}e^{inL(\lambda-S_j)+iS_jX}+\sum_{n=n_1}^{\infty}e^{inL(\lambda-S_j)-iS_jX}\right)\right]\cdot e^{i\Omega\tau}, \tag{2.7}$$

where

$$S_1=\sqrt{2}\sqrt[4]{\Omega^2-2iN-1},\quad S_2=iS_1,\quad A_1=1/(4S_1^3),\quad A_2=iA_1. \tag{2.8}$$

In Eq. (2.7) we have $X \in \langle n_1 L, n_2 L\rangle$, where n_1 and $n_2 = n_1 + 1$ are successive support numbers, that means that Eq. (2.7) describes the solution for the periodic structure element (n_1, n_2). Assuming the convergence of the semi-infinite sums in Eq. (2.7) one obtains

$$W(X, \tau) = 8e^{i(n_1 \lambda L + \Omega\tau)} \cdot \sum_{j=1}^{2} A_j \frac{\sin S_j(n_2 L - X) + e^{i\lambda L} \sin S_j(X - n_1 L)}{\cos S_j L - \cos \lambda L}, \tag{2.9}$$

or

$$W(X, \tau) = W(1-\xi) \cdot e^{i(n_1 \lambda L + \Omega\tau)} + W(\xi) \cdot e^{i(n_2 \lambda L + \Omega\tau)}, \tag{2.10}$$

where

$$\begin{gathered} W(\xi) = Z_1 \sin SL\xi + Z_2 \sinh SL\xi, \quad \xi = X/L, \quad \xi \in \langle 0, 1\rangle, \quad S = S_1, \\ Z_1 = 2/[S^3(\cos SL - \cos \lambda L)], \quad Z_2 = -2/[S^3(\cosh SL - \cos \lambda L)]. \end{gathered} \tag{2.11}$$

Generally, Eqs. (2.9) and (2.10) represent a travelling and spatially attenuated wave in the periodic structure. In the case $n_1 = 0$ the expression (2.9) has a form which is similar to that presented in paper [4]. The relation between the wavenumber λ and wave frequency Ω, which is obtained by means of the condition of zero displacements at the rigid supports, can be written in the following form:

$$\cos \lambda L = f(S(\Omega)) = \frac{\sin SL \cosh SL - \sinh SL \cos SL}{\sin SL - \sinh SL}. \tag{2.12}$$

In the pure elastic case $N = 0$ the above relation is satisfied by λ-values which are either real numbers or have the form $\lambda = (k\pi + i\lambda_i)/L$, where k is an integer. In the first case, Eq. (2.10) represents a travelling wave propagating in the whole periodic structure, and according to the well-known nomenclature (cf. [1]) the corresponding frequency range is called a passing band. In the latter case, Eq. (2.10) describes an exponential wave, and the corresponding frequency range is called a stopping band. Since for the continuous periodic system considered the number of degrees of freedom in a single cell is infinite, the number of passing and stopping bands in the frequency Ω-wavenumber λ-plane is also an infinite one.

The curves representing relation (2.12) in the (Ω, λ)-plane which are determined for a few passing bands are presented in Fig.2, where also the curves $S = S(\Omega)$ for the corresponding model (C) are shown. Figure 2 illustrates the case of a non-dimensional support spacing $L = 2\pi$. The relation $\Omega = \Omega(\lambda)$ is a periodic one with the period $T_L = 2\pi/L$ and is symmetrical with respect to the Ω-axis and λ-axis. The region in the (Ω, λ)-plane corresponding to the two intervals $\lambda \in \left(-\frac{k\pi}{L}, -\frac{(k-1)\pi}{L}\right)$ and $\lambda \in \left(\frac{k\pi}{L}, \frac{(k+1)\pi}{L}\right)$, where k is a natural number, represents the so-called k-th propagation zone or k-th Brillouin zone, cf. [1]. The points of

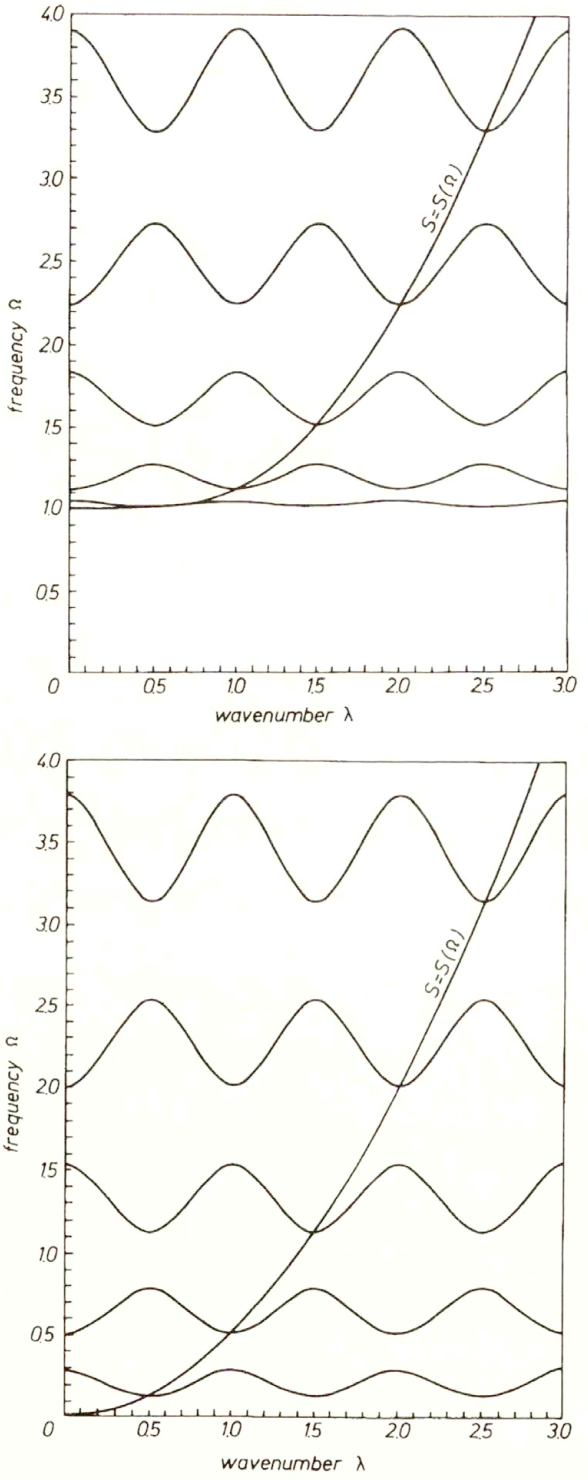

FIG. 2. Dispersion courves in the (Ω, λ)-plane [model(A), model (B)].

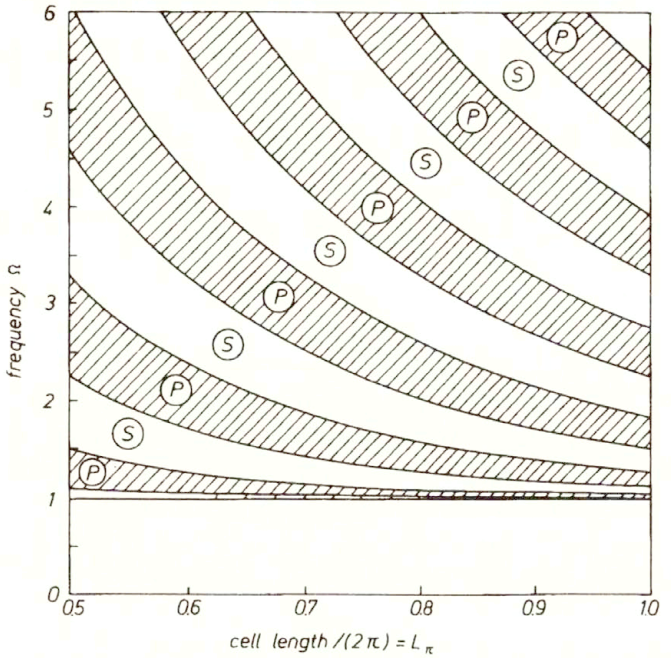

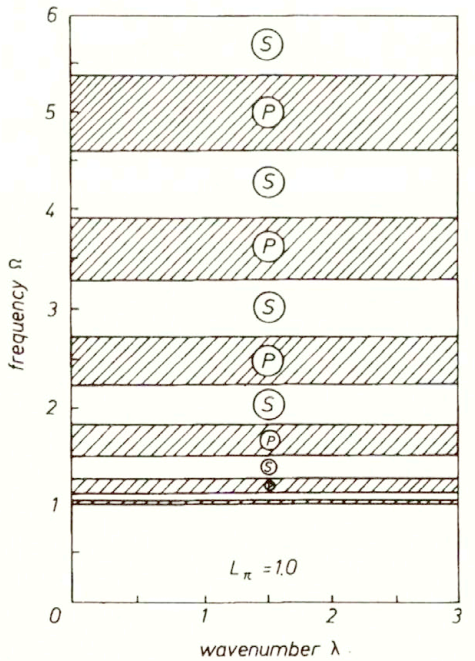

FIG. 3. Configuration of passing bands (P) and stopping bands (S) [model (A)].

extrema on the dispersion curves $\Omega=\Omega(\lambda)$ correspond to the cut-off frequencies Ω_C, i.e. the frequencies bounding the passing and stopping bands. These points $\left(\lambda_C=\frac{m\pi}{L},\ \Omega_C\right)$, where m is an integer, represent standing waves in the infinite periodic structure. It is interesting to note that the curve $S=S(\Omega)$ for the corresponding model (C) intersects the j-th dispersion curve $\Omega=\Omega(\lambda)$ at the i-th extremum point $(\lambda^{(i)}_{C(j)},\ \Omega^{(i)}_{C(j)})$ exactly for $i=j$, cf. Fig.2. The fundamental difference in the dispersion curves for models (A) and (B) consists in the position of the first passing band. Since in case (A) the beam on the elastic foundation acts as a mechanical filter by itself, the first passing band can be found for $\Omega>1.0$, cf. Fig.2.

The configuration of passing and stopping bands depending on the ratio $L_\pi=L/2\pi$ is presented in Fig.3, where also the scheme corresponding to Fig.2 (A) is shown. As follows from Fig.3, for a fixed frequency range the number of passing and stopping bands increases with increasing cell length of the periodic system.

Numerical results presented in the next sections of the paper have been obtained for the case $L=2\pi$.

2.3. Energy flow in passing bands

The analysis of energy flow in continuous systems, and especially the velocity of energy flow is necessary in order to determine critical parameters for a system under travelling disturbance sources, cf. [10, 11]. A detailed investigation of the energy flow velocity can be found in paper [15]. In the following some general remarks are presented.

The velocity of energy flow is defined in the following way:

$$v_{ef}=\frac{\langle P\rangle}{\langle\langle H\rangle\rangle}, \tag{2.13}$$

where $\langle P\rangle$ is the time average energy flow between two infinitesimally near-by beam cross-sections, which is defined as the average power absorbed by the beam cross-section during the period $T=2\pi/\omega$

$$\langle P\rangle=\frac{1}{T}\int_0^T\left[-\left(\frac{\partial^2 w}{\partial x\partial t}\right)\cdot\left(-EI\frac{\partial^2 w}{\partial x^2}\right)+\left(\frac{\partial w}{\partial t}\right)\cdot\left(-EI\frac{\partial^3 w}{\partial x^3}\right)\right]dt. \tag{2.14}$$

The integrand in Eq. (2.14) represents the sum of respective products of pairs of quantities like shear force – displacement velocity and bending moment – rotation velocity. The term $\langle\langle H\rangle\rangle$ in Eq. (2.13) is the time and space average energy density which can be expressed as

$$\langle\langle H\rangle\rangle=\frac{1}{l}\int_0^l\frac{1}{2T}\int_0^T\left[EI\left(\frac{\partial^2 w}{\partial x^2}\right)^2+qw^2+\rho A\left(\frac{\partial w}{\partial t}\right)^2\right]dt\,dx. \tag{2.15}$$

The velocity of energy flow v_{ef} equals the group velocity v_{gp} which is the derivative of the wave frequency ω with respect to $\bar{\lambda}$. An expression for v_{gp} can be obtained by means of the following considerations. Since

$$\cos\lambda L = f(S),$$

$$\frac{d(\cos\lambda L)}{d\Omega} = -L\cdot\sin\lambda L\cdot\frac{d\lambda}{d\Omega} = \frac{d[f(S)]}{d\Omega}, \tag{2.16}$$

then

$$V_{GP} = \frac{d\Omega}{d\lambda} = \frac{-L\cdot\sin\lambda L}{\dfrac{d[f(S)]}{d\Omega}} = \frac{-L\cdot\sin\lambda L}{\dfrac{d[f(S)]}{d\Omega}}\cdot V_{GC}, \tag{2.17}$$

where $V_{GP}=v_{gp}/v_0$ is the non-dimensional group velocity, $V_{GC}=d\Omega/dS$ is the non-dimensional group velocity for the corresponding model (C), and $f(S)$ is expressed by means of Eq. (2.12).

3. Periodic structures under travelling disturbance sources

3.1. Solution method

The equation of motion for model (A) under the action of a force travelling with constant velocity V and oscillating harmonically in time with frequency Ω takes the following form:

$$\frac{\partial^2 W}{\partial X^4}+4\frac{\partial^2 W}{\partial\tau^2}+8N\frac{\partial W}{\partial\tau}+4W = 8\cdot\delta(X-V\tau)\cdot e^{i\Omega\tau}. \tag{3.1}$$

In the case under consideration the displacements of the system are measured in terms of the quantity $w_0=F_0/(8EIa_0^3)$, where F_0 is the magnitude of the force, cf. Eqs. (A).

The conditions of zero displacements and continuity of beam cross-section rotations and bending moments at the rigid supports can be expressed as follows:

$$W(nL,\tau)=0,\quad \frac{\partial W(nL^-,\tau)}{\partial X} = \frac{\partial W(nL^+,\tau)}{\partial X},$$

$$\frac{\partial^2 W(nL^-,\tau)}{\partial X^2} = \frac{\partial^2 W(nL^+,\tau)}{\partial X^2}. \tag{3.2}$$

The steady-state solution of Eq. (3.1) which satisfies the conditions (3.2) is obtained by means of the following integral transformation:

$$W(X,\tau) = \frac{8}{2\pi}\int_{-\infty}^{\infty} T(X,\lambda)\,e^{i\lambda(X-V\tau)+i\Omega\tau}\,d\lambda, \tag{3.3}$$

(3.3) [cont]
$$\delta(X-V\tau)=\frac{1}{2\pi}\int_{-\infty}^{\infty}e^{i\lambda(X-V\tau)}\,d\lambda\,.$$

Introducing relation (3.3) into Eq. (3.1) yields an ordinary differntial equation for the function $T=T(X,\lambda)$

(3.4)
$$\frac{d^4T}{dX^4}+4i\lambda\frac{d^3T}{dX^3}-6\lambda^2\frac{d^2T}{dX^2}-4i\lambda^3\frac{dT}{dX}+(\lambda^4-S^4)T=1\,,$$

where

(3.5)
$$S^4=4(\overline{\Omega}^2-2Ni\overline{\Omega}-1)),\qquad \overline{\Omega}=-\lambda V+\Omega\,.$$

Corresponding to Eqs. (3.2), the conditions for the function $T=T(T,\lambda)$ read:

(3.6)
$$T(n_1L,\lambda)=0,\qquad T(n_2L,\lambda)=0,$$
$$\frac{dT(n_1L,\lambda)}{dX}=\frac{dT(n_2L,\lambda)}{dX},$$
$$\frac{d^2T(n_1L,\lambda)}{dX^2}=\frac{d^2T(n_2L,\lambda)}{dX^2},\quad n_2=n_1+1\,.$$

The solution of Eq. (3.4) can be expressed as

(3.7)
$$T(X,\lambda)=\sum_{j=1}^{4}a_j\cdot e^{\alpha_jX}+\frac{1}{\lambda^4-S^4},$$

where

$$\alpha_{1,2}=-i(\lambda\mp S),\qquad \alpha_{3,4}=-i(\lambda\mp iS)\,.$$

The relations (3.6) take the following form

(3.8)
$$\begin{bmatrix}1 & 1 & 1 & 1\\ e^{\alpha_1L} & e^{\alpha_2L} & e^{\alpha_3L} & e^{\alpha_4L}\\ \alpha_1(1-e^{\alpha_1L}) & \alpha_2(1-e^{\alpha_2L}) & \alpha_3(1-e^{\alpha_3L}) & \alpha_4(1-e^{\alpha_4L})\\ \alpha_1^2(1-e^{\alpha_1L}) & \alpha_2^2(1-e^{\alpha_2L}) & \alpha_3^2(1-e^{\alpha_3L}) & \alpha_4^2(1-e^{\alpha_4L})\end{bmatrix}\cdot\begin{bmatrix}\bar{a}_1\\ \bar{a}_2\\ \bar{a}_3\\ \bar{a}_4\end{bmatrix}=\begin{bmatrix}\frac{1}{S^4-\lambda^4}\\ \frac{1}{S^4-\lambda^4}\\ 0\\ 0\end{bmatrix},$$

where $\bar{a}_i=a_je^{\alpha jnL}$, $j=1,2,3,4$. The solution of Eq. (3.4) can be written in the following form satisfying the conditions (3.6):

(3.9)
$$T(\xi,\lambda)=\frac{A_1(\lambda)e^{iS\xi}+A_2(\lambda)e^{-iS\xi}+A_3(\lambda)e^{S\xi}+A_4(\lambda)e^{-S\xi}+e^{i\lambda\xi}\cdot D}{(\lambda^4-S^4)\cdot D}\cdot e^{-i\lambda\xi},$$

where

(3.10)
$$D=2\cdot[\cos\lambda L(\sin SL-\sinh SL)+\sinh SL\cos SL-\sin SL\cosh SL]$$

is the determinant of the square matrix in Eq. (3.8) and

$$
\begin{aligned}
&\xi = X - n_1 L, \quad \xi \in \langle 0, L \rangle, \\
&A_1 = (\cosh SL - \cos \lambda L)\left[(\sin \lambda L + \sin SL) - i(\cos \lambda L - \cos SL)\right], \\
&A_2 = (\cosh SL - \cos \lambda L)\left[-(\sin \lambda L - \sin SL) + i(\cos \lambda L - \cos SL)\right], \\
&A_3 = (\cos SL - \cos \lambda L)\left[(e^{-SL} - \cos \lambda L) - i \sin \lambda L\right], \\
&A_4 = (\cos SL - \cos \lambda L)\left[(-(e^{-SL} - \cos \lambda L) + i \sin \lambda L\right],
\end{aligned} \tag{3.11}
$$

3.2. Solution for the elastic system

The function $T = T(X, \lambda)$ has an infinite number of poles in the complex λ-plane which are determined from the relation $D = 0$, where D is given by Eq. (3.10). The poles corresponding to the relation $\lambda^4 - S^4 = 0$ contribute to the solution only for a currently loaded cell, what is discussed in details in paper [15]. The integration expressed by Eq. (3.3) can be carried out by means of Cauchy's theorem taking into account only a certain finite number of poles following from $D = 0$. In case of elastic systems the poles can also be found on the real axis of the complex λ-plane. In such a case the important question is whether the real number λ corresponds to the solution behind or ahead of the load. To answer this question, the method of „small damping" ($N \approx 0$) can be used or one can apply the energetic analysis which is discussed in the next section of this paper. Denoting the number of the poles corresponding to the solution behind (left) and ahead (right) of the load by k_L and k_R, respectively, we obtain the solution for $X \in \langle n_1 L, n_2 L \rangle$

$$
W(X, \tau) = \mp \sum_{k=1}^{K} Q_k \left[W_k(\bar{\eta}_k)\, e^{i\lambda_k (n_1 L - V\tau)} + W_k(\bar{\xi}_k)\, e^{i\lambda_k (n_2 L - V\tau)} \right] e^{i\Omega\tau}, \tag{3.12}
$$

where $-$ and $+$ correspond to the solution ahead of the load ($n_1 L \geqslant V\tau$, $K = k_R$) and behind the load ($n_2 L \leqslant V\tau$, $K = k_L$), respectively, and

$$
Q_k = \frac{8i(\cosh S_k L - \cos \lambda_k L)(\cos S_k L - \cos \lambda_k L)}{(\lambda_k^4 - S_k^4)(\sin S_k L - \sinh S_k L)\left(-L \sin \lambda_k L + \dfrac{df(S)}{dS} \cdot \dfrac{dS_k L}{d\bar{\Omega}} \cdot V \right)},
$$

$$
f(S) = \frac{\sin SL \cosh SL - \sinh SL \cos SL}{\sin SL - \sinh SL},
$$

$$
W_k(\bullet) = Z_{1k} \sin(\bullet) + Z_{2k} \sinh(\bullet), \tag{3.13}
$$

$$
Z_{1k} = 1/(\cos S_k L - \cos \lambda_k L), \quad Z_{2k} = -1/(\cosh S_k L - \cos \lambda_k L),
$$

$$
\bar{\xi} = S_k \xi, \quad \bar{\eta}_k = S_k (L - \xi), \quad \xi = X - n_1 L.
$$

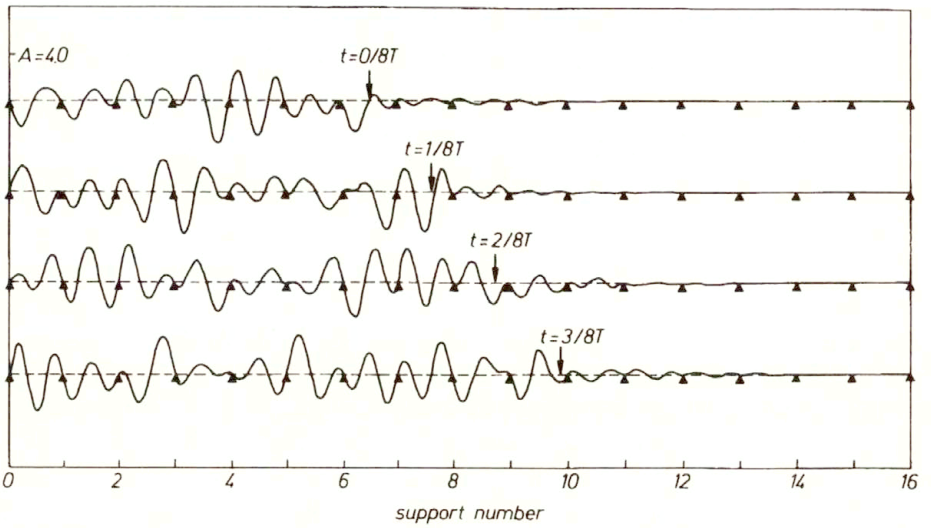

FIG. 4. System (A) displacements for selected times and for $V = 0.9$, $\Omega = 0.1$.

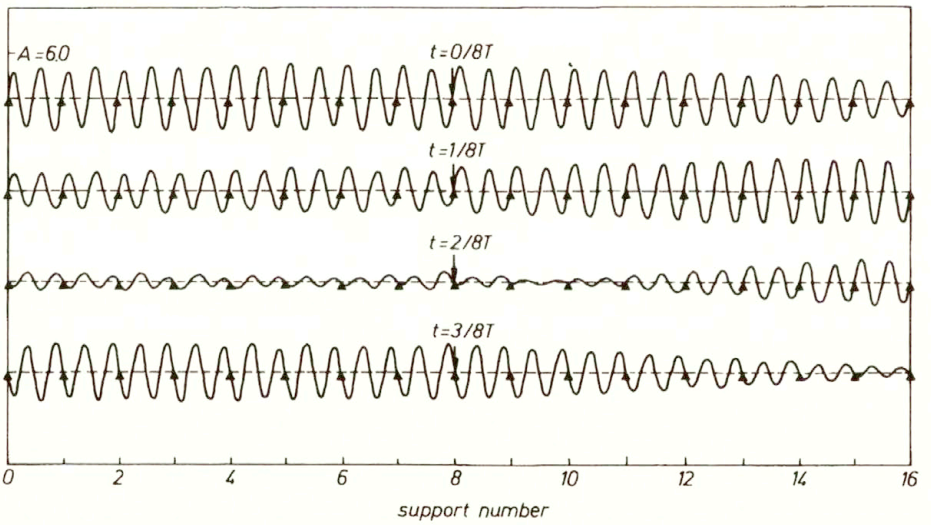

FIG. 5. System (A) displacements for selected times and for $V = 0.118$, $\Omega = 2.0$.

In Eqs. (3.13) the number $S_k = S(\overline{\Omega}(\lambda_k))$ corresponds to the k-th wavenumber λ and is determined by means of the relations (3.5) for $N = 0$.

The dynamic response of the system (A) is illustrated in Figs. 4 and 5 where the beam displacements are shown for times $t = 0$, $T/8$, $T/4$ and $3T/8$ ($T = 2\pi/\Omega$) and selected values of the load parameters.

3.3. Discussion of the solution

The obtained solution has the form of a sum of waves travelling in the periodic system. Each component of the sum has the form which is similar to expression (2.10) for elastic waves propagating in the unloaded periodic system. The wave amplitudes are constant or they decrease with increasing distance from the load depending on the form of the wavenumber λ_k. Since the characteristic equation $D=0$ (cf. (3.10)) has exactly the same form as the dispersion relation (2.12) and the wave freqency is $\overline{\Omega} = -\lambda_k V + \Omega$ (cf. (3.4)), then the real wavenumber $\lambda_k = \alpha_k$ corresponding to constant amplitude waves can be determined by means of simple geometrical considerations. Namely, the wavenumbers $\lambda_k = \alpha_k$ are the intersection points of the dispersion curves given by Eq. (2.12), cf. Fig.2, and the straight line $\overline{\Omega} = -\alpha_k V + \Omega$ in the wavenumber-frequency plane, where all four quarters of the plane should be taken into account. The question at which side of the load the wave $\lambda_k = \alpha_k$ propagates, i.e. behind or ahead of the load, can be answered by means of an energetic analysis. The group velocity V_{GP} of the travelling wave generated by the load is given by Eq. (2.17) where the sign should be changed. The sign change is related to the fact that V_{GP} in Eq. (2.17) is positive for left-going waves, cf. (2.10), and now we assume that the positive group velocity has the same direction as the load velocity V. The condition for the wave $\lambda_k = \alpha_k$ to propagate ahead of the load is $V_{GP}^{(k)} < V$ and behind the load is $V_{GP}^{(k)} > V$. These conditions concern the energy to be radiated away from its source. It should be noted that the complex wavenumbers $\lambda_k = \alpha_k \pm i\beta_k$ satisfying the relation $D=0$ can be found as conjugate pairs and thus they correspond to waves propagating behind and ahead of the load as well. Their frequencies $\overline{\Omega} = -\alpha_k V + \Omega$ can be found in stopping bands and, in some cases, in passing bands too.

The obtained solution has a typical quasi-periodic nature. When we consider the displacement and the corresponding velocity of a fixed beam cross-section we find it very irregular. This feature is illustrated in Fig. 6, where the phase plane for $X = 0.5L$ and selected load parameters is presented. Each point from Fig.$6_{(I)}$ represents the displacement and the corresponding velocity which have been determined at times $\tau = nL/V$, where n is a natural number, and these times are related to the „crossing frequency" $\Omega_{CR} = 2\pi V/L$. Figure $6_{(II)}$ is a result of observations made at times $\tau = nT$ where T is the period of harmonic oscillations of the load.

In both cases (I) and (II) the initial position of the load is $X = 10.5L$. Increasing the number of travelling waves in solution (3.12) one can find the phase plane to become more and more irregular. It is intersting to note that the results shown in the phase plane for $X = V\tau$, i.e. for the immaterial point under the travelling load, look slightly different, cf. Fig. 7. As follows from Fig. $7_{(I)}$ in the case where the ratio Ω_{CR}/Ω is a natural number, one can find the same number of points in the phase plane. In the case where the ratio of the two characteristic frequencies of the load is not a natural number, one can observe closed lines instead of the points in the phase plane, cf. Fig. $7_{(II)}$.

For certain velocities and frequencies of the load, the solution obtained tends to infinity, i.e. the amplitude of one wave propagating in the periodic system increases

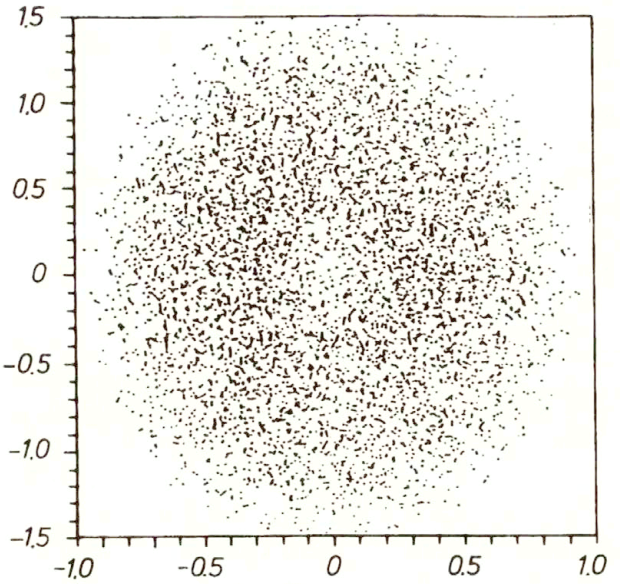

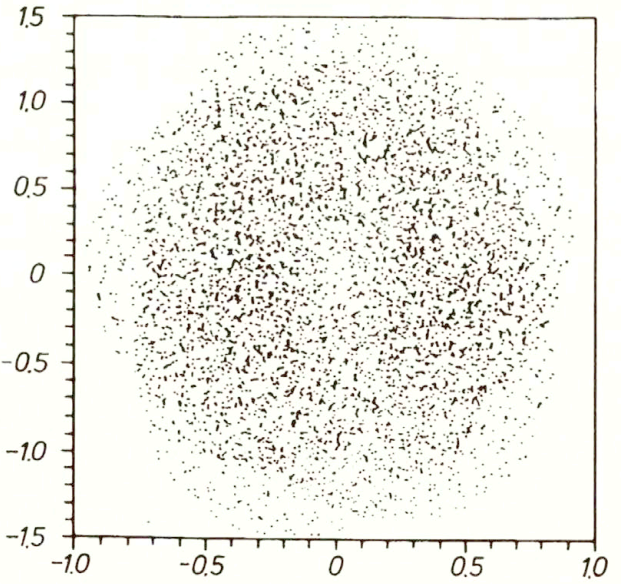

FIG. 6. Phase plane for $X=0.5L$ and $V=0.1$, $\Omega=1.7$; (I) – for times $\tau=nL/V$, (II) – for times $\tau=nT$ [model (A)].

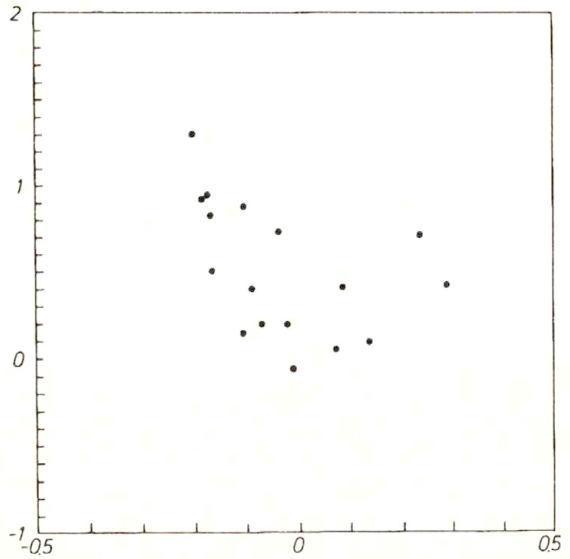

scaling factor=0.5
(I)

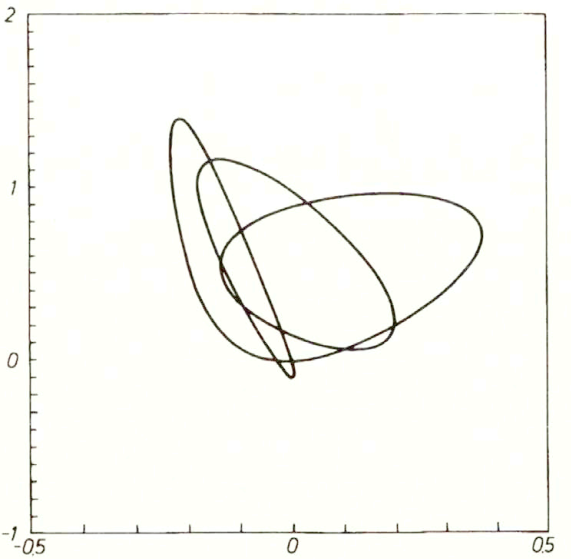

scaling factor=0.5
(II)

FIG. 7. Phase plane for $X=V\tau$; (I) – for $V=0.1$, $\Omega=1.7$; (II) – for $V=0.111$, $\Omega=1.7$ and for times $\tau=nT$ [model (A)].

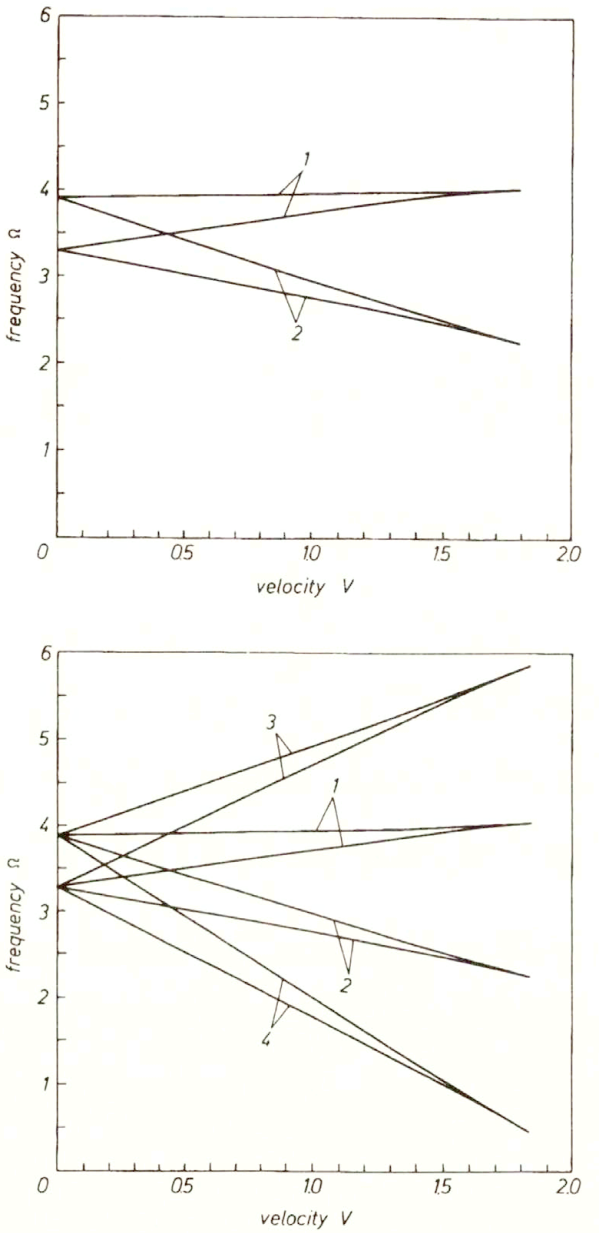

FIG. 8. Critical parameters of the load for the 5th passing band and selected Brillouin zones [model (A)].

infinitely in time. The load parameters corresponding to this infinite increase can be determined from the denominator of the expression for Q_k cf. Eq. (3.13)

$$-L \cdot \sin \lambda_k L + \frac{df(S_k)}{dS} \cdot \frac{dS_k}{d\bar{\Omega}} \cdot V \to 0 . \tag{3.14}$$

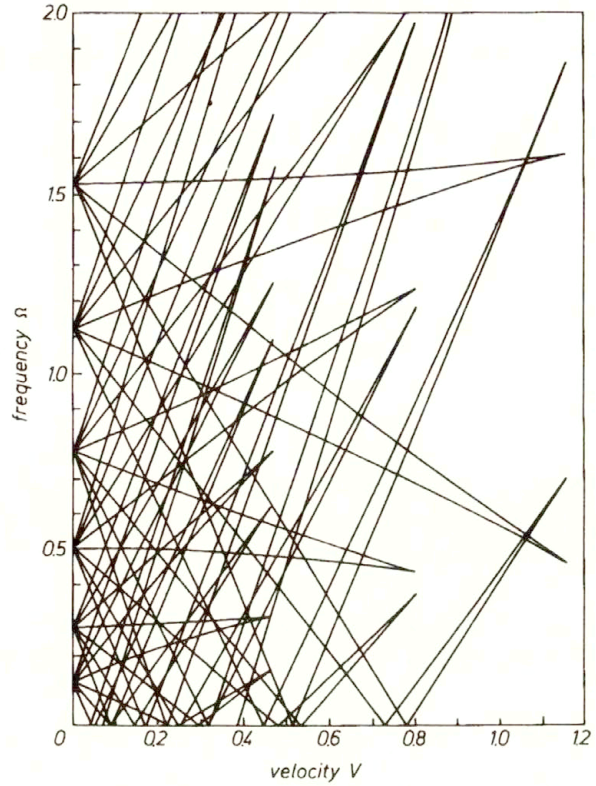

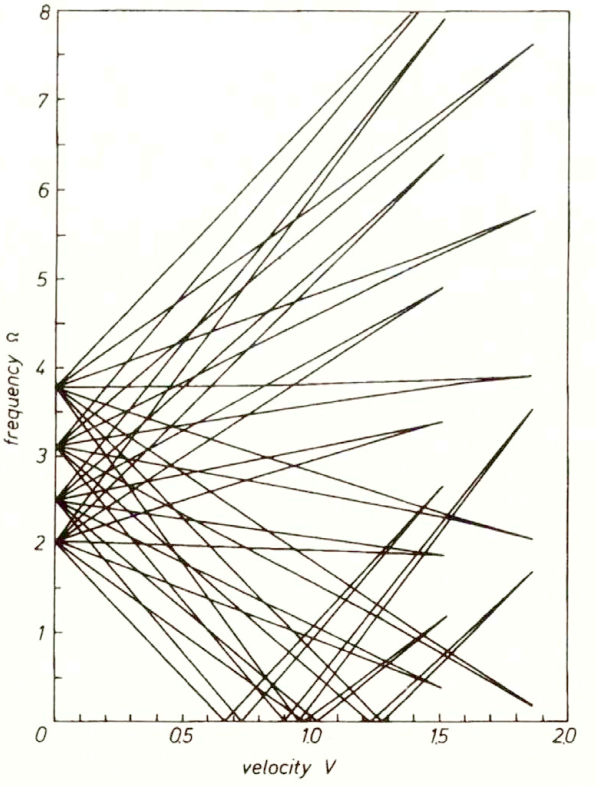

FIG. 9. Critical parameters of the load [model (B)].

Relation (3.14) can also be written in the following form:

$$-L \cdot \sin \lambda L \cdot \left(1 - \frac{V}{V_{GP}}\right) \to 0, \tag{3.15}$$

which means that the discussed phenomenon takes place in case when the load moves with the group velocity of the wave generated. The energy supplied to the system cannot be radiated in such a case and it increases infinitely in time. From a geometrical point of view the relation (3.15) correspond to the case when the straight line $\overline{\Omega} = -V\lambda + \Omega$ is tangential to the dispersion curves in the frequency-wavenumber plane. The critical curves in the Ω, V-plane which are determined for the 5th passing band and selected Brillouin zones are presented in Fig. 8. As follows from Fig. 8, the number of critical curves increases with increasing the number of Brillouin zones taken into account. The critical curves in the Ω, V-plane which are determined for the first six passing bands and the first eight Brillouin zones are presented in Fig. 9. It should be noted that the considered load can also be a source of standing waves in the unbounded periodic system. In such a case the load parameters can be determined from the relation $\Omega_C = -\lambda_C V + \Omega$ where Ω_C is the cut-off frequency and λ_C is the corresponding wavenumber discussed in Sec.2.2 of this paper.

4. Conclusions

A source of disturbance in the form of a harmonic force travelling over a periodic system creates the propagation of an infinite number of travelling waves the frequencies of which differ from each other. From the mathematical point of view the infinite number of waves follows from the infinite number of the poles of the function $T = T(X, \lambda)$ in the complex λ-plane. From the physical point of view, the discussed phenomenon is related to the infinite number of passing and stopping bands. The solution presented in this paper is determined as a sum of finite number of waves. The analysis of the energy flow and its velocity in the systems enables us to explain the phenomenon of an infinite increase of wave amplitudes. The number of critical curves in the Ω, V-plane increases infinitely with increasing number of Brillouin zones and passing bands taken into account. The qualitative analysis for continuous periodic systems under travelling disturbance sources by means of geometrical considerations, which is presented in this paper, seems to be applicable not only to the specific models analyzed. The solutions obtained in the whole load parameters range make it possible to study the problem of hybrid system stability in case of periodic structures treated as continuous subsystems.

References

1. L. BRILLOUIN, *Wave propagation in periodic structures*, Dover Publ., 1953.
2. D.J. MEAD, *Free wave propagation in periodically supported infinite beams*, J. Sound Vibr., **11**, 187–197, 1970.

3. D.J. MEAD, *A general theory of harmonic wave propagation in linear periodic systems with multiple coupling*, J. Sound Vibr., **27**, 2, 235–260, 1973.
4. D.J. MEAD, *A new method of analyzing wave propagation in periodic structures; application to periodic Timoshenko beams and stiffened plates*, J. Sound Vibr., **104**, 1, 9–27, 1986.
5. Y. YONG and Y.K. LIN, *Dynamics of complex truss-type space structures*, AIAA J., **28**, 7, 1250–1258, 1990.
6. K. SINGH and A.K. MALIK, *Parametric instabilities of a periodically supported pipe conveying fluid*, J. Sound Vibr., **62**, 3, 379–397, 1979.
7. C.C. SMITH and D.N. WORMLEY, *Response of a periodically supported guideway beams to travelling vehicle loads*, ASME J. Dyn. Syst., Measur., Control, **97**, 21–29, 1975.
8. K. POPP and P.C. MÜLLER, *On the stability of interactive multibody systems with an application to Maglev-vehicle-guideways control systems*, [in:] Dynamic of Multibody Systems, Proc. IUTAM Symp., 260–273, Springer-Verlag, 1978.
9. K. POPP, *Contributions to the dynamic analysis of Maglev vehicles on elevated guideways*, Shock Vibr. Bull., **50**, part 3, 39–61, 1980.
10. R. BOGACZ, T. KRZYŻYŃSKI and K. POPP, *On the generalization of Mathews problem of the vibrations of a beam on elastic foundation*, Z. Angew. Math. Mech., **69**, 8, 243–252, 1989.
11. R. BOGACZ, T. KRZYŻYŃSKI and K. POPP, *On the group-phase velocities relations for continuous systems under moving loads*, Z. Angew. Math. Mech., **70**, 4, 202–203, 1990.
12. R. BOGACZ, T. KRZYŻYŃSKI and K. POPP, *On self-excitation of hybrid systems with travelling waves*, Z. Angew. Math. Mech., **71**, 4, 219–221, 1991.
13. L. JEZEQUEL, *Response of periodic systems to a moving load*, ASME J. Appl. Mech., **48**, 613–618, September 1981.
14. T. KRZYŻYŃSKI, *On energy flow in a certain class of periodic structures*, Z. Angew. Math. Mech., **72**, 4, 35–38, 1992.
15. R. BOGACZ, T. KRZYŻYŃSKI and K. POPP, *On the vertical and lateral dynamics of periodic guideways for Maglev vehicles*, 1993, (to be published in Proc. 3rd Polish-German Workshop on „Dynamical Problems in Mechanical Systems").

POLISH ACADEMY OF SCIENCES
INSTITUTE OF FUNDAMENTAL TECHNOLOGICAL RESEARCH
and
INSTITUTE OF MECHANICS
UNIVERSITY OF HANNOVER, GERMANY.

Received September 3, 1993.

Arch. Mech., 45, 5, pp. 595-614, Warszawa 1993

Approximate friction treatment in sheet metal forming simulation

W. SOSNOWSKI (WARSZAWA)

THIS PAPER has been devoted to the numerical analysis of frictional contact problems. At the beginning some important computational aspects of existing algorithms are presented. Contact conditions at the interfaces are modelled using a penalty method. Certain modifications of the contact search algorithm are discussed and some remarks about mesh requirements for typical closest point search routines are given. Possible improvements in the contact algorithm are described. In particular, double side contact situations can be treated in a more efficient way. The blank holder zone treatment is especially important. Some remarks about the contact space description are also given. Certain proposition concerning rigid surfaces with prescribed forces is given, with the objective of applying it to a single degree of freedom model of blank holder. Additional regularization of Coulomb law was necessary to avoid „artificial wrinkling". The slip condition of those neighboring nodal points, where small strain velocities increments with different signs are observed, is replaced by stick condition. This gives especially good results in case of plane strain type of analysis. The example corresponds to a case proposed in NUMISHEET'93 conference held in September 1993 in Tokyo.

1. Introduction

IN THE LAST YEARS, much attention has been devoted to the numerical analysis of frictional contact problems. Despite that, contact mechanics is not so well developed as continuum mechanics, and further work in this area is still needed.

Contact and friction appears as a consequence of the interaction between different bodies. Such interaction is typical of sheet metal forming problems where the sheet is formed by means of a punch or gas pressure. During the forming process the sheet interacts with the tools, adding a new source of complexity to the numerical simulation due to the nonlinear nature of the boundary conditions. The numerical treatment of frictional contact problems involves two main steps. First, a contact search procedure must be done in order to detect the penetrations (kinematic incompatibilities) between the different bodies involved in the analysis.

Second, the penetrations detected must be cancelled and the kinematic compatibility constraints must be satisfied.

2. Contact search

Using the slave-master terminology it is imposed that the slave nodes do not penetrate the master surface.

In order to detect if penetration has taken place, a search procedure for each slave node must be performed. Here a different algorithm has been proposed (SCHWEIZERHOFF and HALLQUIST [18]; AGELET DE SARACIBAR [13]). If the search is done using the element normals, special care must be taken in order to treat different situations arising from the discontinuity of the field of normals.

An alternative has been proposed by DALIN and ONATE [5] and later modified by AGELET DE SARACIBAR [6], in which an assumed continuous normal field based on the normals at the nodes is considered.

3. Frictional contact formulations

Different formulations for the numerical analysis of frictional contact problems have been proposed. In the penalty method a penalized functional is added to the standard functional of the unconstrained problem.

The main drawback of this method is that the constraints are exactly satisfied for values of the penalty parameter only which leads to ill-conditioning of the tangent operator. Otherwise, this is a very simple way to enforce the constraints and it is quite easy to implement.

Frictional contact models can be described using a plasticity theory framework where the penalty or regularization parameters may be viewed as constitutive parameters (WRIGGERS *et al.* [24]; AGELET DE SARACIBAR [7]).

In the Lagrange multipliers technique a new field (the multipliers) is introduced by means of a contact functional. This leads to an increase of the number of unknowns and of the system of equations to be solved. Furthermore the tangent operator is indefinite (zero diagonal block associated with the multipliers) and special care must be taken during the solution process. Its main advantage is that the constraints are satisfied exactly.

Using the perturbed Lagrange multipliers method one can bypass this drawback as the tangent operator is positive definite. With this approach both the penalty and Lagrange multipliers methods can be formulated in a unified manner (JU *et al.* [10]).

In the augmented Lagrangian method, traditionally used in conjunction with Uzawa's algorithm, the constraints are satisfied exactly at finite values of the penalty parameter. This overcomes the problems associated with the choice of the penalty parameter and the ill-conditioning of the tangent operator mentioned before. However, no increase of number of the equations to be solved is produced and the multipliers are simply updated after each converged equilibrium step (nested Uzawa's algorithm) or after each equilibrium iteration (simultaneous Uzawa's algorithm) (SIMO and LAURSEN [19]). In the first case an outer loop is needed but otherwise quadratic rate of convergence must be expected if consistent tangent operators have been used. In the latter case, no extra loops are needed but the update of the multipliers destroys the quadratic rate of asymptotic convergence of the consistent Newton–Raphson scheme (SIMO and LAURSEN [10]).

Different augmented Lagrangian formulations for frictional contact problems have been recently proposed (SIMO and LAURSEN [19]; ALART and CURNIER [2]).

In the context of frictionless contact problems a formulation based on a three-field Hu–Washizu-type functional has been proposed recently by PAPADOPOULOS and TAYLOR [16]. In such a formulation contacts between elements rather than between node and elements are postulated, introducing an assumed gap function that is taken as an independent variable in the formulation.

A similar procedure was previously proposed by WRIGGERS *et al.* [23] using a two-field functional.

4. Contact and friction

4.1 Contact search algorithms and possible improvements, mesh dependency for the closest point search technique

Contact and friction play a important role in many sheet metal forming processes. The analysis of such effects involves two main steps. In the first one a contact searching algorithm must be used in order to detect the kinematic incompatibilities produced between the interacting bodies. In the second step these kinematic incompatibilities are eliminated by introducing the contact kinematic restrictions in the finite element formulation. Within the framework of the finite element analysis there are two well established formulations in order to introduce the kinematic restrictions imposed by the interacting bodies. These are the Lagrange multipliers and the penalty methods. It is interesting to note that both methods can be considered as a particular case of a perturbed Lagrangian formulation [25]. Using standard variational procedures the *exact linearization* of the first variation of the perturbed (total) functional leads to the contact *consistent residual* and *consistent tangent operators*, for a fully nonlinear kinematics.

For the fully nonlinear contact problem, the kinematic restriction between two interacting bodies takes the form

$$g := (\boldsymbol{\Phi}^2 - \boldsymbol{\Phi}^1) \times \mathbf{n} \geq 0 \quad \text{on } \delta B_c, \tag{4.1}$$

where $\boldsymbol{\Phi}^2$ $\boldsymbol{\Phi}^1$ refer to the configurations of the bodies B^1 and B^2, respectively, n is the normal to the contact surface $\delta B_c = \delta\boldsymbol{\Phi}^1(B^1) \cap \delta\boldsymbol{\Phi}^2(B^2)$, and g is the gap function representing the distance between the surfaces.

The restriction (4.1) can be introduced on the basis of a contact perturbed Lagrangian functional of the form

$$\boldsymbol{\Pi}_c(\boldsymbol{\Phi}^1, \boldsymbol{\Phi}^2) = \int_{\delta B_c} \lambda \left(g - \frac{\lambda}{2\varepsilon} \right) ds, \tag{4.2}$$

where λ refers to the contact forces on the surface δB_c and ε is a perturbation parameter. Within the framework of the finite element method, the perturbed

Lagrangian functional can be obtained by adding the discretized version of Eq. (4.2) to the usual total potential energy of the bodies [23].

$$\Pi_c(\mathbf{v}, \lambda) = \Pi(\mathbf{v}) + \lambda \times \mathbf{g} - \frac{1}{2\varepsilon}\lambda \times \lambda, \tag{4.3}$$

where $\mathbf{v} \in \mathbf{R}^n$ is the nodal velocities vector, $\lambda \in \mathbf{R}^s$ are the nodal contact forces, $\mathbf{g} \in \mathbf{R}^s$ the nodal gaps vector and $\Pi(\mathbf{v})$ the total potential energy of the bodies. In order to express the gap in terms of the velocities, a time integration scheme of the form

$$^{t+\Delta t}\mathbf{x} = {}^{t+\Delta t}\mathbf{x}^{\text{trial}} + \Theta \Delta t\, {}^{t+\Delta t}\mathbf{v} \tag{4.4}$$

is considered, where

$$^{t+\Delta t}\mathbf{x}^{\text{trial}} = {}^{t}\mathbf{x} + (1-\Theta)\Delta t\, {}^{t}\mathbf{v}. \tag{4.5}$$

Restricting our attention to $2D$ problems and using a linear surface discretization, let us consider a slave node s belonging to the deformable body that has penetrated a master segment defined by the nodes (m_1, m_2), which belongs to the rigid surface.

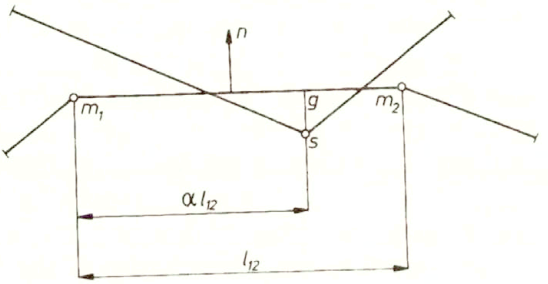

FIG. 1 Geometry of the slave node s with a master segment $m_1 - m_2$.

The current gap $\mathbf{g}$ and contact position αl_{12} for the slave node s are (Fig. 1)

$$\mathbf{g}_s = (\mathbf{x}_s - \mathbf{x}_{m_1}) \times \mathbf{n}, \tag{4.6}$$

$$\alpha = \frac{1}{\| \Delta \mathbf{x}_m \|} (\mathbf{x}_s - \mathbf{x}_{m_1}) \times \mathbf{t}, \tag{4.7}$$

where $\mathbf{t}$ and $\mathbf{n}$ are the unit local tangent and normal to the master segment, respectively, and $\Delta \mathbf{x}_m = \mathbf{x}_{m_2} - \mathbf{x}_{m_1}$.

4.1.1. Consistent operators. The linearized expression of the first variation of the functional leads to the following consistent residual and tangent operators for the contact element (s, m_1, m_2):

$$\mathbf{R}_{c_s} = \left[\lambda_s \mathbf{N}_s, -\frac{1}{\varepsilon}\lambda_s + \mathbf{g}_s \right]^T, \tag{4.8}$$

$$\mathbf{K}_{c_s} = \begin{bmatrix} -\dfrac{\lambda_s}{\| \Delta \mathbf{x}_m \|}\left(\mathbf{T}_s \otimes \mathbf{N}_m + \mathbf{N}_m \otimes \mathbf{T}_s + \dfrac{\mathbf{g}_s}{\| \Delta \mathbf{x}_m \|}\mathbf{N}_m \otimes \mathbf{N}_m\right) & \mathbf{N}_s \\ \mathbf{N}_s^T & -\dfrac{1}{\varepsilon} \end{bmatrix}, \tag{4.9}$$

where $\lambda_s = \varepsilon \mathbf{g}_s$ and the following operators have been introduced:

$$\mathbf{T}_s = \Theta \Delta t [\mathbf{t}, -(1-\alpha)\mathbf{t}, -\alpha \mathbf{t}]^T, \tag{4.10}$$

$$\mathbf{N}_s = \Theta \Delta t [\mathbf{n}, -(1-\alpha)\mathbf{n}, -\alpha \mathbf{t}]^T, \tag{4.11}$$

$$\mathbf{N}_m = \Theta \Delta t [0, -\mathbf{n}, \mathbf{n}]^T. \tag{4.12}$$

The residual force vector $\mathbf{R}_{cs}$ and tangent matrix $\mathbf{K}_{cs}$ for the contact element are added up to the expressions of global residual forces vector $\mathbf{R}$ and global stiffness matrix $\mathbf{H}$, respectively, in the global nonlinear solution scheme.

4.1.2. Lagrange multiplier method. The consistent residual and tangent operator for the Lagrange multiplier method can be obtained by setting the penalty parameter $\varepsilon \to \infty$ in Eq. (4.8)

$$\mathbf{R}_{c_s} = [\lambda_s \mathbf{N}_s, \mathbf{g}_s]^T, \tag{4.13}$$

$$\mathbf{K}_{c_s} = \begin{bmatrix} -\dfrac{\lambda_s}{\| \Delta \mathbf{x}_m \|}\left(\mathbf{T}_s \otimes \mathbf{N}_m + \mathbf{N}_m \otimes \mathbf{T}_s + \dfrac{\mathbf{g}_s}{\| \Delta \mathbf{x}_m \|}\mathbf{N}_m \otimes \mathbf{N}_m\right) & \mathbf{N}_s \\ \mathbf{N}_s^T & 0 \end{bmatrix}. \tag{4.14}$$

4.1.3. Penalty method. The consistent residual and tangent operator for the penalty method can be obtained by static condensation of $\Delta \lambda_s$ at the element level and setting $\lambda_s = \varepsilon \mathbf{g}_s$. This gives

$$\begin{aligned} \mathbf{R}_{c_s} &= \varepsilon \mathbf{N}_s, \\ \mathbf{K}_{c_s} &= \varepsilon \left[\mathbf{N}_s \otimes \mathbf{N}_s - \frac{\mathbf{g}_s}{\| \Delta \mathbf{x}_m \|}\left(\mathbf{T}_s \otimes \mathbf{N}_m + \mathbf{N}_m \otimes \mathbf{T}_s + \frac{\mathbf{g}_s}{\| \Delta \mathbf{x}_m \|}\mathbf{N}_m \otimes \mathbf{N}_m\right)\right]. \end{aligned} \tag{4.15}$$

Contact searching algorithms are very CPU-time consuming. Use of contact searching procedures and efficient algorithms are highly recommended in order to optimize the CPU-time, specially for large-scale computations.

The Lagrange parameter formulation is often an effective procedure. It is well known however that it may lead to singular stiffness matrices. This difficulty may be overcome by a partitioning method [12]. However, the introduction of new variables results in additional computational effort. Therefore the penalty method offers an attractive alternative, since it avoids these two problems. The main drawback of this method is its high sensitivity to the choice of the penalty factor. In this context, an

augmented Lagrangian method has been proposed as a procedure to overcome partially these difficulties and „regularize" the penalty formulation [22, 11, 3].

In the following three sections possible improvements in the contact algorithm are described. In particular, double-side contact situations can be treated in a more efficient way. The blank holder zone treatment is especially important. Some remarks about contact space description are also given.

Serious obstacles appeared when more complex rigid surface geometries were introduced. We observed that standard closest point search technique fails in such cases. The point of specific rigid surface, nearest to the given point of the blank, may belong to an element different from the one which actually is in contact with this point of the blank. These situations, observed sometimes for irregular meshes, may be avoided by regular meshing of the rigid surface – or by introducing additional check in the nearest point search procedure. Elements should be such that each point within one element should be nearest to the one of the nodal points of the element it belongs to.

In Fig. 2 the elements of the blankholder for Tokyo benchmark described in the last section are shown. For the elements in the region of the radius the criterion

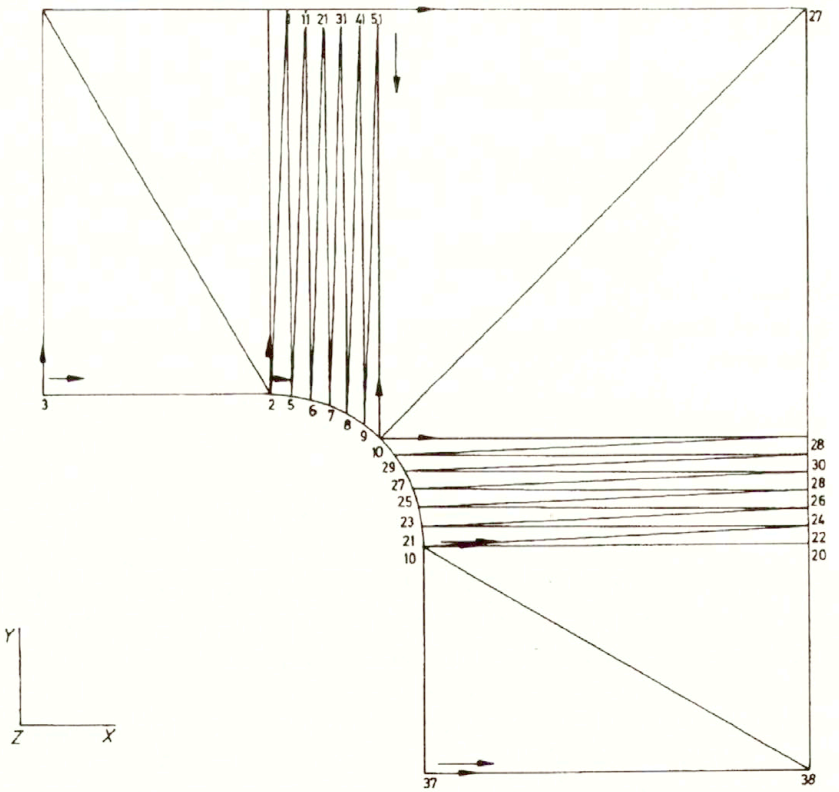

FIG. 2. Blank holder mesh for Tokyo Numisheet benchmark which yields wrinkles in the deformed sheet as shown in the next figure.

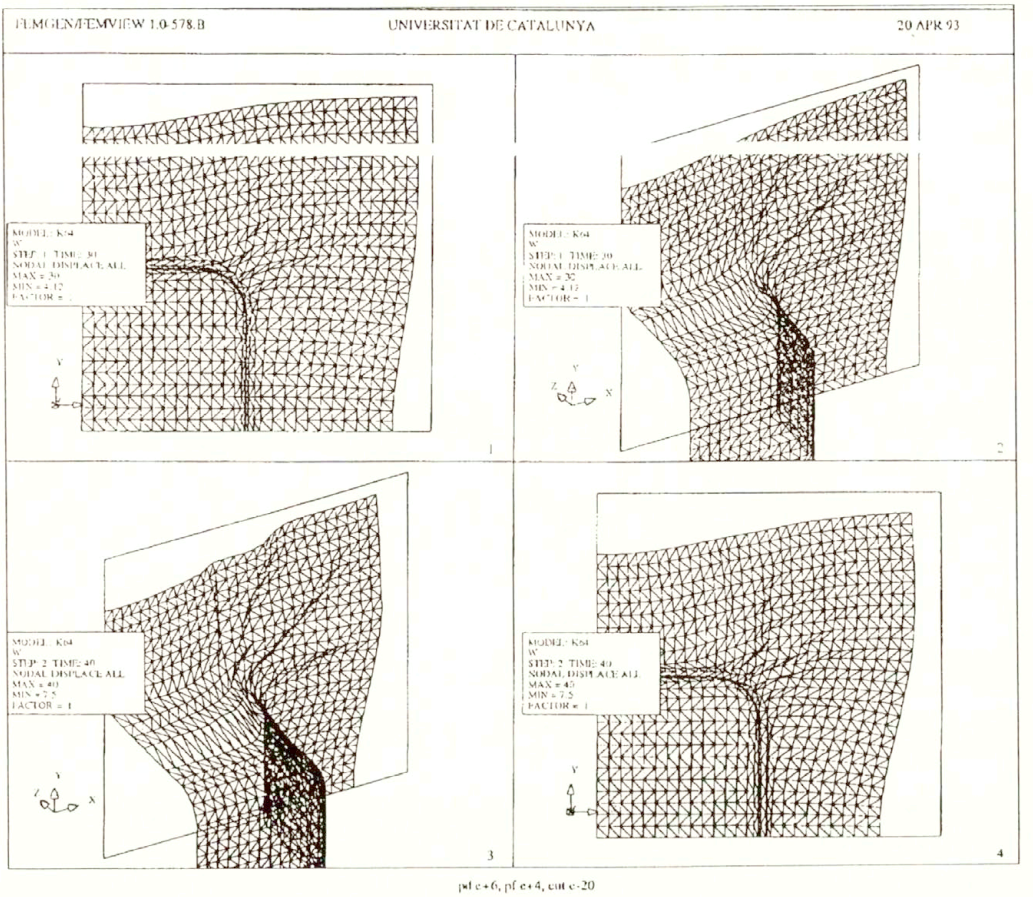

FIG 3. Results obtained by wrong discretization of the blank holder shown in the previous figure.

described above is not given. This leads during the simulation to wrinkles in that region, Fig. 3, since the contact is not correctly detected.

The example of „good", regular mesh for blank holder for this case can be seen in Fig. 4. The results discussed in the last section of this paper have been obtained using this blank holder mesh.

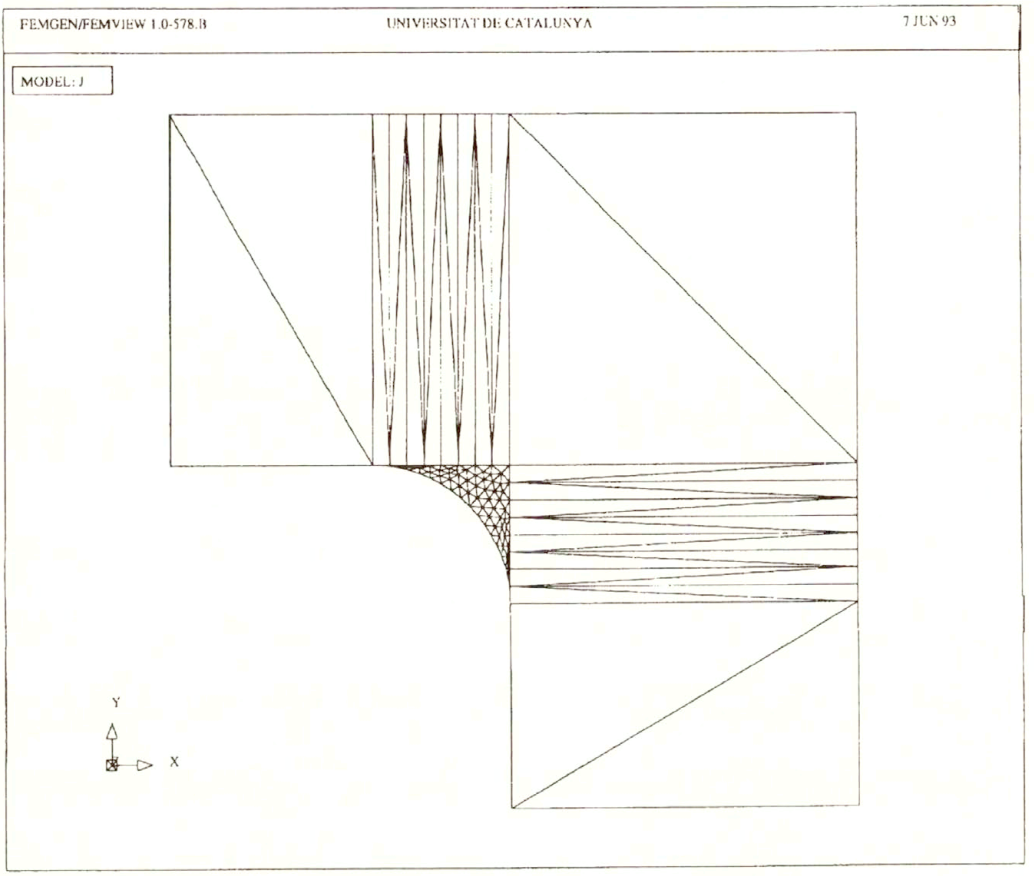

FIG 4. Blankholder mesh for Tokyo Numisheet benchmark, which yields no wrinkles.

4.2. Double side contact approximate treatment

In deep drawing applications attention must be focussed on proper restoration of kinematic conditions for each of the contacting surfaces treated separately. Double side contact situations can be included into the algorithm in this case. Incremental strains are relatively small in deep drawing, so the stiffness matrix is nearly singular. This implies that some initial stretching must be applied at the onset of computations. Double side contact situations treatment was improved recently by some change in kinematics of the process simulation. The contact searching algorithm has been modified so that the contact check is made for each rigid surface separately. A possible simultaneous penetration of specific node of the sheet into different rigid tool surfaces (die and punch for instance) can be detected and eliminated.

In order to simulate deep drawing in $3D$ more realistically, the blank holder as a third rigid surface has been introduced with blank holder force which can be applied in a proper way taking into account friction. Blank holder force is one of the most important parameters in deep drawing processes. Area of the contact between blank holder and blank decreases according to equilibrium conditions between drawing and friction forces. Change of contact area has to be taken into account. Corresponding blank holder pressure values are automatically modified, as it is observed in real deep drawing processes. Validity of this modifications was confirmed by numerical tests known as Wagoner and VDI benchmarks [26, 15, 4].

In some cases additional small in-plane stiffness added for some elements situated on the boundary had a stabilizing effect on the solution process.

An additional stiffness coefficient α of order 0.001 up to 0.1 multiplied by the element area was introduced for such boundary elements.

4.3. Angle versus vector contact space description

The interesting observations were made when the cosine coordinates were used in the contact space description. As we know, the position of any point may be given in many different ways. It is convenient to use in some situations, in axisymmetric analysis for instance, the spherical Θ and r coordinate system, as shown in Fig. 5.

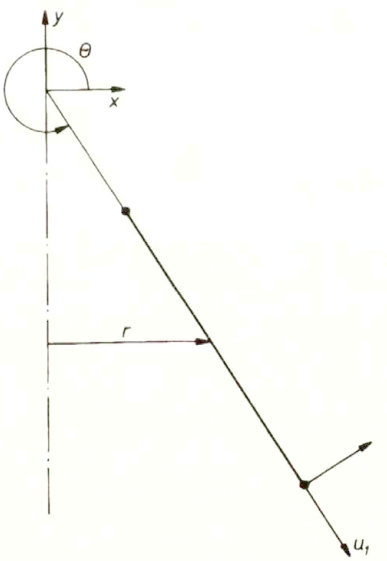

FIG 5. Geometry of the conical shell.

In this figure u_1 and u_2 are displacements in the local coordinate frame. The normals to the elements vary from element to element and often are calculated as cosine functions of angle of inclination of the element to the global coordinate system. In the contact analysis it is necessary to evaluate the mean values of the normals at the nodes.

When the directional cosine functions are applied to describe the element normals in full 2π range of angles, frequently the sums of type $\pi+\theta$ are used.

Let us assume that for some node 1 which belongs to two neighbouring elements, the Θ_1 coordinate after some deformations was calculated as an arccos function

$$\cos\frac{\theta_k+2\pi+\theta_{k+1}}{2}. \tag{4.17}$$

It may happen that node 2 has the same angle coordinate, as shown on Fig. 6, it belongs to elements with similar configuration but different deformation history. Due

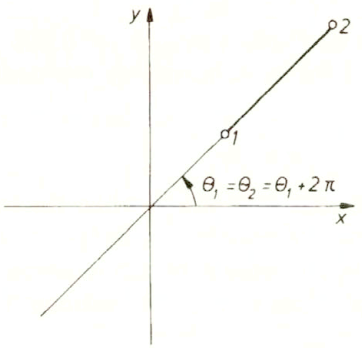

FIG 6. θ_1 and $\theta_2+\pi$ coordinates of points 1 and 2.

to the periodic character of cos function, in directional cosine evaluation often the value of π is added or subtracted in order to keep the θ value inside the $(-\pi - +\pi)$ range.

The θ_2 coordinate after some deformations was calculated as the arccos function

$$\cos\frac{\theta_{k+1}+\theta_{k+2}}{2}, \tag{4.18}$$

but finally we obtain that

$$\theta_1 \neq \theta_2. \tag{4.19}$$

This type of erroneous description, frequently used in programming, may be easily avoided by consequent normal vector space description, were always the resultant of N different directions may by uniquely represented.

We have defined the normal at the node in the general $3D$ case as shown in Fig. 7, i.e.

$$\mathbf{n}^t = \frac{1}{N}\sum_{i=1}^{N}\mathbf{n}_i^t, \tag{4.20}$$

where the sum of N normals of elements connected with this node, $\mathbf{n}_i$, is taken at the specific time t.

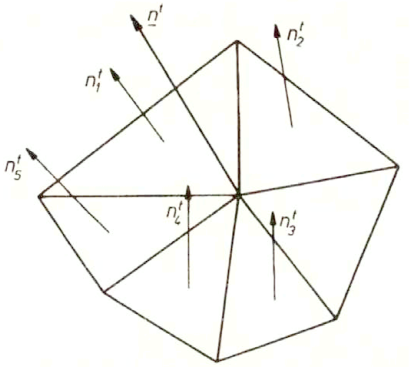

FIG 7. Element and nodal rotation vectors.

4.4. Rigid surfaces with prescribed forces

In typical industrial sheet metal forming processes approximately constant blank holder force is applied. When the sheet is drawn into the die, its area of contact with blank holder decreases, thus increasing the blank holder pressure. In case of the algorithm presented in this section the internal forces and reactions are calculated using a penalized functional similar to Eq. (4.3)

$$\Pi_\varepsilon(\mathbf{u}, \mathbf{u}_r) := \Pi(\mathbf{u}) + \sum_s \frac{1}{2}\varepsilon \mathbf{g}_s^2(\mathbf{u}_s) + \sum_s \frac{1}{2}\varepsilon \mathbf{g}_s^2(\mathbf{u}_s, \mathbf{u}_r) - \mathbf{F}_r \times \mathbf{u}_r, \tag{4.21}$$

where $\mathbf{u} \in \mathbf{R}^n$ is the nodal displacements vector and the energy due to the contact deformations is divided into that due to the rigid surfaces outside the blank holder area (2nd term), and that due to the blank holder (3rd therm). The fourth term is due to the blank holder forces vector $\mathbf{F}_r$. Gaps $\mathbf{g}_s(\mathbf{u})$ and $\mathbf{g}_s(\mathbf{u}_s, \mathbf{u}_r)$ are expressed as follows:

$$\mathbf{g}_s(\mathbf{u}_s) := (\mathbf{x}_s(\mathbf{u}_s) - \mathbf{x}_{ml}) \times \mathbf{n}, \tag{4.22}$$

$$\mathbf{g}_s(\mathbf{u}_s, \mathbf{u}_r) := (\mathbf{x}_s(\mathbf{u}_s) - \mathbf{x}_{ml}(\mathbf{u}_r)) \times \mathbf{n}, \tag{4.23}$$

where index s refers to slave nodes outside the blank holder being in contact with rigid surface and r — to slave nodes contacting with the blank holder only. m as previously refers to master nodes of the rigid surface.

The first variation of Eq. (4.21) leads to the following two variational equations which form the basis for the finite element approximation:

(4.24)

$$D\Pi_\varepsilon(\mathbf{u}, \mathbf{u}_r) \times \delta\mathbf{u} := D\Pi(\mathbf{u}) \times \delta\mathbf{u} + \sum_s \varepsilon \mathbf{g}_s(\mathbf{u}_s) \times (D\mathbf{g}_s \times \delta\mathbf{u}_s) + \sum_s \varepsilon \mathbf{g}_s(\mathbf{u}_s, \mathbf{u}_r)(D\mathbf{g}_s \times \delta\mathbf{u}_s) = 0,$$

$$D\Pi_\varepsilon(\mathbf{u}, \mathbf{u}_r) \times \delta\mathbf{u}_r := \sum_s \varepsilon \mathbf{g}_s(\mathbf{u}_s, \mathbf{u}_r)(D\mathbf{g}_s \times \delta\mathbf{u}_r) - \mathbf{F}_r \times \delta\mathbf{u}_r = 0, \tag{4.25}$$

where

$$D\mathbf{g}_s \times \delta\mathbf{u}_s := \mathbf{n} \times \delta\mathbf{u}_s, \tag{4.26}$$

$$D\mathbf{g}_s \times \delta\mathbf{u}_r := -\mathbf{n} \times \delta\mathbf{u}_r. \tag{4.27}$$

After linearization of the above variational equations the following system of discretized equations can be obtained

$$[\delta\mathbf{u}, \delta\mathbf{u}_r] \begin{bmatrix} \mathbf{K}_T + \mathbf{A}_s \varepsilon \mathbf{n} \otimes \mathbf{n} & -\mathbf{A}_s \varepsilon \mathbf{n} \otimes \mathbf{n} \\ -\mathbf{A}_s \varepsilon \mathbf{n} \otimes \mathbf{n} & \sum \varepsilon \mathbf{n} \otimes \mathbf{n} \end{bmatrix} \begin{bmatrix} \Delta\mathbf{u} \\ \Delta\mathbf{u}_r \end{bmatrix} = -[\delta\mathbf{u}, \delta\mathbf{u}_r] \begin{bmatrix} \mathbf{G}(\mathbf{u}) + \mathbf{A}_s \varepsilon \mathbf{g}_s \mathbf{n} \\ -\sum_s \varepsilon \mathbf{g}_s \mathbf{n} - \mathbf{F}_r \end{bmatrix}, \tag{4.28}$$

where

$$\mathbf{G}(\mathbf{u}) = D\Pi(\mathbf{u})\delta\mathbf{u} \tag{4.29}$$

and $\otimes$ stands for tensor product of the normal vectors $\mathbf{n}$.

Recently the blank holder model with 1 d.o.f. was proposed. After establishing the residual forces

$$\hat{\mathbf{R}} = -[\mathbf{G}(\mathbf{u}) + \mathbf{A}_s \varepsilon \mathbf{g}_s \mathbf{n}, \sum_s \varepsilon \mathbf{g}_s + \mathbf{F}_b]^T, \tag{4.30}$$

the modified tangent operator may be applied

$$\hat{\mathbf{K}} = \begin{bmatrix} \mathbf{K}_T + \mathbf{A}_s \varepsilon \mathbf{n} \otimes \mathbf{n} & -\mathbf{A}_s \varepsilon \mathbf{n} \\ -\mathbf{A}_s \varepsilon \mathbf{n}^t & \sum_s \varepsilon \end{bmatrix} \tag{4.31}$$

with variables

$$\Delta\hat{\mathbf{u}} = [\Delta\mathbf{u}, \Delta u_r]^T; \tag{4.32}$$

Δu_r denotes the displacement increment (usually vertical) of the blankholder. The solution procedure is relatively simple, since only small modifications of the stiffness matrix are necessary. Let us denote

$$\mathbf{v} = -\mathbf{A}_s \varepsilon \mathbf{n}^2 = (\varepsilon \mathbf{n})^2, \tag{4.33}$$

$$e = \sum_s \varepsilon. \tag{4.34}$$

We can write

$$\begin{bmatrix} \mathbf{K} & \mathbf{v} \\ \mathbf{v}^t & e \end{bmatrix} \begin{bmatrix} \Delta\mathbf{u} \\ \Delta u_r \end{bmatrix} = \begin{bmatrix} \mathbf{R} \\ r \end{bmatrix}. \tag{4.35}$$

The displacement field may be obtained as follows:

(4.36) $$\Delta u_r = \frac{r - \mathbf{v}^t \boldsymbol{\Psi}_R}{e - \mathbf{v}^t \boldsymbol{\Psi}_v},$$

(4.37) $$\Delta \mathbf{u} = \boldsymbol{\Psi}_R - \Delta u_r \boldsymbol{\Psi}_v,$$

where:

(4.38) $$\boldsymbol{\Psi}_R = \mathbf{K}^{-1}\mathbf{R}$$

and

(4.39) $$\boldsymbol{\Psi}_v = \mathbf{K}^{-1}\mathbf{v}.$$

This procedure was prepared initially but not tested for the time being. The normal and tangential forces in blank holder zone are very sensitive to velocity field changes, friction treatament etc., and now only blank holder in fixed positions was implemented. Actual normal forces treatment in blank holder zone depends on the relation between reaction $R^{(s)}$ at the specific node and blank holder force component r_s at this node.The following conditions are set into the alghoritm:

(4.40) $$\sum R = r^{(s)} + R^{(s)},$$

also

(4.41) $$\sum R = r^{(s)},$$

i.e. the resultant of reactions $\sum R$ at the specific slave node s is equal to the blank holder force component $r^{(s)}$.

4.5. Friction treatment

A simple procedure to deal with friction can be based on the iterative adjustment of nodal reactions in contact nodes at the blank-punch-tool interfaces until they satisfy a Coulomb type of friction law [17, 14]. A variational finite element formulation of the Coulomb friction model can be found in [13], where also other types of friction models used are discussed in details.

Convergence and other problems appear when relatively small strain velocity increments with different signs for neighboring nodal points are observed. The Coulomb law gives very different friction forces for such nodes, sliding over rigid surfaces with almost the same velocity in fact.

Thus additional regularization of Coulomb law was necessary to avoid such „artificial wrinkling". The slip condition of those neighboring nodal points where small strain velocity increments with different signs are observed is replaced by stick condition. This gives especially good results in case of plane strain type of analysis. Axisymmetric type of analysis seems to be less sensitive to such kind of problems.

Coulomb friction law is usually expressed as

$$\Delta \mathbf{u}^{\text{slip}} = \mathbf{0} \quad \text{if} \quad |\mathbf{f}_t| < \mu |\mathbf{f}_n| , \tag{4.42}$$

$$\Delta \mathbf{u}^{\text{slip}} = -\lambda |\mathbf{f}_t| \quad \text{if} \quad |\mathbf{f}_t| = \mu |\mathbf{f}_n| , \tag{4.43}$$

where $\Delta \mathbf{u}^{\text{slip}}$ denotes relative sliding between two contact points, λ is a positive scalar, $\mathbf{f}_n$ is the normal contact force which may be treated as reaction to the sliding, μ is the friction coefficient. Expression (4.42) corresponds to impossible sliding (condition „STICK") and (4.43) – to the possible sliding (condition „SLIP"). Algorithm modifications were made by the author in search and contact subroutines. Frictional effects can be treated on the basis of Coulomb or kinematic friction models. In the Coulomb model, a variational formulation can be obtained from the expression of the first variation of an unknown friction functional [10]. In the kinematic friction model the formulation is obtained from the expression of a known friction functional. In both cases the exact linearization of the first variation of the functional leads to the frictional consistent residual and tangent operators [10].

Use of consistent tangent operators is essential in order to preserve the asymptotic quadratic rate of convergence of the Newton's method [20, 23].

In Fig. 8 classical and regularized Coulomb rule is presented. Recently the following additional regularization of this low was proposed:

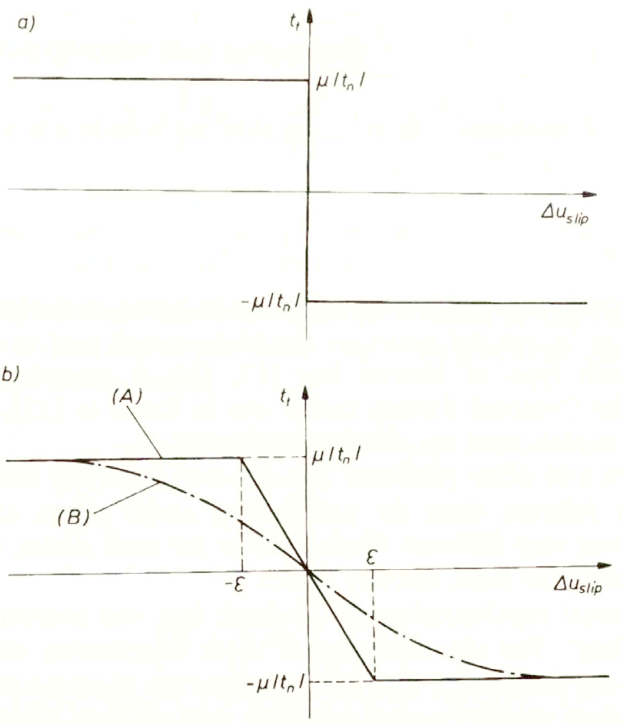

FIG 8. Coulomb friction laws (a) classical, (b) regularized.

(4.44) $$\Delta \mathbf{u}^{\text{slip}} = | \mathbf{u}^{\text{slip}} | .$$

If reverse velocity increment at the specific node is discovered, we set

(4.45) $$\Delta \mathbf{u}^{\text{slip}} = \frac{0.1 \times \mu | \mathbf{f}_n |}{\varepsilon},$$

i.e. local slip condition is transformed to „suave stick" condition with sliding velocity penalized by ε and reduced additionally by 0.1.

5. Tokyo NUMISHEET 93 BENCHMARK — deep drawing of a butter box

The example corresponds to a case proposed in NUMISHEET'93.

The geometry and material properties used can be seen in Fig. 9. Futher details can be obtained from [1, 5, 4, 14].

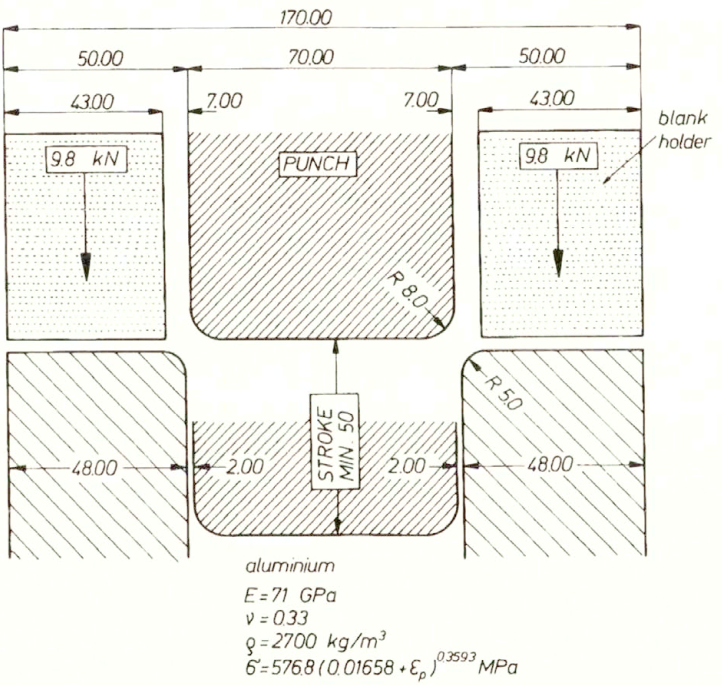

FIG 9. Square cup deep drawing: geometry and material data. Coulomb friction = 0.162.

Finite element model of quasi-static flow

1800 three-node membrane CST triangles were used for the analysis. The results were compared with similar calculations performed using explicit dynamic code [1].

Figure 10 presents the thickness distribution for both the quasistatic flow and explicit dynamic models. The draw-in is shown in Fig. 11 for both models.

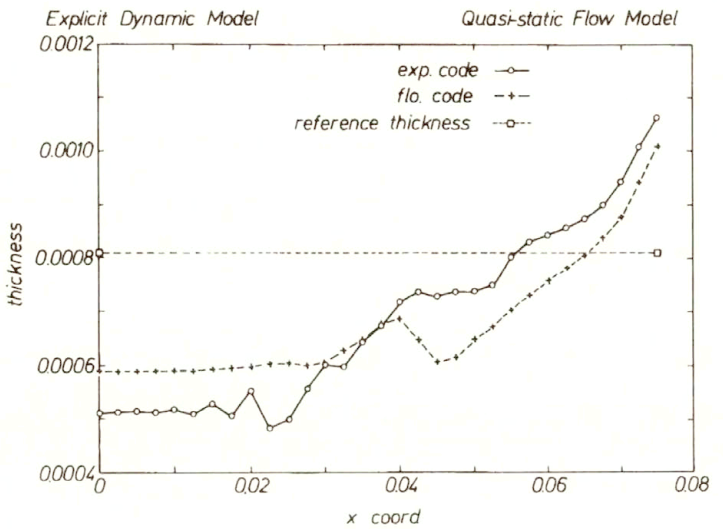

FIG 10. Square cup deep drawing: thickness distribution along line $A-B$ of Fig. 11.

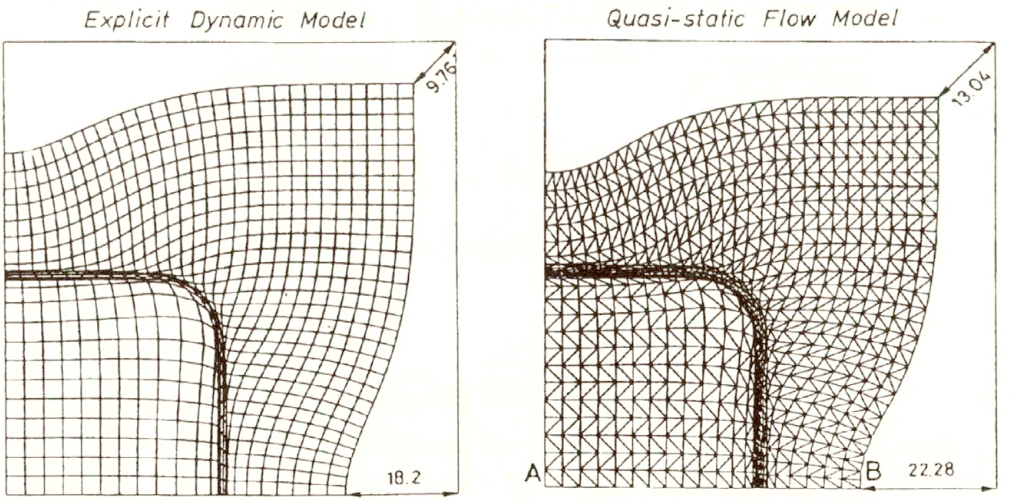

FIG 11. Square cup deep drawing: draw-in effect for a punch travel of 40 mm.

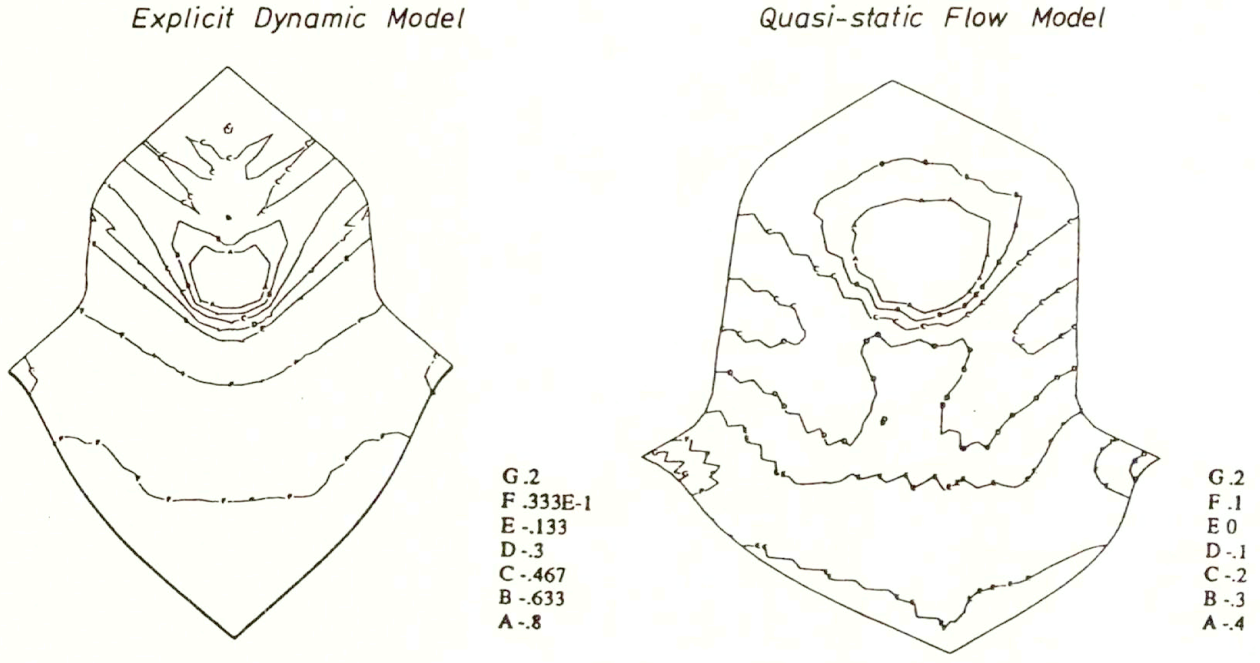

FIG 12. Square cup deep drawing: thickness contours for a punch travel of 40 mm.

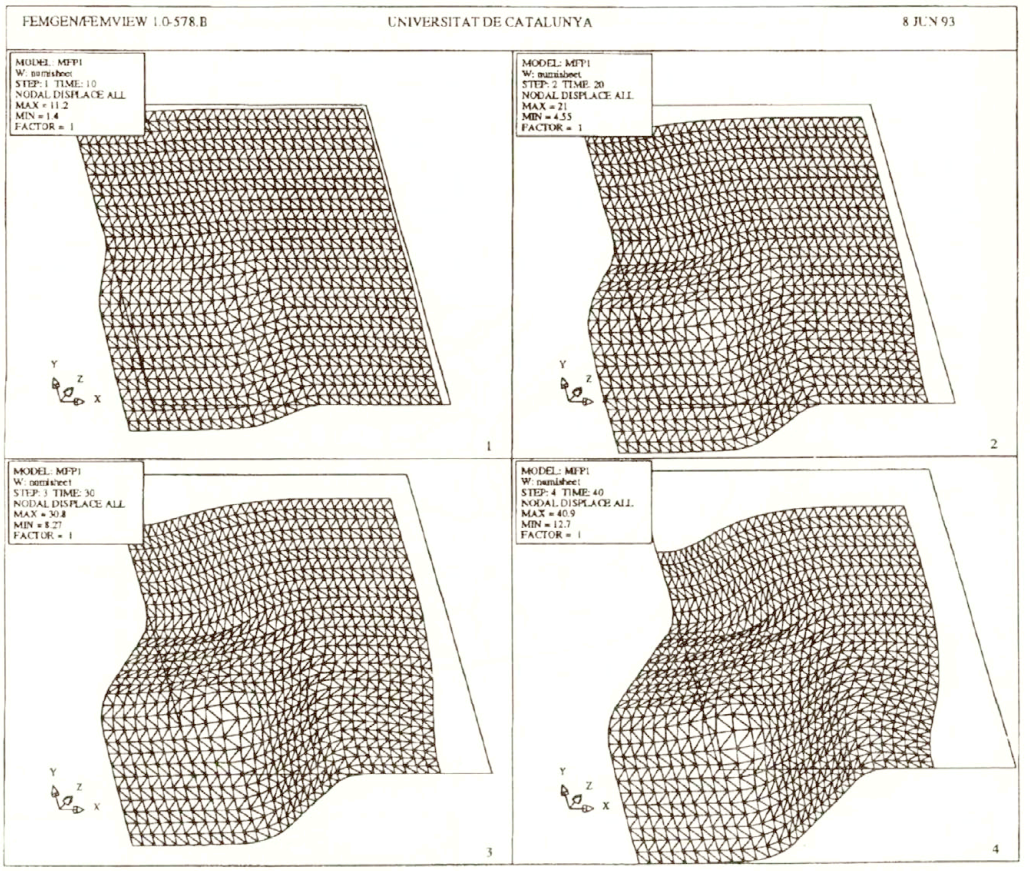

FIG 13. Square cup deep drawing: deformed shape for different punch travels.

Figure 12 shows the thickness contours obtained in both cases. Deformed shape of the blank obtained for different punch travels is shown in Fig. 13.

6. Acknowledgements

The author wishes to acknowledge the help of his colleagues at the International Center for Numerical Methods in Engineering (CIMNE), Polytechnical University of Catalunya and Institute of Fundamental Technological Research, Polish Academy of Sciences. Special thanks are due to Prof. C. AGELET DE SARACIBAR for many useful discussions. He wrote the program MFP3D extended further by author. He is the co-author of all ideas developed during my stay in Barcelona and partially presented in this paper.

The paper presents a part of the work performed during author's stay at CIMNE in 1989–93.

This research was partially supported by EEC-BRITE-EURAM programme under contract RI-1B-240. The author also thanks the enterprises CANDEMAT S.A. and ESTAMPACIONES SABADELL S.A. for their contributions in the performance of experimental tests.

References

1. E. OÑATE, A. MAKINOUCHI, E. NAKAMACHI and R.H. WAGONER, *Metal forming procesess. Verification of simulation with experiment*, [in:] NUMISHEET 2nd Int. Conference on Numerical Simulation of 3-D sheet Metal Forming Processes, 31 August – 2 September 1993, Isekava Japan 1993.
2. P. ALART and A. CURNIER, *A mixed formulation for frictional contact problems prone to Newton-like solution methods*, Comput. Meth. Appl. Mech. Engng. **92**, 1991.
3. D.P. BERTSEKAS, *Constrained optimization and Lagrange multiplier methods*, Academic Press, New York 1982.
4. J.L. CHENOT, *A velocity approach to finite element calculation of elastoplastic and viscoplastic deformation processes*, Engng. Comput., **5**, 2–9, 1988.
5. J.B. DALIN and E. OÑATE, *An automatic algorithm for contact problem: Application to sheet metal forming*, Numerical Methods in Industrial Forming Processes, 1989.
6. C. AGELET DE SARACIBAR, *Finite element analysis of sheet metal forming processes* [in Spanish], Ph.D. Thesis, Univ. Politec. de Catalunya, Barcelona 1990.
7. C. AGELET DE SARACIBAR, *Numerical simulation of frictional contact problems*, [in:] Lecture Notes of the Short Course on Finite Element Procedures for Plasticity and Viscoplasticity, Barcelona, Spain, April 2–3, 1992.
8. A. NEUBERT, W. SOSNOWSKI, A. HEEGE, E. OÑATE and C. AGELET DE SARACIBAR, *Square cup deep drawing – benchmark test*, [in:] International Conference on Metal Forming Numisheet 93, Tokyo, September 1993.
9. C. GARCIA GARINO, S. BOTELLO, F. FLORES, C. AGELET DE SARACIBAR, J. ROJEK, J. OLIVER, W. SOSNOWSKI, A. HEEGE, A. NEUBERT, E. OÑATE and G. OUZUNIDIS, *Numistamp: A research project for assessment of finite element models for stamping processes*, [in:] International Conference on Metal Forming Numisheet 93, Tokyo, September 1993.
10. J.W. JU, R.L. TAYLOR, and L.Y. CHENG, *A consistent finite element formulation of nonlinear contact problems*, Numerical Methods in Engineering and Transient Analysis, A.A. BALKENA J. MIDDLETON *et al.* [Eds.], 1987.
11. D.G. LUENBERGER, *Linear and nonlinear programming*, 2nd Edition, Addison-Wesley Pub., Reading, Massachusetts 1984.
12. R. GLOWINSKY, M. FORTIN, *Augmented Lagrangian Methods*, North-Holland, Amsterdam 1983.
13. E. OÑATE and C. AGELET DE SARACIBAR, *Numerical modelling of sheet metal forming problems*, [in:] P. HARTLEY *et al.* [Eds.], Modelling of Material Deformation Process, Springer–Verlag (in print).
14. E. OÑATE, M. KLEIBER and C. AGELET DE SARACIBAR, *Plastic and viscoplastic flow of void containing metals: Applications to axisymmetric sheet forming problems*, Int. J. Num. Meth. Engng., **25**, 1988.
15. E. OÑATE and O.C. ZIENKIEWICZ, *A viscous shell formulation for the analysis of thin sheet metal forming*, Int. J. Mech. Sci., **25**, 305–335, 1983.
16. P. PAPADOUPOULIS and R.L. TAYLOR, *A mixed formulations for the finite element solution of contact problems*, Comp. Meth. Appl. Mech. Engng., **94**, 373–389, 1992.
17. Z. MRÓZ, R. MICHAŁOWSKI, *Associated and non-associated sliding rules in contact friction problems*, Arch. Mech., **30**, 259–276, 1978.
18. K. SCHWEIZERHOF and J. HALLQUIST, *Fe-simulation of 3d sheet metal forming processes in the automotive industry, vdi benchmark*, Technical Report, Institut für Umformtechnik, ETH-2 Zürich, Mai 14–16, 1991.

19. J. SIMO and T. LAURSEN, *An augmented Lagrangian treatment of contact problems involving friction*, Comput. Struct., **42**, 97–116, 1992.
20. J.C. SIMO, *A framework for finite strain elastoplastic based on maximum plastic dissipation and the multiplicative decomposition, Part II. Computational aspects*, Computer Methods in Applied Mech. and Engng., **68**, 1–31, 1988.
21. E. OÑATE, W. SOSNOWSKI and C. AGELET DE SARACIBAR, *Some computational aspects of the viscous shell approach for sheet metal forming analysis*, Int. J. Mech. Sci., in preparation.
22. P. WRIGGERS and B. NOUR-OMID, *Solution methods for contact problems*. Technical Report, Rep. UCB-SESM 84-09 Dept. Civil Engng., University of California, Berkeley 1984.
23. P. WRIGGES, J.C. SIMO, and R.L. TAYLOR, *Penalty and augmented Lagrangian formulations for contact problems*, Proc. NUMETA'85, pages 97–106, 1985.
24. P. WRIGGERS. T. VU VAN, and E. STAIN, *Finite elements formulation of large deformation impact-compact problems*, **37**, 319–331, 1990.
25. O.C. ZIENKIEWICZ, P.C. JAIN and E. OÑATE, *Flow of solids during forming and extrusion. Some aspects of numerical solutions*, Int. J. Solids Struct., **14**, 14–28, 1978.
26. O.C. ZIENKIEWICZ, E. OÑATE and J.C. HEINRICH, *A general formulation for coupled thermal flow of metals using finite elements*, Int. J. Num. Meth. Engng., **17**, 1497–1514, 1981.

POLISH ACADEMY OF SCIENCES
INSTITUTE OF FUNDAMENTAL TECHNOLOGICAL RESEARCH

Received September 7, 1993.

Arch. Mech., 45, 5, pp. 615-634, Warszawa 1993

A moving boundary problem describing the growth of a droplet in its vapour

V. A. CIMMELLI (POTENZA) and F. DELL'ISOLA (ROMA)

IN [1–5] AND [12] THE THEORY of shells is generalized: nonmaterial bidimensional continua are introduced in order to model capillarity phenomena. In this paper we solve some mathematical problems arising when the quoted models are used to describe the growth in its vapour of a sufficiently small drop in the neighbourhood of an equilibrium state. We start to consider the source terms appearing in the integro-differential parabolic evolution equation (IDE) deduced in [5] for the temperature field in the vapour phase. We prove that, due to coupling between the capillarity and thermomechanical phenomena occurring close to the interface, these terms have both space and time Hölder coefficients equal to that one relative to the second time-derivative of the radius of the droplet. To our knowledge only GEVREY [14] partially treated this case for PDE of parabolic type. We improve his results in order to prove the well-posedness of the moving boundary problem formulated in [5] for IDE.

1. Introduction: physical motivation and discussion of proof strategy

1.1. Physical motivation

THE IMPORTANT role played in technology and applied science by capillarity phenomena (see for instance the classical books [13]–[14]) has drawn a growing interest in the theoretical study of models suitable for their description. Indeed, the classical theoretical studies, of capillarity mainly due to Gibbs (for a more detailed discussion and more references see [12] and [13]), are confined to the consideration of equilibrium states, while non-equilibrium phenomena have a lot of relevance in applications. Our attention was drawn by the surface tension-elastograms like that on p. 92 in [13]: a periodically time-varying surface tension is induced by changing concentrations in a biphasic solution. Our idea was to look for a similar effect induced, in a biphasic mono-component system, by a periodically varying supersaturation vapour temperature and/or pressure. Therefore we want to study, on a theoretical ground, the time evolution of the radius $R(t)$ of a liquid drop in presence of a periodical time variation of supersaturation pressure or temperature, in the neighbourhood of an eqilibrium state for the system

$$S = (\text{liquid small drop} + \text{interface} + \text{surrounding vapour}).$$

1.2. Models for capillarity phenomena

The models we use to develop our theoretical treatment are those proposed in [1–4] and more recently improved in [12]. In those papers, in order to model the interfaces between different phases the concept of bidimensional directed nonmaterial continuous system is introduced, generalizing the one classically introduced in the theory of shells: indeed in this theory such systems are modelled which, during their evolution in time, always consist of the same set of material points, while the study of interfacial phenomena obviously requires the introduction of a continuum which at different time instants contain different sets of material points. To bidimensional nonmaterial continua surface densities of material properties are attached, for which the evolution equations have to be found (see [12] for a more detailed discussion).

Let us now quote some of the results derived in [5], the paper upon which the present one is mainly based.

i. The concept of *Soap-Bubble-like* (SB-) continuum is introduced: it is a nonmaterial bidimensional continuum for which some properties which hold for true soap bubbles are still valid. More precisely, it is assumed that the temperature field is continuous across the interface, the total amount of surface mass is constant, the surface stress tensor is pressure-like so that a surface tension is sufficient to describe the stress state in the interface, the interfacial inner energy is an affine function of specific area. It is clear that one can reasonably expect that, at least when S evolves in the neighbourhood of a given equilibrium state, SB-continua suitably describe the behaviour of considered interface.

ii. For SB – continua the

GIBBS PHASE RULE

is proved; if the equilibrium temperature v and vapour pressure P_e belong to $]\vartheta^t, \vartheta^c[$ and $]P_e^t, P_e^c[$, where the indices t and c denote triple and critical values, then there exists a unique (uniform) field of pressure in the liquid phase, and a unique radius R of the droplet for which the equilibrium conditions are satisfied.

We therefore get some equilibrium functions of the equilibrium parameters, $\mathscr{E} = (\vartheta, P_e)$:

$R(\mathscr{E})$, i.e. the equilibrium droplet radius;

$\rho_v(\mathscr{E})$ i. e. the mass density of vapour phase, which is determined by constitutive equations of the vapour;

$p_l(\mathscr{E})$ i. e the pressure of the liquid phase, which is determined when the surface tension $\gamma(\mathscr{E})$ is given;

$p_v(\mathscr{E}) \equiv P_e$ for consistency of notations;

$\rho_\sigma(\mathscr{E})$ i.e. the equilibrium surface mass density.

iii. It is proved that, if the interface is assumed to be SB-like, the liquid phase is incompressible, the vapour is a perfect gas and all fields are spherically symmetric, then the linearized (1) balance equation for mass, velocity and energy, valid for liquid,

(1) In the neighbourhood of one of the previously characterized equilibrium states.

vapour and interfacial phases yield some evolution equations for mass, velocity and temperature fields which are decoupled.

More precisely, this means that the evolution of temperature field can be determined once an Integro-Differential Equation (IDE) is solved in which only the temperature appears, while the mass and velocity fields are derived from a hyperbolic problem, in which the (known) temperature field appears as source term.

1.3. Physical meaning of IDE and related FMB: their dimensionless forms

The IDE is quoted in Sec. 2, together with the Free Moving Boundary problem for its arising in the treatment exposed in [5].

In IDE the coupling between thermal phenomena, mechanical and capillarity is modelled by:

a) its source terms (cf. Eq. (2.2)), whose space and time Hölder continuity exponents are both equal to that of the function $R(t)$;

b) the initial and boundary conditions for the temperature;

c) the new (with respect the classical Stefan condition) contributions appearing in the free moving boundary condition (2.3); moreover, in the most relevant of them the second derivative of $R(t)$ appears.

We are thus facing the following problem: are the Hölder continuity conditions, satisfied by the source terms in Eq. (2.2), able to assure the Hölder continuity of the heat flux jump? We will see that, in order to get a positive answer to this question, we are obliged to improve the results found by GEVREY [6]. Indeed he manages to find solutions of heat flow equations, starting even from the Hölder continuity properties for the heat source which are weaker than those usually applied in the literature (see for instance CILIBERTO [7]).

We explicitly remark here that, in order to recognize that the IDE and its initial and boundary conditions, as formulated in Sec. 3 can be easily regarded as adimensional equations, we only need to change slightly the meaning of the symbols in Sec. 2 by using the set of physical quantities listed in ii) together with the characteristic time ϑ (also appearing in the following Eq. (2.5)) defined as follows

$$\vartheta = \alpha_3\left(\frac{M}{4\pi R(E)}\right),$$

where M is the total mass of the interface and α_3 appears in the generalized non-equilibrium Laplace equation for pressure at the interface. More precisely, it represents the proportionality coefficient which relates the pressure lag

$$p_v - p_l + 2\gamma/R,$$

which is not vanishing far from equilibrium, with the speed lag

$$v - \dot{R},$$

where v is the normal barycentric speed of the material particles lying in the interface.

For the sake of self-consistence we conclude this subsection recalling that

1. IDE stems from the balance of energy when it is considered in the vapour phase in the case of spherically symmetric fields; moreover (cf. [5]), in the quoted balance of energy the time derivative of mass density field appears; this derivative is determined (also in terms of temperature field) once the system of linearized hyperbolic equations (to which the balance of mass and linear momentum reduce) is solved. This is the reason for which an integral operator acting along some characteristic lines, appears in Eq. (2.2).

2. BE (i.e. the following condition (2.3)) is determined when balance of energy is postulated for the bidimensional continuum modelling of the interface: it generalizes, in the considered instance, the classical Stefan condition. We underline here that, while in the latter only the first order time-derivative of the drop radius $R(t)$ appears, in BE an extra term, containing the second order derivative of $R(t)$ times the capillarity coefficient, is found.

3. The boundary conditions for IDE on the moving boundary (2.5), (2.6) and $(2.9)_{1,2}$ in the following Sec. 2, are obtained from the balance of interfacial mass and linear momentum and the dynamic version, found in [3], of Gibbs' conditions at the interface. In [3] these dynamic conditions are determined assuming that:

3.1. the jump of Gibbs' dynamic potential at the interface is proportional to the average mass flux through the interface;

3.2. the previously introduced speed and pressure lags are mutually proportional;

3.3. the increase of interfacial mass is proportional to the interfacial average Gibbs' potential lag.

1.4. Discussion of the proof strategy

In this paper we prove the existence and uniqueness theorem for the solution of the moving boundary problem formulated in Sec.2, when $R(t)$ is known, in a space of functions which show some regularity properties which are compatible with the free boundary condition (2.3). The proof is based upon a fixed point method which uses the results on the solutions of parabolic equations available in the classical works of GEVREY [6], CILIBERTO [7] and FRIEDMAN [8].

Indeed we always consider a space of functions whose strong derivative are Hölder continuous; however, we cannot use the results found neither in Ciliberto's nor Friedman's papers, but we need to implement them with Gevrey's results (or better to say, with Gevrey's techniques), which are more general. This impossibility is due to the quoted coupling properties between thermodynamic and capillarity phenomena: a thermal source arises in IDE because of surface phenomena, and, as we prove in the following sections, this source is space and time Hölder continuous, but the space Hölder exponent is equal to the Hölder time exponent, and both are equal to time Hölder exponent of the function $\ddot{R}(t)$. Those are difficulties we solve in this paper: indeed, in the literature only space Hölder exponents which are twice the time

exponents, are considered. If one tries to apply the classical results in the Boundary Equation (BE) (2.3), one is lead to regard the boundary value of space derivative of the solution of IDE (i.e. the heat flux), *which is part of the source appering in BE*, as a function of time whose Hölder continuity exponent is one half of that of $\ddot{R}$, which is clearly a contradiction.

We shall prove that this contradition can be solved considering the space of source terms in heat equation whose space and time Hölder exponents are equal to $\alpha < 1/2$. The solution of heat equation still exists in this case (this result is mainly due to Gevrey, who really needs only time Hölder continuity), and is sufficiently regular to supply a heat flux that is space-time Hölder continuous with exponent α.

Therefore we will use the following proof strategy:

a) we study the regularity properties of source terms in IDE as determined by the regularity of the function $R(t)$. We assume that the rate of growth of the drop is smaller than the speed of sound in the vapour (cf. [9] for physical meaning of such an assumption);

b) we define a class $\mathscr{K}$ of functions and discuss the existence and uniqueness in $\mathscr{K}$ of the solution of IDE when $R(t)$ is chosen in the class $C^{2+\alpha}$ and boundary data are given as in Sec.2. We are considering the Moving Boundary Problem MBP which is obtained from the corresponding Free Moving Boundary Problem found in [5];

c) we prove that in BE the heat flux appearing as source term has the same Hölder continuity of the second time derivative of $R(t)$;

d) we prove the continuous dependence of the solution of MBP, as an element of $\mathscr{K}$, on the initial and boundary data.

2. Statement of the problem. Regularity properties of the source terms

In this section we shall summarize the main features of the problem outlined in [5].

Let now $\mathscr{D}$ be a spherical region of R^3 and $\partial\mathscr{D}$ its boundary. We shall consider a spherical liquid droplet $\mathscr{D}^-$, its center coinciding with that of $\mathscr{D}$, with time-dependent radius $R(t) \in [R(0), b]$, where $R(0)$ is a positive number and b the radius of $\mathscr{D}$. We suppose moreover that the droplet is surrounded by its vapour which occupies the domain $\mathscr{D}^+ = \mathscr{D} - \mathscr{D}^-$. The temperature on $\partial\mathscr{D}$ is a given function of time $\Phi_E(t)$. According to the theory exposed in [9], we assume that

$$|\dot{R}(t)| < a, \tag{2.0}$$

where a means the speed of sound in the vapour.

Introducing a spherical system of coordinates and denoting by r the distance of the generic point in $\mathscr{D}$ from its center, we define

$$D^+ \equiv \{(r, t) \in R^+ \times R^+ : \ R(t) \leqslant r \leqslant b\},$$

$$D^- \equiv \{(r, t) \in R^+ \times R^+ : \ 0 \leqslant r \leqslant R(t)\}.$$

In [5] it is proved that the problem of determining the evolution of the radius of the liquid droplet near the equilibrium condition, when surface and convective phenomena are not negligible, is solved if the following problem is solved:

Find a triple $(\vartheta_r^{\pm}, R(t))$ which satisfies the conditions

$$\delta\vartheta_r^- \equiv \vartheta_{r,t}^- - \vartheta_{r,rr}^- = 0 \quad \text{in } D^-, \tag{2.1}$$

$$\vartheta_{r,t}^+ = \vartheta_{r,rr}^+ + \lambda_0 \Phi_{,t} + \tilde{k} \int_0^t \vartheta_{r,rr}^+(\rho, \tau)\Big|_{\rho=I_\tau}^{\rho=F_\tau} d\tau \quad \text{in } D^+, \tag{2.2}$$

$$\lambda_1 \ddot{R} + \lambda_2 \dot{R} + \lambda_3 v' + R^{-1}(C^+ \vartheta_{r,r}^+ - C^- \vartheta_{r,r}^-) + \vartheta' R^{-1} \Delta C = 0, \tag{2.3}$$

$$\vartheta_r(0, t) = 0, \quad \vartheta_r(R(t), t) = \Phi_R(t), \quad \vartheta_r(r, 0) = u_0(r),$$

$$\vartheta_r(b, t) = \Phi_E(t), \quad R(0) = R_0, \quad \dot{R}(0) = \dot{R}_0. \tag{2.4}$$

where:

1) in $(R(0), 0)$ and $(b, 0)$, respectively, the following equalities hold:

$$\dot{\Phi} - u_{0,r}\dot{R} = u_{0,rr} + \lambda_0 \Phi_{,t}; \quad \dot{\Phi}_E = u_{0,rr} + \lambda_0 \Phi_{,t}, \tag{2.4}'$$

2) the physical case which is considered in [5] leads to the identifications

$$\begin{aligned} &\Phi_R(t) = R(t)\vartheta'(t), \quad u_0 = r\vartheta_0(r), \\ &v'(t) = \Big(\int_0^t \dot{R}(\tau)\, e^{\tau/\theta}\, d\tau\Big)\, e^{-t/\theta}/\theta + v_0' \end{aligned} \tag{2.5}$$

where v_0' is an initial value and θ is a given constant,

3) $\tilde{k}$, $C^{\pm}$ and λ_j are suitable constants and $\Delta C = C^+ - C^-$, ϑ' is a linear function of the variables R, $\dot{R}$, v',

$$\vartheta' = b_{1\vartheta}(R - R(0)) + b_{2\vartheta}\dot{R} + b_{3\vartheta}v', \tag{2.6}$$

4) F_τ, I_τ, Φ are functionals depending on (r, t), the function $R(t)$ and, in the case of Φ, on suitable initial and boundary conditions, [5]. They are defined as follows: once the curve $R(t)$ ([2]) is fixed, it is well known (see [10]) that there exists a unique couple of functions $u_1(r, t)$ and $u_2(r, t)$ defined in $\{(r, t) : R(t) \leqslant r\}$ which is the solution of the system:

$$u_{1,t} + c u_{2,r} + c u_2/r = 0, \tag{2.7}$$

$$c u_{2,t} + a^2(u_{1,r} - u_1/r) + d(\vartheta_{r,r} - \vartheta_r/r) = 0, \tag{2.8}$$

satisfying the initial and boundary conditions:

([2]) The curve $R(t)$, because of Eq. (2.0), is not characteristic so that mixed data problem for the hyperbolic system (2.2)–(2.9) in D^+ is well-posed.

$$u_1(r, 0) = u_{10}(r), \qquad u_2(r, t) = u_{20}(r), \quad \forall r \in [R(t), \infty];$$

$$u_1(R(t), t) = R(t)\rho_{v'}(t), \tag{2.9}$$

$$u_2(R(t), t) = m\dot{R}(t)\, R(t), \quad \forall t \in [0, T],$$

where m is a given constant and $\rho_{v'}$ a suitable linear function of v', R, $\dot{R}$:

$$\rho_{v'} = c_1(R(t) - R(0)) + c_2\dot{R}(t) + c_3 v'(t).$$

Moreover, we assume that

$$u_{10}(0) = R(0)\rho_{v'}(0), \qquad u_{20} = m\dot{R}(0)\, R(0),$$

$$u_{10}R(0)\, R^{-1}(0) = u_{10,\xi}R(0) + a u_{20}R(0). \tag{2.9}'$$

Using the results found in [10] we can see that the characteristic curves of Eqs. (2.8)–(2.9) are the lines whose angular coefficient is a.

We set

$$\Phi(R, r, t, IBC) \equiv u_1(r, t).$$

Let

$$D_C(r, t) \equiv \{(\xi, \tau) \in R^+ \times R^+ : \ 0 \leqslant \tau \leqslant t, \quad r + a(\tau - t) \leqslant \xi \leqslant r - a(\tau - t)\}.$$

Once the curve $R(t)$ is fixed, we define the application

$$P_R : R^+ \times R^+ \to R^+ \times R^+,$$

$$P_R(r, t) \equiv (R(\tau_1), \tau_1) \tag{2.10}$$

as follows:

- either it is the unique intersection, if it exists, of the characteristic line stemming from the point (r, t), whose angular coefficient is a, with the curve $R(t)$ ([3]);
- or it is the intersection of the quoted line with the line $t = 0$.

We remark here that $\tau_1 = \tau_1(r, t)$.

Let us moreover assume

$$D^*(r, t) \equiv (D^+ \cap D_C(r, t)) - D_C(P_R(r, t)).$$

The functionals $I_\tau(R, r, t)$ and $F_\tau(R, r, t)$ are defined as follows:

$$D^*(r, t) \equiv \bigcup_{\tau \in [0, t]} \{\tau\} \times [I_\tau, F_\tau]. \tag{2.11}$$

In order to find the regularity of the time derivative of the function Φ we represent the solution of the system (2.7)–(2.8) in the whole plane R^2 using the method of characteristic curves, as it was done in [10], and prove some lemmas.

([3]) Uniqueness of this intersection can be easily proved starting from assumption (2.0).

This solution will be given by a couple (ψ_1, ψ_2) which will satisfy in the interval $[R(0), \infty]$ the initial data (2.9) and (2.9'), and in the interval $[-\infty, R(0)]$, some suitable initial data of the type

$$\psi_1(r, 0) = \chi_1(r), \quad \psi_2 = \chi_2(r).$$

Hence we have

$$\psi_1(R(t), t) = R(t)\rho_{v'}(t), \quad \psi_2(R(t), t) = m\dot{R}(t)R(t).$$

The existence of such initial data is assured by arguments completely analogous to those found in [10].

Due to the uniqueness theorems quoted in [10], together with the D'Alambert representation formula, using some simple algebra we conclude that:

When (r, t) is such that $\tau_1(r, t) > 0$, then

$$\Phi(R, r, t, IBC) = R(\tau_1)\rho_{v'}(\tau_1) - 1/2\, u_{10}(R(\tau_1) + a\tau_1) + 1/2\, u_{10}(r + at) + 1/2\, a \int_{R(\tau_1)+a\tau_1}^{r+at} u_{20}(\xi)\, d\xi, \tag{2.12}$$

while if (r, t) is such that $\tau_1(r, t) = 0$, then

$$\Phi(R, r, t, IBC) = 1/2\,(u_{10}(r + at) + u_{10}(r - at)) + 1/2\, a \int_{r-at}^{r+at} u_{20}(\xi)\, d\xi. \tag{2.12'}$$

LEMMA 1. If $\tau_1(r, t)$ is defined according to Eqs. (2.10), then

$$\frac{\partial \tau_1}{\partial t} = a(a - \dot{R}(\tau_1(r, t)))^{-1},$$
$$\frac{\partial \tau_1}{\partial r} = (\dot{R}(\tau_1(r, t)) - a)^{-1}. \tag{2.13}$$

Proof. It is a trivial application of the Dini Theorem. ■

LEMMA 2. If $\Phi(R, r, t, IBC)$ is given by Eq. (2.12) and $\ddot{R}(t)$ is α-Hölder continuous, then $\Phi_{,t}$ is a continuous function in D^+ which is α-Hölder continuous in both the space and time variables.

Proof. In fact, using Eqs. (2.12) and (2.12') we have: when (r, t) is such that $\tau_1(r, t) > 0$, then

$$\Phi_{,t} = \tau_{1,t}\{\dot{R}(\tau_1\rho_{v'}(\tau_1) + (R(\tau_1) - R(0))[c_1\dot{R}(\tau_1) + c_2\ddot{R}(\tau_1) + (c_3/v)(\dot{R}(\tau_1) - v'(\tau_1))] - 1/2\, u_{10,\xi}(R(\tau_1) + a\tau_1)[\dot{R}(\tau_1) + a] - 1/2a\, u_{20}(R(\tau_1) + a\tau_1)[\dot{R}(\tau_1) + a]\} + a/2\, u_{10,\xi}(r + at) + 1/2\, u_{20}(r + at), \tag{2.13}$$

while, if (r, t) is such that $\tau_1(r, t) = 0$, then

(2.13') $$\Phi_{,t} = a/2\,(u_{10,\xi}(r+at) - u_{10,\xi}(r-at)) + 1/2\,(u_{20}(r+at) + u_{20}(r-at)),$$

so that the regularity of $\Phi_{,t}$ follows from Eqs. (2.9), (2.9') and (2.13) and from the assumed regularity of $\ddot{R}$. ∎

LEMMA 3. Let $f(r, t)$ be a given function whose domain is D^+, and let $G(r, t)$ be defined as follows:

$$G(r, t) = \int_0^t f(\rho, \tau)\Big|_{\rho=I_\tau}^{\rho=F_\tau} d\tau.$$

If $f(r, t)$ is

i) either α-Hölder continuous with respect to r with Hölder constant $H_r(f)$,

ii) or α-Hölder continuous with respect to t with Hölder constant $H_t(f)$, then $G(r, t)$ is α-Hölder continuous with respect to both r and t.

Proof. We prove this statement only in the case i) which will be used later. The proof when ii) holds is completely analogous.

We start defining

(2.14) $$\Lambda(\pm a, B, t) = \int_0^t f(\pm a\tau + B, \tau)\, d\tau,$$

Λ is α-Hölder continuous with respect to B.

Indeed, from (2.14) we get

(2.15) $$|\Lambda(\pm a, B_1, t) - \Lambda(\pm a, B_2, t)| \leqslant H_r(f)t\,|B_1 - B_2|,$$

where $H_r(f)$ is the space Hölder coefficient of f.

We now split $G(r_1, t) - G(r_2, t)$ into four parts and prove that $G(r, t)$ is space Hölder continuous.

In fact, it is easily seen that

$$G(r_1, t) - G(r_2, t) = \int_0^t (f(F(r_1, t, \tau), \tau) - f(F(r_2, t, \tau), \tau)\, d\tau$$

$$+ \int_{\tau_1(r_1,t)}^t (f(I(r_1, t, \tau) - f(I(r_2, t, \tau), \tau)\, d\tau + \int_0^{\tau_1(r_2,t)} (f(I(r_1, t, \tau) - f(I(r_2, t, \tau), \tau)\, d\tau$$

$$+ \int_{\tau_1(r_2,t)}^{\tau_1(r_1,t)} (f(I(r_1, t, \tau) - f(I(r_2, t, \tau), \tau)\, d\tau.$$

Now the first three terms are of the form (2.14), where b_i have suitable values.

In the first two integrals we have

$$B_1 - B_2 = x_1 - x_2,$$

while in the third one we have

$$| B_1 - B_2 | \leqslant | \dot{R} | \ | \partial\tau_1/\partial r | \ | r_1 - r_2 |.$$

Finally, the absolute value of the last integral is easily bounded when we remark that

$$\forall\tau \in [\tau_1(r_1, t), \tau_1(r_2, t)],$$

$$| I(r_1, t, \tau) - I(r_2, t, \tau) | \leqslant | \partial\tau_1/\partial r | \ 2a | r_1 - r_2 |.$$

We can conclude, using Eqs. (2.15) and (2.13'), that

$$(2.16) \quad H_r(G) \leqslant 2H_r(f)t + H_r(f)t \ | a(\dot{R} - a)^{-1} |^{\alpha} + 2H_r(f) \ | (\dot{R} - a)^{-1} | \ abt.$$

In order to prove the time Hölder continuity of G, we split

$$G(r, t_1) - G(r, t_2)$$

in a way similar to that used in space Hölder continuity to obtain finally

$$(2.17) \qquad H_t(G) \leqslant 2H_r(f)\, ta^{\alpha} + 2H_r(f)\, ta^{\alpha} \quad \blacksquare$$

3. Existence and uniqueness of the solution of MBP. Class K

Let us recall some definitions:

A real function f is said to be Hölder continuous with exponent α if there exists $\alpha \in (0, 1)$ such that

$$| f(x+h) - f(x) | \leqslant H_x(f)\, h^{\alpha},$$

where $H_x(f)$ is a constant Hölder coefficient of f.

For every $m \in N$ we shall say that f belongs to the class $C^{m+\alpha}$ if its m-th derivative exists and it is α-Hölder continuous.

A function of n real variables $f(x_1, \ldots, x_n)$, whose domain is a compact subset X of R^n, belongs to the class $C^{m_1+\alpha_1 \ldots m_n+\alpha_n}$ if the m_i-th partial derivative with respect to $x_i (i = 1, \ldots, n)$ is α_i-Hölder continuous with respect to x_i itself.

Let

$$D_T^{+} \equiv D^{+} \cap \{(r, t): \ 0 \leqslant t \leqslant T\}.$$

We now define the class $\mathscr{K}(D_T^{+})$ as follows:

$$\mathscr{K}(D_T^{+}) \equiv \{v: D^{+} \to \mathbb{R} \text{ with } v \in C^{2+\alpha, 1};\ v_r \in C^{1+\alpha, 0+\alpha};\ v_t \in C^{0+\alpha, 0}\}.$$

We define in $\mathscr{K}$ the following norm:

$$\| v \|_{\mathscr{K}} = \sup | v | + \sup | v_r | + \sup | v_{rr} | + H_t(v_r) + H_r(v_{rr}).$$

Let us introduce the following notation:

$$\triangleleft D_T^{+} = \partial D_T^{+} - \{(r, t): \ R(t) \leqslant r \leqslant b; \ \ t = T\},$$

so that we can define

$$\mathscr{K}_0(D_T^+) \equiv \left\{ v \in \mathscr{K},\ v \Big|_{\lhd D_\tau^+} = 0 \right\}.$$

Consider now the problem (2.1)–(2.2) when $R(t)$ is a given function belonging to $C^{2+\alpha}$ and the initial and boundary data, listed in Eq. (2.4) and imposed on the function ϑ_r, are vanishing.

The existence of the solution of Eq. (2.1) is assured by standard theorems on the parabolic equations which can be found, for instance, in [8].

Let us introduce the function

$$\mathscr{S}_R : \mathscr{K}_0 \to \mathscr{K}_0 \tag{3.0}$$

such that $\mathscr{S}_R(v)$ is the solution, satisfying the conditions $\mathscr{S}_R(v)\Big|_{\lhd D_\tau^+} = 0$, of the following equation:

$$\mathscr{S}_R(v)_{,t} - \mathfrak{s}_R(v)_{,rr} = \lambda_0 \Phi_{,t} + \tilde{k} \int_0^t v_{,rr}(\rho, \tau)\Big|_{\rho = I_\tau}^{\rho = F_\tau} d\tau + \mathfrak{s}(r, t) \equiv f \quad \text{in } D^+, \tag{3.1}$$

where $\mathscr{S}_R(r, t)$ is a source term belonging to $C^{0+\alpha,\, 0+\alpha}$.

Moreover, we introduce the following quantity:

$$\mu = \inf_{t \in [0,\ T]} \{ |R(t)|,\ |R(t) - b| \},$$

which will be assumed in the following to be strictly positive.

PROPOSITION 1. As the solution of Eq. (3.1) belongs to $\mathscr{K}_0$, definition (3.0) makes sense and there exists T' such that $\mathscr{S}_R(v)$ is a contraction in $\mathscr{K}_0$. Moreover, there exists a unique solution of Eq. (3.2) with vanishing initial and boundary data.

Proof. As $v \in \mathscr{K}_0$, the Lemmas 2 and 3 assure us that the right-hand member of Eq. (3.1) belongs to $C^{0+\alpha,\, 0+\alpha}$.

Moreover, in Appendix A, theorem A.1, we shall use the last result together with some theorems stated in [6-8] in order to prove that, if $R(t)$ belongs to $C^{2+\alpha}$, then $\mathscr{S}_R(v) \in \mathscr{K}_0$ and there exists a constant $L(\mu^{-1}, T, b, a)$, which is bounded when T tends to zero, such that:

$$\forall (w_1, w_2) \in \mathscr{K}_0^2 \qquad \| \mathscr{S}_R(w_1) - \mathscr{S}_R(w_2) \|_{\mathscr{K}_0} \leqslant L(\mu^{-1}, T, b, a) \, \| w_1 - w_2 \|_{\mathscr{K}_0} t. \tag{3.2}$$

Obviously, for suitable value T' of t, we have $LT' < 1$ so that $\mathscr{S}_R(v)$ is a contraction in $\mathscr{K}_0(D_T^+)$.

Using the Banach–Caccioppoli fixed point theorem we conclude that

$$\exists!\, v \in \mathscr{K}_0 : \mathscr{S}_R(v) = v,$$

i.e., when $R(t)$ is fixed, there exists a unique solution of Eq. (2.1) with vanishing initial and boundary data (4). ■

Let us consider a couple

$$(\Phi_R(t),\ \Phi_E(t)) \in C^{1+\alpha} \times C^{1+\alpha}$$

and use it to define the function

$$v_2(r,\ t) = A(r,\ t) + B(r,\ t), \tag{3.3}$$

where

$$A(r,\ t) \equiv [\Phi_E(t) - \Phi_R(t)]\,(r - R(t))\,(b - R(t))^{-1} + \Phi_R(t),$$

$$B(r,\ t) \equiv v_0(\xi(r,\ t)) \equiv u_0(\xi) - A(\xi,\ 0) \equiv u_0(\xi) - p\xi + q,$$

$$\xi \equiv [(b - R(0))\,(b - R(t)^{-1}]\,(r - R(t)) + R(0),$$

$$p \equiv (\Phi_E(0) - \Phi_R(0))\,(b - R(0))^{-1},$$

$$q \equiv -R(0)\,(\Phi_E(0) - \Phi_R(0))\,(b - R(0))^{-1} - \Phi_R(0).$$

It is easily seen that

$$v_2(R(t),\ t) = \Phi_R(t), \qquad v_2(b,\ t) = \Phi_E(t), \qquad v_2(r,\ 0) = u_0(r).$$

If $R(t) \in C^{2+\alpha}$ then, because of Proposition 1, we can assume that $\Phi_R(t) = \vartheta_r(R(t),\ t)$ belongs to $C^{1+\alpha}$.

LEMMA 4. If the functions

$$(\Phi_E(t),\ \Phi_R(t)) \in C^{1+\alpha} \times C^{1+\alpha}$$

and $u_0(r)$ belong to $C^{2+\alpha}$, then the functions $v_{2,rr}$ and $v_{2,t}$ are α-Hölder continuous both in the space and time.

P r o o f. Since evidently $v_{2,t}$ and $v_{2,rr}$ exist and are continuous, in order to prove this statement it is sufficient to calculate the space and time Hölder constants of both $v_{2,t}$ and $v_{2,rr}$. Now it is easily seen that

$$A_{,rr} = 0,$$

$$H_r(B_{,rr}) \leqslant b^3\mu^{-3} H_r(v_{0,rr}),$$

$$H_t(B_{,rr}) \leqslant b^4\mu^{-4} H_r(v_{0,rr}) + \sup\ |\ v_{0,rr}\ |\ 2ab\mu^{-3},$$

$$H_r(A_{,t}) \leqslant \sup\ |\ \Phi_{E,t} - \Phi_{R,t}\ |\ a^2 b\mu^{-1} + \sup\ |\ \Phi_E - \Phi_R\ |\ a\mu^{-2},$$

$$H_t(A_{,t}) \leqslant (H(\Phi_{R,t} - \Phi_{E,t}) b\mu^{-1} + H(\Phi_{R,t}) + \sup\ |\ \Phi_E - \Phi_R\ |\ 2ba^2\mu^{-3},$$

$$H_r(B_{,t}) \leqslant H(v_{0,r}) ab\mu^{-2},$$

$$H_t(B_{,t}) \leqslant \sup\ |\ v_{0,r}\ |\ a^2 b^3.$$

so that the lemma is proved ■.

(4) Note that Eq. (2.1) coincides with Eq. (2.2) when $s(r,\ t) = 0$.

We put now

$$v = v_1 + v_2, \tag{3.4}$$

where v_1 is the solution of Eq. (3.1) with vanishing initial and boundary data.

Lemma 4 assures us that the function

$$-\tilde{k}\int_0^t v_{2,rr}(\rho,\tau)\Big|_{\rho=I_\tau}^{\rho=F_\tau} d\tau + c_1 v_{2,t} - c_2 v_{2,rr} = \mathfrak{g}(r,t) \tag{3.5}$$

belongs to $C^{0+\alpha,\,0+\alpha}$.

Setting $\mathfrak{g}(r,t) = \mathfrak{s}(r,t)$ we conclude that v satisfies Eq.(2.2) with arbitrary initial and boundary conditions.

In this way we have proved the following:

THEOREM 1. *If* $R(t)\in C^{2+\alpha}$ is such that $\mu>0$, *then in the interval* $[0, T']$ *there exists a unique solution of* Eqs.(2.1), (2.2) *with initial and boundary conditions given by* Eq. (2.4) *and satisfying* Eq. (2.4').

4. Continuous dependence of the solution of MBP on initial and boundary data

We now introduce the space $\mathscr{D}$, i.e. the space of initial and boundary data:

$$\mathscr{D} = C^{1+\alpha}[0,T]\times C^{1+\alpha}[0,T]\times C^{2+\alpha}[R(0),b]\times C^{1+\alpha}[R(0),b]\times C^{0+\alpha}[R(0),b], \tag{4.1}$$

which satisfy all compatibility conditions, in $(R(0), 0)$ and $(b, 0)$, listed in Sec.2.

An element of $\mathscr{D}$ is the set $(\Phi_E, \Phi_R, u_0, u_{10}, u_{20})$ which will be denoted in what follows by IBD.

In order to define a norm in $\mathscr{D}$, we recall that:

if $f(x)\in C^{n+\alpha}$,

$$\|f(x)\|_{C^{n+\alpha}} \equiv \sup|f| + \sup|f_{,x}| + \ldots + \sup|f_{,x^n}| + |f_{,x^n}|_x^{\alpha}, \tag{4.2}$$

so that we can define

$$\|\mathrm{IBD}\|_{\mathscr{D}} \equiv \|\Phi_R\|_{C^{1+\alpha}} + \|\Phi_E\|_{C^{1+\alpha}} + \|u_0\|_{C^{1+\alpha}} + \|u_{10}\|_{C^{1+\alpha}} + \|u_{20}\|_{C^{0+\alpha}}. \tag{4.3}$$

■ We begin with the observation

$$v_2(r,t) = A(r,t) + B(r,t). \tag{4.4}$$

Simple calculations yield the result

$$\|A\|_{\mathscr{K}} \leqslant \|\mathrm{IBD}\|_{\mathscr{D}}[a_1 + a_2\|R_{,t}\|_{C^{1+\alpha}} + a_3\|R_{,t}\|^2_{C^{1+\alpha}}], \tag{4.5}$$

$$\|B\|_{\mathscr{K}} \leqslant \|\mathrm{IBD}\|_{\mathscr{D}}[a_1 + a_2\|R_{,t}\|_{C^{1+\alpha}} + a_3\|R_{,t}\|^2_{C^{1+\alpha}}], \tag{4.6}$$

where a_1, a_2, a_3, are three suitable constans such that the following limits are finite:

$$\lim_{\mu\to 0} \mu^2 a_1, \quad \lim_{\mu\to 0} \mu^3 a_2, \quad \lim_{\mu\to 0} \mu^4 a_3 . \tag{4.7}$$

Consider now function v_1. We remark that v_1 is the solution of the following equation:

$$v_{1,t} - v_{1,rr} = \lambda_0 \Phi_{,t} + \tilde{k} \int_0^t v_{1,rr}(\rho, \tau)\Big|_{\rho=I_\tau}^{\rho=F_\tau} d\tau + \mathfrak{s}(r, t) \qquad \text{in } D^+ , \tag{4.8}$$

where $\mathfrak{s}(r, t) = -\delta v_2$ is a source term belonging to $C^{0+\alpha, 0+\alpha}$ which vanishes on $\lhd D_T^+$.

We split the function v_1 in the following way:

$$v_1 = V_1 + U_1 . \tag{4.9}$$

V_1 is such that

$$V_{1,t} - V_{1,rr} = \lambda_0 \Phi_{,t} + \mathfrak{s}(r, t) \tag{4.10}$$

and U_1 satisfies the equation

$$U_{1,t} - U_{1,rr} = \tilde{k} \int_0^t U_{1,rr}(\rho, \tau)\Big|_{\rho=I_\tau}^{\rho=F_\tau} d\tau + \tilde{k} \int_0^t V_{1,rr}(\rho, \tau)\Big|_{\rho=I_\tau}^{\rho=F_\tau} d\tau . \tag{4.11}$$

We can apply to the solution of Eq. (4.10) the Theorem A.2 of the Appendix and Lemma 4 in order to prove that $V_1 \in \mathscr{K}_0$ and, moreover,

$$\| V_1 \|_{\mathscr{K}_0} \leqslant L(R(t), t) K_0 , \tag{4.12}$$

where K_0 is $\| \lambda_0 \Phi_{,t} + \mathfrak{s}(r, t) \|_{C^{0+\alpha, 0+\alpha}}$.

Let now U_1^1 be such that

$$U_{1,t}^1 - U_{1,rr}^1 = \tilde{k} \int_0^t V_{1,rr}(\rho, \tau)\Big|_{\rho=I_\tau}^{\rho=F_\tau} d\tau . \tag{4.13}$$

Lemma 3 assures us that the right-hand side of Eq. (3.13) $\in C^{0+\alpha, 0+\alpha}$, so that we have

$$\| U_1^1 \|_{\mathscr{K}_0} \leqslant L_1(R(t), t) K_1 , \tag{4.14}$$

where K_1 is the $C^{0+\alpha, 0+\alpha}$ norm of $\tilde{k} \int_0^t V_{1,rr}(\rho, \tau)\Big|_{\rho=I_\tau}^{\rho=F_\tau} d\tau$..

On the other hand, owing to Lemma 3, we can write

$$K_1 \leqslant J(R(t), t) K_0 t . \tag{4.15}$$

Using Eqs. (4.12), (4.13), (4.15) we conclude that

$$\| v_1^1 \|_{\mathscr{K}_0} \leqslant L(R(t), t) K_0 + J(R(t), t) K_0 t, \tag{4.16}$$

where

$$v_1^1 = V_1 + U_1^1.$$

Consider now the solution of the equation

$$U_{1,t}^n - U_{1,rr}^n = \tilde{k} \int_0^t U_{1,rr}^{n-1}(\rho, \tau)\Big|_{\rho = I_\tau}^{\rho = F_\tau} d\tau + \tilde{k} \int_0^t V_{1,rr}(\rho, \tau)\Big|_{\rho = I_\tau}^{\rho = F_\tau} d\tau.$$

As proved in the Appendix, the application

$$\mathscr{S} : U_1^n \longrightarrow U_1^{n+1}$$

is contracting in $\mathscr{K}_0$, so we conclude that

$$\lim_{n \to \infty} U_1^n = U_1 \tag{4.17}$$

and, if $v_1^n \equiv V_1 + U_1^n$,

$$\lim_{n \to \infty} v_1^n = v_1. \tag{4.18}$$

On the other hand, for every n we have

$$\| v_1^n \|_{\mathscr{K}_0} \leqslant L(R(t), t) K_0 + J(R(t), t) K_{n-1} t, \tag{4.19}$$

where K_{n-1} is the $C^{0+\alpha, 0+\alpha}$ norm of

$$\tilde{k} \int_0^t U_{1,rr}^{n-1}(\rho, \tau)\Big|_{\rho = I_\tau}^{\rho = F_\tau} d\tau + \tilde{k} \int_0^t V_{1,rr}(\rho, \tau)\Big|_{\rho = I_\tau}^{\rho = F_\tau} d\tau.$$

As n tends to infinity, the constant K_{n-1} is bounded by $\| v_1 \|_{\mathscr{K}_0}$ so that we can write

$$\| v_1 \|_{\mathscr{K}_0} \leqslant (L(R(t), t) K_0)(1 - J(R(t), t) t)^{-1}. \tag{4.20}$$

On the other hand, we have

$$K_0 \leqslant (L_R) \| \mathrm{IBD} \|_{\mathscr{D}}, \tag{4.21}$$

so that (4.20) reads

$$\| v_1 \|_{\mathscr{K}_0} \leqslant (L_R)'(\| \mathrm{IBD} \|_{\mathscr{D}})(1 - J(R(t), t) t)^{-1}, \tag{4.22}$$

where $J(R(t), t)$ is found in the proof of Lemma 3, and is easily seen to be bounded when

$$\inf_{t\in[0,T]} \mid \dot{R}(t) - a \mid \equiv \mu' > 0.$$

■

The last formula, together with Eqs. (4.5) and (4.6), proves the

THEOREM 2. *If $R(t) \in C^{2+\alpha}$ and is such that μ and μ' are not vanishing and the initial and boundary data belong to $\mathscr{D}$, then the operator which maps* IBD *onto the unique solution v of* MBP, *$v \in \mathscr{K}$, in a suitable interval $[0, T']$ is continous and*

$$\| v \|_{\mathscr{K}^0} \leqslant (L_R)'' \| \text{IBD} \|_{\mathscr{D}}. \tag{4.23}$$

Appendix

In this section we prove

THEOREM A.1. *If $v \in \mathscr{K}_0$, $IBD \in \mathscr{D}$ ([5]) and* Eqs. $(2.4)_1$ *holds, then $\mathscr{S}_R(v) \in \mathscr{K}_0$ and* Eqs. (2.2) *holds.*

P r o o f. We note that $\mathscr{S}_R(v)$ is the solution of the heat equation with a source term ([6]) $f \in C^{0+\alpha, 0+\alpha}$, satisfying

$$\text{IBD} = 0. \tag{A.0}$$

As it is well known (see for instance [6]) we can write $\mathscr{S}_R(v)$ as follows:

$$\mathscr{S}_R(v) = Z_f(r, t) - z_0(r, t), \tag{A.1}$$

where

i) $Z_f(r, t)$ represents the following integral:

$$Z_f(r, t) = -(4\pi)^{-1/2} \int_{D^+} U_P(r, t, \xi, \eta) f(\xi, \eta)\, d\xi\, d\eta, \tag{A.2}$$

$$U_P(r, t, \xi, \eta) = e^{(r-\xi)^2/4(t-\eta)} (t-\eta)^{-1/2}. \tag{A.3}$$

ii) $z_0(r, t)$ is the solution of $\delta z_0 = 0$ corresponding to the IBD given by $Z_f\Big|_{\lhd D^+}$.

In GEVREY [6] it is proved that:

a) $\mid Z_{f,r} \mid < (L)$ ([7]) $H(f)\, t^{\alpha+1/2}$ (p.344),

b) $H_t(Z_{f,r}) < (L) \mid f \mid t^{1/2-\alpha}$ (p.360),

c) $\mid Z_f \mid < (L) \mid f \mid t$ (p.358),

([5]) The space $\mathscr{D}$ of initial and boundary data *IBD* is defined by Eq. (3.1).

([6]) The source f was defined in (2.1) where $\mathfrak{s} = -\mathfrak{g}$ and $\mathfrak{g}$ is given by Eq. (2.5).

([7]) (L) is a constant which is bounded, when t tends to zero, and its value is varying in different formulas.

d) $Z_{f,t}$ exists and is time-Hölder continous with exponent $\gamma \leqslant \alpha$; its Hölder constant will be denoted by $H_t^{\gamma}(Z_{f,t})$ (p.361 – 362).

Note moreover that, as it is easily seen from Eq. (A.2),

$$Z_f(r,0) = 0, \quad Z_{f,r}(r, 0) = 0\,. \tag{A.4}$$

In the hypotheses d) and (A.4) the following results hold (Gevrey, p.342 and footnote 3 p.362):

e) $| z_0 | < (L) H_t(f)\, t$;

f) $| z_{0,r} | < (L) H_t(f)\, t^{1/2-\alpha}$;

g) $H_t(z_{0,r}) < (L) H_t(f)\, t^{1/2-\alpha}$.

h) $z_{0,t}$ exists and is time-Hölder continous with exponent $\gamma \leqslant \alpha$; its Hölder constant will be denoted by $H_t^{\gamma}(z_{0,t})$. The last result is an obvious consequence of d), the footnote at p.361 and the theorem before Eq. (22), p.342 in GEVREY [6].

i) Statements d) and h) imply that $\mathscr{S}_R(v)_{,t}$ exists and is time Hölder continous with Hölder constant $H_t^{\gamma}(\mathscr{S}_R(v)_{,t})$.

Moreover,

$$H_t^{\gamma}(\mathscr{S}_R(v)_{,t}) \leqslant (L)\mathrm{H}(f)$$

because of Eq. (34)″ p.363, the footnote p.361, and footnote 3 p.362 in Gevrey.

The inequalities a)...c) and e)...g) prove that

$$| \mathscr{S}_R(v) | + | \mathscr{S}_R(v)_{,r} | + H_t \mathscr{S}_R(v)_{,r} < (L) \, \| f \|_{C^{0+\alpha,\, 0+\alpha}}. \tag{A.5}$$

On the other hand, using d), h), i) and Eq. (A.0) we can see that

$$| \mathscr{S}_R(v)_{,rr} \leqslant t^{\gamma} H_t^{\gamma} (\mathscr{S}_R(v)_{,rr}) \leqslant t^{\gamma} (H_t^{\gamma}(\mathscr{S}_R(v)_{,t}) + H_t(f)) \leqslant (L) t^{\gamma} H(f)\,. \tag{A.6}$$

In order to prove that $H_r(\mathscr{S}_R(v)_{,rr})$ exists and is bounded by $(L)H(f)$, we perform the following transformation:

$$\xi \equiv [(b - R(0))\,(b - R(t))^{-1}]\,(r - R(t)) + R(0)\,,$$

$$\tau \equiv \int_0^t (b - R(0))^2\,(b - R(\sigma))^{-2}\, d\sigma\,, \tag{A.7}$$

which maps the domain D^+ on the rectangle $R^+ \equiv [R(0),\, b] \times [0,\, T]$.

If we introduce the notation $(\mathscr{S}_R = \mathscr{S}_R(v))$

$$\mathscr{S}_R(r(\xi,\, \tau),\, t(\tau)) \equiv \mathscr{I}_R(\xi,\, \tau)\,, \tag{A.9}$$

we have

$$\mathscr{S}_R(r(\xi,\, \tau)_{,r} = \mathscr{I}_R(\xi,\, \tau)_{,\xi}\, \xi_{,r}\,, \tag{A.10}$$

$$\mathscr{S}_R(r(\xi,\, \tau)_{,rr} = \mathscr{I}_R(\xi,\, \tau)_{,\xi\xi}\, (\xi_{,r})^2\,, \tag{A.11}$$

$$\mathscr{S}_R(r(\xi,\, \tau)_{,t} = \mathscr{I}_R(\xi,\, \tau)_{,\tau}\, \tau_{,t} + \mathscr{I}_R(\xi,\, \tau)_{,\xi}\, \xi_{,t}\,. \tag{A.12}$$

Under such a transformation the equation $\delta \mathscr{S}_R = f$ becomes

(A.13) $$\mathscr{I}_R(\xi, \tau)_{,\xi\xi} - \mathscr{I}_R(\xi, \tau)_{,\tau} = \mathfrak{f},$$

where

$$\mathfrak{f} = f(r(\xi, \tau), t(\tau))t_{,\tau} + \mathscr{I}_R(\xi, \tau)_{,\xi}\,\xi_{,t}\,t_{,\tau}.$$

We note that as $\mathscr{S}_{R,rr} = \mathscr{S}_{R,t} + f$ we have

(A.14) $$H_r(\mathscr{S}_{R,rr}) \leqslant H_r(\mathscr{S}_{R,t}) + H_r(f).$$

Moreover,

(A.15) $$H_r(\mathscr{S}_{R,t}) = H_r((\mathscr{I}_{R,\tau}\tau_{,t} + \mathscr{I}_{R,\xi}\xi_{,t})(r, t) \leqslant H_r((\mathscr{I}_{R,\tau}\tau_{,t})(r, t))$$

$$+ H_r((\mathscr{I}_{R,\xi}\xi_{,t})(r, t)) \leqslant |\ \tau_{,t}\ |\ H_r((\mathscr{I}_{R,\tau})(r, t)) + H_r((\mathscr{I}_{R,\xi}\xi_{,t})(r, t).$$

(A.16) $$H_r((\mathscr{I}_{R,\xi}\xi_{,t})(r, t)) = H_r((\mathscr{S}_{R,r}r_{,\xi}\xi_{,t})(r, t)$$

$$\leqslant |\ \mathscr{S}_{R,rr}\ |\ ab^3\mu^{-3} + a\mu^{-1}\ |\ \mathscr{S}_{R,r}\ | \leqslant (L)H_t(f)\,a\,(b^3\mu^{-3}t^{\gamma} + \mu^{-1}t^{1/2}),$$

where we used formula (A.6).

(A.17) $$H_r((\mathscr{I}_{R,\tau})(r, t) \leqslant H_\xi((\mathscr{I}_{R,\tau})(r, t))\ |\ \xi_{,x}\ |^{\alpha} \leqslant b^{\alpha}\mu^{-\alpha}H_\xi(\mathscr{I}_{R,\tau}).$$

We split now $\mathscr{I}_R(\xi, \tau)$ as in Eq. (A.3) and write

(A.18) $$\mathscr{I}_R(\xi, \tau) = \mathscr{Z}_{\mathfrak{f}}(\xi, \tau) + \mathfrak{z}_0(\xi, \tau).$$

Because of Eq. (A.18) we have

(A.19) $$H_\xi(\mathscr{I}_{R,\tau}) \leqslant H_\xi(\mathscr{Z}_{\mathfrak{f}}(\xi, \tau)_{,\tau}) + H_\xi(\mathfrak{z}_0(\xi, \tau)_{,\tau}).$$

In order to apply to $\mathscr{Z}_{\mathfrak{f}}$ the results found by FRIEDMAN in [11] we remark that, because of the hypothesis (2.4') $\mathscr{Z}$ is vanishing in $(R(0), 0)$ and $(b, 0)$ so that (see [11] Lemma 1 and its proof):

(A.20) $$H_\xi(\mathscr{Z}_{\mathfrak{f}}(\xi, \tau)_{,\tau}) \leqslant (L)H_\xi(\mathfrak{f}).$$

On the other hand it is possible to find an upper bound for $H_\xi(\mathfrak{z}_0(\xi, \tau)_{,\tau})$ by using the following arguments:

I. Owing to footnote p.361 Eq. (21′) p.338, and to the results quoted at the beginning of p.362 in GEVREY [6]

$$\mathscr{Z}_{f,\tau}(R(0), t) \in C^{0+\alpha/2}, \quad \mathscr{Z}_{f,\tau}(b, t) \in C^{0+\alpha/2}. \tag{A.21}$$

II. Owing to Eq. (3) p.469, which is obtained only for rectangular domains, we conclude, taking again into account footnote 3 p.362 in Gevrey:

$$H_\xi(\mathfrak{z}_0(\xi, \tau)_{,\tau}) \leqslant (L)(H_\xi(\mathfrak{f}) + H_\tau(\mathfrak{f})). \tag{A.22}_1$$

Finally, we have to estimate $H_\xi(\mathfrak{f})$ and $H_\tau(\mathfrak{f})$ in terms of $\| f \|_{C^{0+\alpha, 0+\alpha}}$. It is easily seen that

$$H_\xi(\mathfrak{f}) \leqslant 1(L)\mathscr{Q}_1(\mu^{-1}) \| f \|_{C^{0+\alpha, 0+\alpha}}, \tag{A.22}_2$$

$$H_\tau(\mathfrak{f}) \leqslant (L)\mathscr{Q}_2(\mu^{-1}) \| f \|_{C^{0+\alpha, 0+\alpha}}, \tag{A.22}_3$$

where $\mathscr{Q}_i$ are bounded functions of the variable μ^{-1}.

Using now all results (A.15) ... $(A.22)_{1,2,3}$ we observe that (A.14) becomes

$$H_\xi(\mathscr{S}_R(r, t)_{,rr}) \leqslant \mathscr{Q}(\mu^{-1}) \| f \|_{C^{0+\alpha, 0+\alpha}}, \tag{A.23}$$

where $\mathscr{Q}$ is a bounded function of the variable μ^{-1}.

Equations (A.5), (A.6) and (A.23) prove that $\mathscr{S}_R(v) \in \mathscr{K}_0$.

Consider now v_1 and $v_2 \in \mathscr{K}_0$. The function $\mathscr{S}_R(v_1) - \mathscr{S}_R(v_2)$ belongs to $\mathscr{K}_0$ and is a solution of the following equation:

$$\delta[\mathscr{S}_R(v_1) - \mathscr{S}_R(v_2)] = \tilde{k} \int_0^t (v_1 - v_2)_{1,rr}(\rho, \tau) \Big|_{\rho = I_\tau}^{\rho = F_\tau} d\tau. \tag{A.24}$$

The right-hand side of Eq. (A.24) belongs to $C^{0+\alpha, 0+\alpha}$, owing to Lemma 3, and vanishes when $t \to 0$ so that we can apply to $\mathscr{S}_R(v_1) - \mathscr{S}_R(v_2)$ formulas (34″) p.363 in Gevrey and (A.23).

In our notation they read

$$\| \mathscr{S}_R(v)_1 - \mathscr{S}_R(v_2) \|_{\mathscr{K}_0} \leqslant S(R(t), T, b) \| \Xi \|_{C^{0+\alpha, 0+\alpha}}, \tag{A.25}$$

where

$$\Xi = \tilde{k} \int_0^t (v_1 - v_2)_{,rr}(\rho, \tau) \Big|_{\rho = I_\tau}^{\rho = F_\tau} d\tau.$$

On the other hand, using the estimates found in proving the Lemma 3, it is easily seen that there exists a constant K, bounded when t tends to zero, such that

$$\| \Xi \|_{C^{0+\alpha, 0+\alpha}} \leqslant K(R(t), t, b)\, t \| v_1 - v_2 \|_{\mathscr{K}_0}. \tag{A.26}$$

Equation (3.2) is proved when we choose $L = SK$ ■

We remark that in proving Theorem A.1, we also proved the following

THEOREM A.2 *If* $l \in C^{0+\alpha, 0+\alpha}$ *and* V_1 *is the solution of*

$$V_{1,t} - V_{1,rr} = l(r, t)$$

which vanishes on $\lhd D^+$, *then* $V_1 \in \mathscr{K}_0$ *and, moreover,*

$$\| V_1 \|_{\mathscr{X}_0} \leqslant L(R(t), t) \| l \|_{C^{0+\alpha, 0+\alpha}},$$

where $L(R(t), t)$ is bounded when μ and μ' are not vanishing.

References

1. F. DELL'ISOLA and A. ROMANO, *On a general balance law for continua with an interface*, Ric. di Mat., **35**, 325–337, 1986.
2. F. DELL'ISOLA and A. ROMANO, *On the derivation of thermomechanical balance equations for continuous systems with a nonmaterial interface*, Int. J. Engng. Sci., **25**, 11/12, 1459–1468, 1987.
3. F. DELL'ISOLA and A. ROMANO, *A phenomenological approach to phase transition in classical field theory*, Int. J. Engng. Sci., **25**, 11/12, 1469–1475, 1987.
4. A. ROMANO, *Continuous systems with an interface and phase transitions*, Mediterranean Press, Commenda di Rende, 1989.
5. F. DELL'ISOLA, *Linear growth of a liquid droplet divided from its vapour by a soap bubble–like fluid interface*, Int. J. Engng Sci., **27**, 9, 1053–1067, 1989.
6. M. GEVREY, *Sur les équations aux dérivées partielles du type parabolique*, J. de Math., (6_e série), IX, IV, 1913.
7. C. CILIBERTO, *Formule di maggirazione e teoremi di esistenza per le soluzioni delle equazioni paraboliche in due variabili*, Ric. di Mat., III, 40–75, 1954
8. A. FRIEDMAN, *Partial differential equations of parabolic type*, Prentice Hall, Englewood Cliffs, N.J. 1961.
9. R. COURANT, K.O. FRIEDRICS, *Supersonic flow and shock waves*, Appl. Math. Sci., 21, Springer Verlag, New York 1976.
10. R. COURANT, D. HILBERT, *Methods of mathematical physics* II, Intersci. Publ., 1962.
11. A. FRIEDMAN, *Boundary estimates for second order parabolic equations and their applications*, J. Math. Mech., 7, 5, 1958 771–790, 1958.
12. F. DELL'ISOLA and W. KOSIŃSKI, *Deduction of thermodynamic balance laws for bidimensional nonmaterial directed continua modelling interphase layers*, Arch. Mech., **45**, 3, 333–359, 1993.
13. A.W. ADAMSON, *Physical chemistry of surfaces*, Interscience, New York–London 1983.
14. I.N. LEVINE, *Physical chemistry*, Mc Graw–Hill, New York 1978.

DIPARTIMENTO DI MATEMATICA
UNIVERSITÁ DELLA BASILICATA, POTENZA
and
DIPARTIMENTO DI INGEGNERIA STRUTTURALE
UNIVERSITÁ DI ROMA „LA SAPIENZA", ROMA, ITALIA.

Received October 22, 1993.

Computer Assisted Mechanics and Engineering Sciences (CAMES)

to be published quarterly starting in 1994

Editor: M. Kleiber, Warsaw Associate Editor: H.A. Mang, Vienna

Scope of the Journal

Computer Assisted Mechanics and Engineering Sciences (CAMES) is a refereed international journal, published quarterly, providing an international forum and an authoritative source of information in the field of computational mechanics and related problems of applied science and engineering.

The specific objective of the journal is to support researchers and practitioners based in Central Europe by offering them a means facilitating (a) access to newest research results by leading experts in the field (b) publishing their own contributions and (c) dissemination of information relevant to the scope of the journal.

Papers published in the journal will fall largely into three main categories. The first will contain state-of-the-art reviews with the emphasis on providing the Central European readership with a guidance on important research directions as observed in the current world literature on computer assisted mechanics and engineering sciences.

The second category will contain contributions presenting new developments in the broadly understood field of computational mechanics including solid and structural mechanics, multi-body system dynamics, fluid dynamics, constitutive modeling, structural control and optimization, transport phenomena, heat transfer, etc. Variational formulations and numerical algorithms related to implementation of the finite and boundary element methods, finite difference method, hybrid numerial methods and other methodologies of computational mechanics will clearly be the core areas covered by the journal.

The third category will contain articles describing novel applications of computational techniques in engineering practice; areas of interest will include mechanical, aerospace, civil, naval, chemical and architectural engineering as well as software development.

The journal will also publish book reviews and informations on activities of the Central European Association of Computational Mechanics.

Subscription and sale of single issues is managed by the Editorial Office (for 1994).
Price of single issue: 20 USD (in Poland: 40 000 zł)

Address: Editorial Office, CAMES
Polish Academy of Sciences
Institute of Fundamental Technological Research
ul. Świętokrzyska 21, PL 00-049 Warsaw, Poland

Our Bankers: IV Oddz. Pekao SA Warszawa 501132-40054492-3111